LASER RAMAN SCATTERING STUDIES OF VIBRATIONAL RELAXATION AND NON-COINCIDENCE EFFECT OF THE ISOTROPIC AND ANISOTROPIC RAMAN SPECTRAL COMPONENTS OF MOLECULAR LIQUIDS

ABSTRACT

Anusree Purkayastha
DEPARTMENT OF PHYSICS
SCHOOL OF PHYSICAL SCIENCES
NEHU

A THESIS
SUBMITTED
IN
FULFILMENT OF THE REQUIREMENT OF THE DEGREE OF
DOCTOR OF PHILOSOPHY

To

THE NORTH-EASTERN HILL UNIVERSITY
SHILLONG
INDIA

December, 1986

LASER RAMAN SCATTERING STUDIES OF VIBRATIONAL RELAXATION AND NON-COINCIDENCE EFFECT OF THE ISOTROPIC AND ANISOTROPIC RAMAN SPECTRAL COMPONENTS OF MOLECULAR LIQUIDS

ANUSREE PURKAYASTHA

Synopsis of the dissertation for Ph.D. degree of the North-Eastern Hill University, Shillong

Thesis Supervisor: Dr. Kamal Kumar,
Reader in Physics.

Forwarded

K. Kumar
29/12/86

Dr. Kamal Kumar
Reader in Physics
North Eastern Hill University
Shillong-793003

SYNOPSIS

Laser Raman Scattering studies of vibrational relaxation and Non-coincidence effect of the isotropic and anisotropic Raman spectral components of molecular liquids.

The above mentioned thesis is based on the results of studies which involved the vibrational relaxation studies of liquid N,N-Dimethylacetamide, N,N-Dimethylformamide and Cyclohexanone. Particularly, studies in which solvents were used as an experimental variable have contributed in a major way to our understanding of vibrational relaxation mechanism in liquids. The thesis is limited to Laser Raman scattering studies of liquids with some help from IR band intensities. Raman scattering studies are restricted usually to simpler liquids but provide detailed information about specific dynamic processes in liquids. The main goal of this thesis is to show that solvent is an essential experimental variable in all studies that attempt to improve our basic understanding of the liquid state and the effect of environment on the molecular vibrations and coupled oscillators.

Chapter I presents a brief introduction to the work embodied in the thesis. It highlights the importance of laser Raman scattering studies of vibrational relaxation, the importance of analyzing the experimentally measured lineshapes of the isotropic and anisotropic components of the Raman spectrum of a molecular liquid. The careful investigation of Raman

spectra shows that the peak frequencies of the isotropic and anisotropic components do not coincide and lead to the non-coincidence effect. These studies are performed for the totally symmetric modes of the molecules. The important aspects of the mechanism of vibrational relaxation have been mentioned and the role of Transition dipole-Transition dipole interactions in the dephasing process has been indicated. In case of polar Raman bands such as C=O stretching vibration it is possible to separate the vibrational relaxation from reorientational effects, hence the studies have been limited to the C=O stretching mode vibrations of the polar molecules.

Chapter II gives the general theoretical background in order to understand the different types of mechanisms involved in vibrational relaxation and parameters affecting the band shape of the Raman active vibrations of totally symmetric type. In liquids with strong intermolecular interactions, broadening parameters normally taken into account are second moment $\langle \Delta \omega^2 \rangle$ and the linewidth (FWHH). Sometimes the shift of the maximum frequency or the first moment of the band against the gas frequency is also taken into consideration. Theoretical background for all these parameters has been outlined and the relation to the intermolecular potential mainly of the dipole-dipole type has been given. The various types of potential and the intermolecular potential parameters have been discussed. The van der waal type of interactions and

their role in the bandshpe broadening and other effects has to be considered in a detailed manner which has been attempted in this Chapter.

Chapter III deals with the experimental aspects and describes the various aspects which have to be taken into consideration for accurate measurements of the lineshapes of the Raman bands. Mention has been made for the errors involved in the measurement of the depolarization ratio which has to be kept in mind in order to separate the isotropic component from the polarized (I_{VV}) component of the Raman spectrum. The spectrometer used and the importance of the slitwidth etc. on the Raman band has also been indicated.

Chapter IV gives an account of the experimental work performed by us on the N,N-Dimethyl acetamide (DMA) molecule in neat liquid and under varying environmental conditions by varying solvents. The solvents chosen were acetonitrile (CH_3CN), chloroform ($CHCl_3$), carbontetrachloride (CCl_4) and benzene (C_6H_6). These four solvents were found suitable after considerable screening taking into consideration, no overlapping bands, avoiding strong hydrogen bonding effects. Out of these four solvents two ($CHCl_3$ and CH_3CN) solvents belong to the category of polar molecules and two (CCl_4 and C_6H_6) are non-polar in nature. The dipolar effects may be studied using $CHCl_3$ and CH_3CN and these solvents are therefore quite effective

in reducing the interactions between the solute molecules. Besides the dipolar interactions, the inductive and dispersion forces are also operative and play quite significant role in liquid structure. These interactions are easily studied in non-polar solvents as dipole-dipole interactions are absent here. In case of polar molecules all the three types of interactions are effective. The screening effects due to the dielectric constant of the medium may also be investigated using these four solvents as their dielectric constants are quite different from each other. The studies on dilute solutions are especially of considerable importance as it deals with the situation where the solute molecule is surrounded mainly by solvent molecules. Under these conditions the influence of the solvent molecules becomes quite important. The van der Waals attractions (dipole-dipole, dipole-induced dipole and dispersion type) have been taken into consideration to see their role in the line broadening mechanism. The variation of the linewidth of the isotropic component, Γ_{iso} (FWHH) has been studied as a function of the total interaction energy involving D-D, D-ID and dispersion forces. It is seen that Γ_{iso} varies linearly as a function of the dispersion energy parameter given as $F(n,I) = \frac{3}{2n^4}\frac{I_i I_j}{I_i+I_j}\alpha_i\alpha_j$ where I_i, I_j are the ionization potential of the molecules i and j, α_i, α_j are the polarizabilities and n is the refractive index of the medium. This parameter is for a pair of interacting molecules i and j.

The calculations of D-D, D-ID and dispersion energy have been carried out for the systems DMA-$CHCl_3$, DMA-CH_3CN, DMA-CCl_4 and DMA-C_6H_6 taking into consideration the dielectric constant and refractive index of the medium. These calculations clearly show that the dispersion energy is the most significant one even in case of polar solvent molecules due to the presence of high dielectric constant in the denominator of D-D and D-ID energy expressions. The solvent dependence has also shown that the transition dipole-transition dipole (TD-TD) interaction is the main coupling mechanism responsible for the noncoincidence effect in DMA molecule.

Chapter V deals with the vibrational relaxation studies on N,N-Dimethylformamide (DMF) molecule. This molecule is similar to N,N-Dimethylacetamide except that it has H atom in place of the methyl group near the C=O bond. The hydrogen bonding effect may therefore be present in linear chain. This system is quite interesting from intermolecular interaction point of view. The studies were performed in dilute solutions using the polar and nonpolar solvents which clearly show same type of behaviour of Γ_{iso} in dilute solutions. The relation between the Γ_{iso} and the dispersion energy parameter is linear here too indicating that dispersion forces override all other forces (electrical forces) so far as the line broadening is concerned. One very interesting thing which we have

investigated in case of DMF molecule is the combined effect of the parameters related to the hydrodynamic force, and dispersion force on the lineshape. For the hydrodynamic force, η, the dynamic viscosity, and for the dispersion force the quantity $\frac{n^2-1}{2n^2+1}$, which comes from Lorentz's local field have been taken into consideration. The vibrational relaxation rate $(\tau_v^{-1}) = \pi c \Gamma_{iso}$, is found to be clearly related to a parameter f $(\rho,\eta,n) = \rho\eta\left(\frac{n^2-1}{2n^2+1}\right)^{-1}$ in a linear fashion, where being the density and n is the refractive index of the medium. This is an interesting empirical finding as it takes care of many aspects related to the molecular parameters. The solvents have been varied from polar to non-polar and it has been found that τ_v^{-1} is a linear function of $f(\rho,\eta,n)$ for dilute solutions. The TD-TD type of interactions are again seem to be responsible for noncoincidence effect in DMF. In addition we have studied the variation of $\delta\nu\ (2\epsilon + n^2)^2\,\epsilon^{-1}$ as a function of volume fraction of solute (φ). It is seen that this variation is also linear in nature. This correlation is indicative of the screening effects due to dielectric properties of the medium.

Chapter VI has been mainly devoted to studies on Cyclohexanone molecule showing the effect of the dispersion energy parameter on linebroadening in a system where the dipole moment of the entire molecule is almost concentrated on the C=O bond only. The C=O is the only polar group in cyclohexanone molecule. The dipole, as well as the transition-dipole both will be in

the same direction in this case. The system is considered to be in the chair conformation. It is quite interesting to see that the relationship which we observed in case of N,N-Dimethylacetamide and N,N-Dimethylformamide are also holding good in this molecule. The dispersion energy parameter is well correlated with the Γ_{iso} and the parameters $f(\varphi, \eta, n)$ is found to be very well fitting with the τ_v^{-1} in a linear fashion. The non-coincidence effect is again very well explained in terms of TD-TD interactions.

The last Chapter VII gives the conclusions drawn from the present work.

LASER RAMAN SCATTERING STUDIES OF VIBRATIONAL RELAXATION AND NON-COINCIDENCE EFFECT OF THE ISOTROPIC AND ANISOTROPIC RAMAN SPECTRAL COMPONENTS OF MOLECULAR LIQUIDS

Anusree Purkayastha
DEPARTMENT OF PHYSICS
SCHOOL OF PHYSICAL SCIENCES
NEHU

A THESIS
SUBMITTED
IN
FULFILMENT OF THE REQUIREMENT OF THE DEGREE OF
DOCTOR OF PHILOSOPHY

To

THE NORTH-EASTERN HILL UNIVERSITY
SHILLONG
INDIA

December, 1986

Thesis.

DS
544.64
PUR

Phone
Grams : NEHU

North - Eastern Hill University

Bijni Complex
Bhagyakul, Shillong-793003 (Meghalaya)

Department of..PHYSICS.....

Dr. Kamal Kumar
Reader in Physics

I certify that the thesis entitled "Laser Raman scattering studies of vibrational relaxation and Noncoincidence effect of the isotropic and anisotropic Raman spectral components of Molecular liquids", submitted by Miss Anusree Purkayastha for the Degree of Doctor of Philosophy of the North-Eastern Hill University, Shillong, embodies the record of original investigations carried out by her under my supervision. She has been duly registered and the thesis presented is worthy of being considered for the award of the Ph.D. degree. This work has not been submitted for any Degree of any other University.

K. Kumar

Date: 29th December, 1986 Signature of the Supervisor

Place: Shillong.

Phone 24558
Grams : NEHU

North - Eastern Hill University

Bijni Complex
Bhagyakul, Shillong-793003 (Meghalaya)

Department of...PHYSICS.....

C E R T I F I C A T E

This is to certify that Miss Anusree Purkayastha has cleared the following Pre-Ph.D. courses as prescribed by this University and obtained 'A' grade in all of them.

Course	Grade
Experimental Techniques - II	A
Nuclear Physics - II	A
Chemical Binding	A
French Language	A

(C.S. Shastry)
Professor & Head
Department of Physics,
NEHU, Shillong.

ACKNOWLEDGEMENTS

I take the opportunity to express my deep sense of gratitude to Dr. Kamal Kumar, Reader, Department of Physics, N.E.H.U. for suggesting me the research problem and offering me his valuable guidance throughout the entire course of my Ph.D. programme. I am thankful to him especially for his constant supervision, encouragement and help but for which this work would not have been possible. I am grateful to Prof. A.L. Verma, Department of Physics, N.E.H.U. for his kindness in allowing me to make use of the facilities available in his laboratory and encouraging me during the course of this work. I am immensely grateful to the Vice-Chancellor, N.E.H.U., the Dean of the School of Physical Sciences, the Head of the Department of Physics, Prof. C.S. Shastry and the Head of R.S.I.C., N.E.H.U. for kindly allowing me to use all the research facilities available in the University. Special thanks are due to Mr. Anil Kumar Rathore for his help in recording the laser Raman spectra.

I am priviledged to thank my friends for their helpful co-operation during the course of this work. Thanks are also due to Mrs. Rajamma K. for her adept typing.

Lastly, I am indebted to my parents for their keen interest, patience and encouragement over all these years of my research work.

Dated: 29th Dec 1986
Shillong

(ANUSREE PURKAYASTHA)

CONTENTS

SYNOPSIS

Laser Raman Scattering studies of vibrational relaxation and Non-coincidence effect of the isotropic and anisotropic Raman spectral components of molecular liquids.

The above mentioned thesis is based on the results of studies which involved the vibrational relaxation studies of liquid N,N-Dimethylacetamide, N,N-Dimethylformamide and Cyclohexanone. Particularly, studies in which solvents were used as an experimental variable have contributed in a major way to our understanding of vibrational relaxation mechanism in liquids. The thesis is limited to Laser Raman scattering studies of liquids with some help from IR band intensities. Raman scattering studies are restricted usually to simpler liquids but provide detailed information about specific dynamic processes in liquids. The main goal of this thesis is to show that solvent is an essential experimental variable in all studies that attempt to improve our basic understanding of the liquid state and the effect of environment on the molecular vibrations and coupled oscillators.

Chapter I presents a brief introduction to the work embodied in the thesis. It highlights the importance of laser Raman scattering studies of vibrational relaxation, the importance of analyzing the experimentally measured lineshapes of the isotropic and anisotropic components of the Raman spectrum of a molecular liquid. The careful investigation of Raman

spectra shows that the peak frequencies of the isotropic and anisotropic components do not coincide and lead to the non-coincidence effect. These studies are performed for the totally symmetric modes of the molecules. The important aspects of the mechanism of vibrational relaxation have been mentioned and the role of Transition dipole-Transition dipole interactions in the dephasing process has been indicated. In case of polar Raman bands such as C=O stretching vibration it is possible to separate the vibrational relaxation from reorientational effects, hence the studies have been limited to the C=O stretching mode vibrations of the polar molecules.

Chapter II gives the general theoretical background in order to understand the different types of mechanisms involved in vibrational relaxation and parameters affecting the band shape of the Raman active vibrations of totally symmetric type. In liquids with strong intermolecular interactions, broadening parameters normally taken into account are second moment $\langle \Delta\omega^2 \rangle$ and the linewidth (FWHH). Sometimes the shift of the maximum frequency or the first moment of the band against the gas frequency is also taken into consideration. Theoretical background for all these parameters has been outlined and the relation to the intermolecular potential mainly of the dipole-dipole type has been given. The various types of potential and the intermolecular potential parameters have been discussed. The van der Waal type of interactions and

their role in the bandshpe broadening and other effects has to be considered in a detailed manner which has been attempted in this Chapter.

Chapter III deals with the experimental aspects and describes the various aspects which have to be taken into consideration for accurate measurements of the lineshapes of the Raman bands. Mention has been made for the errors involved in the measurement of the depolarization ratio which has to be kept in mind in order to separate the isotropic component from the polarized (I_{VV}) component of the Raman spectrum. The spectrometer used and the importance of the slitwidth etc. on the Raman band has also been indicated.

Chapter IV gives an account of the experimental work performed by us on the N,N-Dimethyl acetamide (DMA) molecule in neat liquid and under varying environmental conditions by varying solvents. The solvents chosen were acetonitrile (CH_3CN), chloroform ($CHCl_3$), carbontetrachloride (CCl_4) and benzene (C_6H_6). These four solvents were found suitable after considerable screening taking into consideration, no overlapping bands, avoiding strong hydrogen bonding effects. Out of these four solvents two ($CHCl_3$ and CH_3CN) solvents belong to the category of polar molecules and two (CCl_4 and C_6H_6) are non-polar in nature. The dipolar effects may be studied using $CHCl_3$ and CH_3CN and these solvents are therefore quite effective

in reducing the interactions between the solute molecules. Besides the dipolar interactions, the inductive and dispersion forces are also operative and play quite significant role in liquid structure. These interactions are easily studied in non-polar solvents as dipole-dipole interactions are absent here. In case of polar molecules all the three types of interactions are effective. The screening effects due to the dielectric constant of the medium, may also be investigated using these four solvents as their dielectric constants are quite different from each other. The studies on dilute solutions are especially of considerable importance as it deals with the situation where the solute molecule is surrounded mainly by solvent molecules. Under these conditions the influence of the solvent molecules becomes quite important. The van der Waals attractions (dipole-dipole, dipole-induced dipole and dispersion type) have been taken into consideration to see their role in the line broadening mechanism. The variation of the linewidth of the isotropic component, Γ_{iso} (FWHH) has been studied as a function of the total interaction energy involving D-D, D-ID and dispersion forces. It is seen that Γ_{iso} varies linearly as a function of the dispersion energy parameter given as $F(n,I) = \frac{3}{2n^4}\frac{I_i I_j}{I_i+I_j}\alpha_i\alpha_j$ where I_i, I_j are the ionization potential of the molecules i and j α_i, α_j are the polarizabilities and n is the refractive index of the medium. This parameter is for a pair of interacting molecules i and j.

The calculations of D-D, D-ID and dispersion energy have been carried out for the systems DMA-$CHCl_3$, DMA-CH_3CN, DMA-CCl_4 and DMA-C_6H_6 taking into consideration the dielectric constant and refractive index of the medium. These calculations clearly show that the dispersion energy is the most significant one even in case of polar solvent molecules due to the presence of high dielectric constant in the denominator of D-D and D-ID energy expressions. The solvent dependence has also shown that the transition dipole-transition dipole (TD-TD) interaction is the main coupling mechanism responsible for the noncoincidence effect in DMA molecule.

Chapter V deals with the vibrational relaxation studies on N,N-Dimethylformamide (DMF) molecule. This molecule is similar to N,N-Dimethylacetamide except that it has H atom in place of the methyl group near the C=O bond. The hydrogen bonding effect may therefore be present in linear chain. This system is quite interesting from intermolecular interaction point of view. The studies were performed in dilute solutions using the polar and nonpolar solvents which clearly show same type of behaviour of Γ_{iso} in dilute solutions. The relation between the Γ_{iso} and the dispersion energy parameter is linear here too indicating that dispersion forces override all other forces (electrical forces) so far as the line broadening is concerned. One very interesting thing which we have

investigated in case of DMF molecule is the combined effect of the parameters related to the hydrodynamic force, and dispersion force on the lineshape. For the hydrodynamic force, η, the dynamic viscosity, and for the dispersion force the quantity $\frac{n^2-1}{2n^2+1}$, which comes from Lorentz's local field, have been taken into consideration. The vibrational relaxation rate $(\tau_v^{-1}) = \pi c \Gamma_{iso}$, is found to be clearly related to a parameter $f(\rho,\eta,n) = \rho\eta(\frac{n^2-1}{2n^2+1})^{-1}$ in a linear fashion, where ρ being the density and n is the refractive index of the medium. This is an interesting empirical finding as it takes care of many aspects related to the molecular parameters. The solvents have been varied from polar to non-polar and it has been found that τ_v^{-1} is a linear function of $f(\rho,\eta,n)$ for dilute solutions. The TD-TD type of interactions are again seem to be responsible for noncoincidence effect in DMF. In addition we have studied the variation of $\delta\nu\ (2\epsilon + n^2)^2\ \epsilon^{-1}$ as a function of volume fraction of solute (φ). It is seen that this variation is also linear in nature. This correlation is indicative of the screening effects due to dielectric properties of the medium.

Chapter VI has been mainly devoted to studies on Cyclohexanone molecule showing the effect of the dispersion energy parameter on linebroadening in a system where the dipole moment of the entire molecule is almost concentrated on the C=O bond only. The C=O is the only polar group in cyclohexanone molecule. The dipole, as well as the transition-dipole both will be in

the same direction in this case. The system is considered to be in the chair conformation. It is quite interesting to see that the relationship which we observed in case of N,N-Dimethylacetamide and N,N-Dimethylformamide are also holding good in this molecule. The dispersion energy parameter is well correlated with the Γ_{iso} and the parameters $f(\varphi,\eta, n)$ is found to be very well fitting with the τ_v^{-1} in a linear fashion. The non-coincidence effect is again very well explained in terms of TD-TD interactions.

The last Chapter VII gives the conclusions drawn from the present work.

CHAPTER I

Introduction

The study of dynamical behaviour in molecular liquids is very difficult since in the liquid state the molecules are in a state of chaotic motion. However, some progress has been made towards a better understanding of the molecular motions in liquids on the basis of experimental and theoretical work. The NMR relaxation experiments provide information about molecular motions and intermolecular interactions in liquids. Laser Raman scattering experiments, however, provide detailed information about a specific dynamic process in the liquid.[1-9] During the past decade vibrational relaxation and molecular reorientation processes in liquids have been studied by analyzing [1-5,10-12] the line shape of the isotropic (I_{iso}) and anisotropic(I_{aniso}) components of the Raman band of the molecule. The sensitivity of the Raman peak position and linewidth (FWHH) on the environment has been demonstrated by the solvent, and pressure dependent studies. The temperature dependent studies of the linewidth have been useful in obtaining the information on the dynamics of liquid.

Theoretical models for lineshape may often be applied to data obtained by different techniques like NMR, ESR and vibrational spectroscopy. In these cases the electromagnetic field causes a change of state in a reference system of nuclear

spin or electronic spin states or the vibrational modes (vibrational energy levels) of molecules. The reference molecular system is immersed in a solid, liquid or dense gas and interacts with many degrees of freedom (eg. translational and rotational) of the bath. Thus the states of the reference system will have a finite lifetime and energy width. This amounts to a decay of the time correlation function corresponding to the reference transition. The lineshape may give valuable information about the interaction of the reference molecule with its environment. In addition it may provide information about the dynamics of the bath.

The experimental set-up is normally such that an ensemble of reference molecules is under observation. In case one wants to examine the reorientation and vibrational relaxation processes separately using vibrational (IR and Raman) Spectroscopy one has to study the well isolated vibrational modes. From the experimentally observed polarized (I_{VV}) and depolarized (I_{VH}) Raman bandshapes, one can obtain the isotropic scattering intensity, $I_{iso}(\omega)$, and the anisotropic scattering intensity, $I_{aniso}(\omega)$[13]. Only vibrational processes contribute to $I_{iso}(\omega)$, whereas both vibrational and reorientational processes contribute to $I_{aniso}(\omega)$.

The broadening of isotropic Raman bandshapes may be influenced by several mechanisms.[10,14] The two dominant ones are the energy relaxation and phase relaxation. The energy

relaxation involves inelastic processes and it may occur due to intermolecular transfer of energy between the vibrational degrees of freedom and the bath. The phase relaxation involves only quasi-elastic interactions of the molecules with their surroundings, leading to perturbation of the phases of the vibrational wave functions without changing their quantum states. Both mechanisms have been investigated and it has been found that phase relaxation (dephasing) in liquids occur much faster than energy relaxation. Many different theories[15] of dephasing have recently been developed, examples of which are the isolated binary collision (IBC) model,[16,17] the hydrodynamic model,[18] the cell model[19] and the model based on resonant energy transfer[10].

Different theoretical models have been used to predict rate constants for vibrational relaxation process. In the IBC model, the transition rate is assumed to be the product of the collision rate in the liquid and the transition probability per collision in the gas phase. The probability per collision may be obtained either from scattering calculations or by independent experiments on low-density gases. Various models have been proposed for the collision rate in liquid phase. Litovitz[20] approximated the time between collisions to an Enskog time for the rate of binary collision of hard spheres using cell model. Oxtoby[15] has shown that the relaxation time of the random force is responsible for the viscosity dependence of the diffusion coefficient. Fluctuations with wavelengths longer than a

molecular diameter decay hydrodynamically with rates characterized by the liquid viscosity but for shorter wavelengths this simple nature is lost.

One of the important mechanisms that may contribute significantly to dephasing process in liquids is the coupling between the similar modes of identical molecules that results in resonant energy transfer. The interaction responsible for this coupling usually depends strongly on the relative orientation of the molecules. An important coupling mechanism is the transition dipole-transition dipole (TD-TD) type which is possible when strongly infrared active transitions are present[5]. The resonance transfer mechanism is identified by dilution experiments with inert solvents, which reduces the coupling. Such experiments exhibit line narrowing when dilution studies are carried out with isotopically substituted species.

It has been observed in case of many molecules that the peak frequencies of the Raman bands corresponding to the isotropic and anisotropic components do not coincide in liquid state. The differences in the peak positions may sometimes be even more than 10 cm^{-1}. This noncoincidence has been observed for many IR active modes such as SO stretch of sulfoxides and sulfones[2], the OH stretch of carbonyls[21], CN stretch of nitriles[1] and NH stretch of amines[22]. The concentration studies have shown that the magnitude of the splitting decreases with decreasing concentration of the

solvent and may go to zero in the limit of infinite dilution[23]. This effect is often, but not always associated with vibrational modes having large dipole moment derivatives. Facts such as these have led some investigators[24] to attribute the noncoincidence effect to a frequency difference between in-phase and out-of-phase collective oscillations of molecular aggregates aligned by angular dependent intermolecular forces. This concept does not contradict the dynamic nature of the liquid phase, since it is only necessary that the lifetimes of the supposed quasicrystalline regions be long compared to the vibrational period. In order to see whether this qualitative comparison to correlation field splitting in solids is a correct analogy for the splitting of nondegenerate polar modes in the liquid phase, a quantitative theoretical treatment of the noncoincidence effect is necessary. Wang and McHale[4] presented the results of the calculation of the first moments of the isotropic and anisotropic Raman spectral components of a molecule with an axially symmetric polarizability tensor. An important feature of the derivation is that it is not necessary to postulate short-range order to explain the noncoincidence effect; a strong angular dependent intermolecular potential is predicted to give rise to the concentration dependent isotropic and anisotropic peak frequencies. Recently, McHale[5] formulated a model which distinguishes the solvent systems with strong short-range order from those in which noncoincidence is attributed to angular dependent forces of a less directional

nature. In order to see whether the concentration dependence of the Raman spectra of a variety of solvent systems can be explained without invoking short-range order, a particular type of vibrational coupling, the transition dipole-transition dipole interaction (TD-TD) has been considered. The first moment of the infrared absorption band was also evaluated in order to investigate the potential influence of intermolecular forces on the peak frequency of the IR spectrum.

Although the vibrational resonance coupling due to the TD-TD interaction may be important in some polar modes, it has been pointed out earlier by Wang[25] that the vibrational resonance coupling Hamiltonian given by the form $\frac{1}{2} \sum_{i,j}' V_{ij}^{(2)} Q_i Q_j$ may originate from quadrupole-quadrupole interaction, hydrogen bonding interaction, or any other type of intermolecular interactions. Here i and j designate molecules, and Q_i and Q_j refer to the same vibrational mode of molecules i and j, respectively. The prime on the summation sign indicates the summation of the term with i = j to be excluded. This coupling term provides a pathway for an efficient exchange of vibrational energy between vibrational normal modes of the same symmetry but of different molecules. The Hamiltonian[11] which determines the time evolution of the dynamic variables is written as

$$H = H_{osc} + H_B + H'$$

where Hosc is the sum of the harmonic oscillator Hamiltonians, H_B is the Hamiltonian for the rotational and translational

degrees of freedom (the bath molecules) and H' is the part of the Hamiltonian which couples the internal vibrational coordinates of the bath molecules. Considering the total potential V as a Taylor series expansion about all $Q_i = 0$, H' is written as

$$H' = \sum_i V_i^{(1)} Q_i + \tfrac{1}{2} \sum_{i,j} V_{ij}^{(2)} Q_i Q_j$$

where $V_i^{(1)} = (\partial V / \partial Q_i)_0$ and $V_{ij}^{(2)} = \tfrac{1}{2}(\partial^2 V / \partial Q_i \partial Q_j)_0$.

It is the off-diagonal elements of $V_{ij}^{(2)}$ which give rise to the concentration dependent resonance transfer effects. The diagonal terms $V_{ii}^{(2)}$ along with $V_i^{(1)}$ are also expected to make a contribution to the linewidth which results from dephasing due to fluctuations in the vibrational frequency. It was shown that $V_i^{(1)}$ and $V_{ii}^{(1)}$ do not affect the first moment or the frequency at the maximum, but do contribute to the second moment or the linewidth.

Fini and Mirone[26] showed for the first time that the C = O stretching mode frequency for liquid ethylene carbonate and propylene carbonate is higher in IR spectrum than the Raman one. The difference in frequency being 13 cm^{-1} for ethylene carbonate at 313 K. Later, it was shown[1] by them that for the pure liquids the Raman anisotropic component of the C = O stretching mode falls at a higher frequency than the isotropic one. The IR band maximum appears almost at the same frequency as the Raman anisotropic component. In some cases IR band may be resolved into two components, the stronger

coinciding with the anisotropic and the weaker with the isotropic Raman component.

The non-coincidence of the isotropic and anisotropic Raman band components of few polar molecules like acetone, N,N-dimethylformamide, γ-butyrolacetone and dimethylsulfoxide have been studied by Mirone et al.[23] as a function of solvent concentrations in various solvents. The noncoincidence effect reduces with dilution and ultimately almost disappears on high dilution. With increasing temperature, a decrease in anisotropy shift is observed. This behaviour is explained on the basis of the coupling between the transition dipole moments of neighbouring molecules, which is made possible by some degree of alignment of dipoles of these highly polar molecules. The anisotropy shift was shown to depend linearly on the ratio between the volume fraction and the static dielectric constant of the solution. It may become zero at a finite concentration. It has been suggested that this concentration threshold is related to vibrational energy relaxation.

The benzaldehyde molecule has been studied by Yarwood and Arndt[27] who observed that the I_{VV} component of the C = O stretching mode gives an asymmetric shape whereas I_{VH} component is almost symmetric with its maximum shifted to higher wavenumbers. For 98 mole per cent dilution of benzaldehyde in carbondisulfide solvent the I_{VV} component narrows to a symmetric band and its maximum frequency coincides with the I_{VH} component.

The asymmetry of the I_{VV} component (or anisotropy shift) is explained as due to the TD-TD interactions. On dilution the effects of resonant transfer of vibrational energy due to TD-TD interactions on the band shape are reduced as the benzaldehyde molecules become separated. The isotopic dilution studies of benzaldehyde in benzaldehyde-d_6 show that with increasing dilution the anisotropy shift decreases from ~ 4.5 cm^{-1} to ~ 1 cm^{-1} in the most dilute solution.

A Raman study of the C = O stretching vibration band of liquid methyl-ethyl-ketone has been carried out by Scheibe[28]. A simple theoretical approach to the behaviour of various band shape parameters in terms of dipole-dipole (D-D) interactions has been worked out in the frequency domain. The structural effects seem to play an important role in influencing the band shape of polar Raman bands in liquids with dipole-dipole interaction energies of the order of kT. The asymmetry of the I_{VV} component of the band was explained on the basis of the change of the orientation probability distribution into the direction of energetically favourable orientations. However, the theoretical approach is too simple to allow more than a qualitative interpretation of the experimental data. Therefore further theoretical and experimental work is required in this direction.

The relative role of slowly varying attractive interactions and rapidly varying repulsive interactions on the frequency shifts and dephasing process in liquids has been studied by

Schweizer and Chandler[29]. Their theoretical model correctly predicts the isothermal density dependence of C = CH_2 bandwidth in isobutylene and the C = O bandwidth in acetone. Schindler and Jonas[30], however found a very different density dependence for the frequency shifts of the C = CH_2 and C-CH_3 modes in isobutylene. They have also shown that anisotropy shift for the $\nu_2 + 2\nu_7$ bands of ethylene carbonate is proportional to $(\partial\mu/\partial Q)^2$, which clearly indicates that TD-TD coupling is responsible for the observed effect.

Recently Steiger et. al.[31] have studied the Raman spectrum of trimethylchlorosilane and have observed the anisotropy shift (~3 cm^{-1}) for the ν(SiCl) bond. The non-coincidence of the Raman frequencies of the two scattering components indicates a local clustering of the molecules for at least a certain time (~ 0.1 ps). Further investigations are however needed to confirm the influences drawn by these authors.

The influence of vibrational resonance coupling on spectral linewidths has been discussed by a number of investigators[32-35]. It is generally recognized now that the problem of deducing the separate vibrational and reorientational correlation functions from experimental band shapes is not as simple as it was once thought to be. In order to investigate the expected concentration trends of the half-widths of vibrational spectra, Wang and McHale[4] evaluated the second moments of infrared, polarized and depolarised Raman spectra. It is

shown that the intermolecular forces which are strong enough to result in noncoincidence effect may also be responsible for the Raman and IR band-width dependence on concentration. Concentration dependent IR band-widths have been reported for both the bending and asymmetric stretching modes of CS_2, and have been attributed to the effects of resonant transfer of vibrational energy[32]. Although the full band shape and half-widths are not accounted for unless all the spectral moments are evaluated, the results should provide a basis for further investigation of the effects of intermolecular vibrational coupling on Raman linewidths.

In order to understand the nature of intermolecular interactions and molecular dynamics, there is a definite need for additional systematic studies on vibrational relaxation, reorientational motion and frequency shifts in various liquids. The information content of temperature and solvent effects on frequency shifts of various vibrational bands has not yet been fully explored. In particular, the anisotropy shift in dipolar liquids may offer new information about strong dipolar interactions. The study of the influence of solvents on the band shape parameters is of paramount importance not only in connection with molecular structure and liquid dynamics but also in connection with solution kinetics. The N,N-dimethylacetamide (DMA), N,N-dimethylformamide (DMF) and cyclohexanone molecules were chosen for the vibrational relaxation studies as these

molecules contain C = O bond which is highly polar in nature. The DMA and DMF are also of great value because of their biophysical significance. The amide I band of DMA and DMF provide vital information regarding the protein molecules. The solvent dependent studies of Raman band shape parameters may also serve as a model for the environmental effects on the vibrational modes. The Raman experimental data on the protein-ligand interactions especially enzyme-substrate interactions where line broadening or frequency shifts are observed may also be interpreted in these lines to provide information about the nature of the interacting site in proteins. It may help in the mapping of the active site of the enzyme where the substrate is bound during the catalytic process. These studies are therefore expected to throw light on the nature of the inter-molecular forces playing key role in the interactions of great biophysical significance.

References

[1] G. Fini and P. Mirone, J. Chem. Soc. Faraday Trans.II. 70, 1776 (1974).

[2] G. Fini and P. Mirone, Spectrochim. Acta Part A, 32, 625(1976).

[3] W. Schindler, P.T. Sharko and J. Jonas, J. Chem. Phys. 76, 3493 (1982).

[4] C.H. Wang and J. McHale, J. Chem. Phys. 72, 4039 (1980), and references therein.

[5] J. McHale, J. Chem. Phys. 75, 30 (1981).

[6] W. Schindler and J. Jonas, J. Chem. Phys. 72, 5019 (1980).

[7] J. Schroeder and J. Jonas, J. Chem. Phys. 34, 11 (1978).

[8] T.W. Zerda, S. Perry and J. Jonas, Chem. Phys. Lett. 83, 600 (1981).

[9] B. Hegemann and J. Jonas, J. Chem. Phys. 79, 4683 (1983).

[10] D.W. Oxtoby, J. Phys. Chem. 87, 3028 (1983).

[11] W. Schindler, T.W. Zerda and J. Jonas, J. Chem. Phys. 81, 4306 (1984).

[12] J. Jonas, Acc. Chem. Res. 17, 74 (1984), and references therein.

[13] L.A. Nafie and W.L. Peticolas, J. Chem. Phys. 57, 3145 (1972).

[14] F. Seifert, K.L. Oehme, G. Rudakoff, W. Hölzer, W. Carius and O. Schrötter, Chem. Phys. Lett. 105, 635 (1984).

[15] D.W. Oxtoby, Ann. Rev. Phys. Chem. 32, 77 (1981).

[16] S.F. Fischer and A. Laubereau, Chem. Phys. Lett. 35, 6(1975).

[17] D.W. Oxtoby and S.A. Rice, Chem. Phys. Lett. 42, 1 (1976).

[18] D.W. Oxtoby, J. Chem. Phys. 70, 2605 (1979).

[19] D.J. Diestler and J. Manj, J. Mol. Phys. 33, 227 (1977).

[20] F.J. Bartoli and T.A. Litovitz, J. Chem. Phys. 56, 404, 413 (1972).

[21] C. Perchard and J.P. Perchard, J. Raman Spectrosc. 3 277 (1975).

[22] C. Perchard and J.P. Perchard, J. Raman Spectrosc. 6 74(1975).

[23] P. Mirone and G. Fini, J. Chem. Phys. 71, 2241 (1979).

[24] J.P. Perchard, in "Proceedings of the Fifth International Conference on Raman Spectroscopy" (Schulz, Freiburg; 1976) p. 235.

[25] C.H. Wang, Mol. Phys. 33, 207 (1977).

[26] G. Fini and P. Mirone, J. Chem. Soc. F. Trans II 69, 1243 (1973).

[27] J. Yarwood and R. Arndt, in "Molecular Association", Vol.2. Ed. by R. Foster (Academic Press, London, 1979) p-312.

[28] D. Scheible, J. Raman Spectrosc. 13, 103 (1982).

[29] K.S. Schweizer and D. Chandler, J. Chem. Phys.. 76, 1128 (1982).

[30] W. Schindler and J. Jonas, J. Chem. Phys. 72, 5019 (1980); 73, 3547 (1980).

[31] Th. Steiger, K.W. Brzezinka and P. Reich, J. Raman Spectrosc. 17, 65 (1986).

[32] M. Kakimoto and T.Fuhiyama, Bull. Chem. Soc. Jpn. 45, 2970 (1972).

[33] R.M. Lynden Bell, Mol. Phys. 33, 907 (1977).

[34] R.K. Wertheimer, Mol. Phys. 36, 1631 (1978).

[35] R.G. Gordon, J. Chem. Phys. 40, 1973 (1964); 41, 1819 (1964); 43, 1307 (1965).

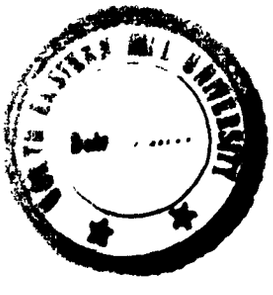

CHAPTER II

CHAPTER II

Theoretical aspects

In recent years there has been a resurgence of interest in the study of vibrational relaxation in liquids and considerable progress has been made through experiment, theory and computer simulation towards a deeper understanding of the physical processes involved. The vibrations of a molecule are sensitive probes of local structure and dynamics in molecular liquids, and therefore provide microscopic information about a state of matter which is still relatively poorly understood. Vibrational relaxation occurs through the coupling of a quantum vibrational system to a classical "heat bath" of rotational and translational degrees of freedom[1]. Vibrational phase and energy relaxation time can be as short as few picoseconds and may thus be comparable to bath relaxation time. This has important consequences for the dynamics of the coupled systems. In small molecules, reorientation provides the primary relaxation mechanism for allowed transitions. For larger molecules, vibrational relaxation mechanisms play an increasingly important role[2]. Laser Raman scattering experiments are used to provide detailed information about a specific dynamic process in liquids.

2.1 Vibrational relaxation in liquids

In case of totally symmetric vibration, the contribution to the band shape from reorientational motion can be separated from the contribution arising from vibrational relaxation by

appropriate choice of scattering geometry. This provides the opportunity to study the relative importance of two processes and the mechanism of reorientational and vibrational relaxation. The vibrational relaxation process is generated by a large variety of inter and intra-molecular forces including dipole-dipole, dipole-induced dipole, dispersion, short range repulsion, centrifugal and Coriolis forces[3,4]. Vibrational relaxation originates either in the dephasing of molecular vibrations or in the depopulation of vibrational levels, or sometimes a combination of two processes. The former process is analogous to the T_2-type spin-spin and the latter to the T_1-type spin-lattice relaxation in NMR[5].

In order to explain the mechanism of vibrational relaxation, one has to consider the coupling potential between the molecules and the bath, which includes rotational and translational degrees of freedom[3,4,6]. There are different mechanisms that may lead to coupling potential and contribute in this process. The dipole and multipole interactions, dispersion interactions, repulsive forces etc. are some of the important ones. The coupling potential V may be expanded in a Taylor series as a function of the normal co-ordinate Q,

$$V = V_0 + \left(\frac{\partial V}{\partial Q_i}\right)_0 Q_i + \frac{1}{2}\left(\frac{\partial^2 V}{\partial Q_i^2}\right)_0 Q_i^2 + \frac{1}{2}\sum_{i,j}\left(\frac{\partial^2 V}{\partial Q_i \partial Q_j}\right)_0 Q_i Q_j + \cdots\cdots \quad ..(2.1)$$

The first three terms are similar to the potential of a harmonic oscillator corresponding to a normal co-ordinate Q_i. By choosing the zero of energy so that the energy of the equilibrium configuration is zero, V_o may be eliminated. The last term is responsible for the resonant energy transfer from one oscillator to another and this is the term which leads to different shifts of the isotropic and anisotropic components of the Raman (vibrational) band. This frequency splitting is known as Anisotropy shift or non-coincidence effect.

The Hamiltonian has the form

$$H = H_o + H_B + V, \qquad \ldots\ldots\ldots(2.2)$$

where H_o is the Hamiltonian for the vibrational degrees of freedom (independent harmonic oscillator in the scattering volume), H_B is the bath Hamiltonian (translational and rotational degrees of freedom) and V is the coupling potential. The interaction potential V provides for the coupling of the oscillators to the bath and to one another. Before going into the details of perturbing potential we may discuss in brief the harmonic oscillator.

2.1a. The vibrational energies of a harmonic oscillator

The classical Hamiltonian for the harmonic oscillator described[7] by a single co-ordinate x and a parameter depending on the masses and structure of the system is given by the expression,

$$H = \frac{p_x^2}{2m} + \tfrac{1}{2} kx^2 \qquad \ldots.(2.3)$$

The motion of the harmonic oscillator is governed by the Hooke's law that the force is - kx. The px is the momentum conjugate to the co-ordinate x. The expression (2.3) is the quantum mechanical Hamiltonian for the system if the variables px and x satisfy the quantum condition $[q_i, p_i] = i\delta_{ij}$, which they do if $p_x = -i\frac{\partial}{\partial x}$. Two variants of our basic Hamiltonian are,

$$H = \tfrac{1}{2}(p^2 + \omega^2 \Omega^2), \qquad \ldots\ldots (2.4)$$

where $\Omega = \sqrt{m}\, x$ and $\omega = \sqrt{k/m}$, and $H = \tfrac{1}{2}\omega(p^2 + q^2)$ ....(2.5)

where $q = \sqrt{m}\, x$. A general simple harmonic oscillator expression may be written as,

$$H = \alpha p^2 + \beta q^2, \qquad \ldots\ldots (2.6)$$

where the associated frequency $\omega = 2\sqrt{\alpha\beta}$ or $\alpha\beta = \tfrac{1}{4}\omega^2$. The Hamiltonian (2.4) is closely related to the general expression for vibrational energy in terms of normal co-ordinates.

The H represented by (2.5) may be factorized as $H = \tfrac{1}{2}\omega(F^{\pm} F^{\mp} \mp 1)$ where $F^{\pm} = q \pm ip$ are the shift operators. F^{+} ladders down through eigenfunctions which have eigenvalues successively reduced by units of ω. The set of functions $|, \psi_n\rangle$ has a lower bound function with an energy $\tfrac{1}{2}\omega$ known as zero point energy. Laddering up by successive applications of F^{-} allows us to generate the infinite sets of eigenfunctions each separated by energy quanta of ω. Note that

$$\int \psi^* \psi \, d\tau \equiv (F^{+} |\, v\rangle)^{\dagger} F^{+} |v\rangle = \langle v | F^{-} F^{+} | v \rangle$$

$\ldots\ldots (2.7)$

The general energy-level expressions can be written as,

$$E(v) = \omega(v + \tfrac{1}{2}), \qquad \ldots.(2.8)$$

where we can now specify the eigenfunction by a quantum number v. The diagonal matrix of H may be determined, where $\langle v/H/v \rangle = E(v)$ which can be written

H	$\|0\rangle$	$\|1\rangle$	$\|2\rangle$	
$\langle 0 \|$	$\omega/2$	0	0	.
$\langle 1 \|$	0	$3\omega/2$	0	.
$\langle 2 \|$	0	0	$5\omega/2$	.
	.	.	.	.

$\ldots.(2.9)$

The matrix properties of p andq can be determined from those of $F^{\pm}$. We have

$$F^{+}|v\rangle = N_v|v-1\rangle \quad \ldots.. \quad (2.10)$$

Where N_v is a number. A self consistent set of numbers, N_v, can be determined for a normalised set of functions

$|v\rangle$ (i.e. $\langle v \mid v\rangle = 1$), $\langle v|F^{-}F^{+}|v\rangle = N_v^{*}N_v$ $\ldots.(2.11)$

Note that $F^{\pm}$ are not Hermitian and that $(F^{\pm})^{\dagger} = F^{\mp}$. It can be seen that $(N_v)^2 = \langle v \left| \frac{2H}{\omega} - 1 \right| v\rangle = 2v$ $\ldots\ldots(2.12)$

A similar procedure can be applied to derive the appropriate factor for F^{-}. Thus we see that

$$\langle v-1 \mid F^{+} \mid v\rangle = \sqrt{2v}\langle v+1 \mid F^{-}|v\rangle = \sqrt{2(v+1)} \qquad \ldots. \quad (2.13)$$

The matrix elements of p and q are now directly obtainable as $q = \frac{1}{2}(F^{-} + F^{+})$ and $p = \frac{1}{2}i(F^{-} - F^{+})$. The matrices can be

written as

$$\alpha \begin{bmatrix} 0 & \sqrt{1} & 0 & \cdot & \cdot \\ \sqrt{1} & 0 & \sqrt{2} & \cdot & \cdot \\ 0 & \sqrt{2} & 0 & \sqrt{3} & \cdot \\ 0 & 0 & \sqrt{3} & 0 & \cdot \\ \cdot & \cdot & \cdot & \cdot & \cdot \end{bmatrix} \quad i\alpha \begin{bmatrix} 0 & -\sqrt{1} & 0 & 0 & \cdot \\ 1 & 0 & -\sqrt{2} & 0 & \cdot \\ 0 & \sqrt{2} & 0 & -\sqrt{3} & \cdot \\ 0 & 0 & \sqrt{3} & 0 & \cdot \\ \cdot & \cdot & \cdot & \cdot & \cdot \end{bmatrix} \qquad (2.14)$$

The matrices of p and q are not diagonal but they are Hermitian. The matrix elements are obtained by having the convention satisfying $N_v = \ldots e^{i\delta}$ and in fact has been shown to zero. We would obtain the matrix of q imaginary instead of p if we had chosen an imaginary phase convention. The explicit expressions for the matrix elements are listed in

Table II.1 Matrix elements of q and q^2.

	$\langle v/q/v' \rangle$	$\langle v/q^2/v' \rangle$
$\langle v/q^n/v+2 \rangle$		$\alpha^2\sqrt{(v+1)\ (v+2)}$
$\langle v/q^n/v+1 \rangle$	$\alpha\sqrt{v+1}$	
$\langle v/q^n/v \rangle$		$\alpha^2(2\ v+1)$
$\langle v/q^n/v-1 \rangle$	$\alpha\sqrt{v}$	
$\langle v/q^n/v-2 \rangle$		$\alpha^2\sqrt{v(v-1)}$

$\alpha = \frac{1}{\sqrt{2}}$

In general the harmonic oscillator potential may be expanded in Taylor series in vibrational co-ordinate Q_i,

$$V = V_o + \left(\frac{\partial V}{\partial Q_i}\right)_o Q_i + \tfrac{1}{2}\left(\frac{\partial^2 V}{\partial Q_i^2}\right)_o Q_i^2 + 1/6\left(\frac{\partial^3 V}{\partial Q_i^3}\right)_o Q_i^3 + \ldots\ldots \quad (2.15)$$

The subscript zero indicates the position of minimum energy so that $\left(\frac{\partial V}{\partial Q_i}\right)_o = 0$. The quantity V_o is a constant independent of **Q** and may be ignored since it does not affect the vibrational frequencies (or the constant V_o may be taken as zero). The force constant $F_{\alpha\alpha}$ is defined by,

$$F_{\alpha\alpha} = \frac{\partial^2 V}{\partial Q_i^2} \quad \ldots\ldots (2.16)$$

The selection rule for a vibrational transition to be induced by electromagnetic radiation is

$$\Delta v = \pm 1, \quad \ldots\ldots (2.17)$$

where v is the vibrational quantum number. It can now be recognized that this implies that only for $\Delta v = \pm 1$, can $\langle n/\mu/m \rangle$ for a vibrational transition (from a state m to n) be non zero. μ may be equal to αE for Raman transition, α being the polarizability and E is the electric field.

2.1b. Anisotropy shift or non-coincidence effect:

Coming back to eqn. (2.1) for the coupling potential and considering the theory based on perturbation calculation, the frequency difference between the ground ($|0\rangle$) and first excited ($|1\rangle$) states can be written as,[3,8]

$$\Delta E = \left(\frac{\partial V}{\partial Q}\right)_0 (\langle 1/Q/1\rangle - \langle 0/Q/0\rangle) + \tfrac{1}{2}\left(\frac{\partial^2 V}{\partial Q^2}\right)_0 (\langle 1/Q^2/1\rangle - \langle 0/Q^2/0\rangle) + \left(\frac{\partial^2 V}{\partial Q_i \partial Q_j}\right)_0 (\langle 1/Q/0\rangle)^2 + \ldots\ldots \quad ..(2.18)$$

The term $(\langle 1/Q/1\rangle - \langle 0/Q/0\rangle)$ represents mechanical anharmonicity and it vanishes for a harmonic oscillator; but in real molecules we deal with anharmonic oscillators. The second term contains the electrical anharmonicity which arises if dipole moment is not a linear function of normal co-ordinate Q. Let us consider the Hamiltonian for the vibrational degrees of freedom, Ho as,

$$Ho = F_{\alpha\alpha}\, Q^2 + F_{\alpha\alpha\alpha}\, Q^3, \qquad \ldots. (2.19)$$

where $F_{\alpha\alpha}$ is the principal force constant and $F_{\alpha\alpha\alpha}$ is the anharmonic force constant associated with the isolated molecule. For an isolated vibration of the diatomic molecule with reduced mass m_r, the quantum mechanical value is given as:

$$(\langle 1/Q/1\rangle - \langle 0/Q/0\rangle) \propto \frac{h}{2m_r \nu_g} \left(-3\frac{F_{\alpha\alpha\alpha}}{F_{\alpha\alpha}}\right) \qquad \ldots.(2.20)$$

$$(\langle 1/Q^2/1\rangle - \langle 0/Q^2/0\rangle) \propto \frac{h}{m_r \nu_g} \qquad \ldots. (2.21)$$

where ν_g denotes the gas frequency. Therefore the frequency shift of the band relative to the unperturbed gas frequency, ν_g, is proportional to,

$$\Delta\nu = \nu - \nu_g \propto \frac{1}{2m_r \nu_g}\left[-\frac{3F_{\alpha\alpha\alpha}}{F_{\alpha\alpha}}\left(\frac{\partial V}{\partial Q}\right)_0 + \left(\frac{\partial^2 V}{\partial Q^2}\right)_0\right] \qquad \ldots. (2.22)$$

The usefulness of eqn. (2.22) to interpret the experimental data will require the assumption for the functional radial and angular dependence of V. It has to be then averaged over the configuration space. These type of calculations are almost impossible and approximate results can be best obtained through computer simulation studies. For most of the liquids the computer simulations are much more complicated. In order to examine eqn. (2.22), it must be extremely simplified. It has been shown by Drickamer and co-workers[9,10] that dispersion and dipolar forces produce a red-shift (decrease in frequency) whereas repulsive forces lead to blue shift (increase in frequency).

For highly polar molecules the interaction energy for the two interacting dipoles (Fig. 2.1) of dipole moments μ_i and μ_j is given by the relation:

$$V = \left(\frac{\mu_i \mu_j}{R_{ij}^3} - 3 \frac{(\mu_i \cdot R_{ij})(\mu_j \cdot R_{ij})}{R_{ij}^5} \right),$$

or $$V = \frac{\mu_i \mu_j}{R_{ij}^3} K_{ij} \quad , \qquad \ldots\ldots (2.23)$$

where $K_{ij} = [-2 \cos\theta_i \cos\theta_j + \sin\theta_i \sin\theta_j \cos(\phi_i - \phi_j)]$

$\ldots\ldots(2.24)$

is the orientation factor for point dipoles. This interaction energy will exceed the randomizing thermal energy, kT, for strong dipole-dipole type interactions and it may predominate

in neat liquid phase. If only pair interactions are considered and the first order term is the only one taken into account the frequency shift may be given as[3],

$$\Delta\nu \propto \left(\frac{K_{ij}}{R_{ij}^3}\right) \qquad \left(-\frac{F_{\alpha\alpha\alpha}}{F_{\alpha\alpha}}\ \mu\frac{\partial\mu}{\partial Q}\right) \quad \ldots.(2.25)$$

Since the evaluation of the factor $\frac{K_{ij}}{R_{ij}^3}$ is not possible the simplified proportionality relation may be written as,

$$\Delta\nu \propto F_{\alpha\alpha\alpha}\ \mu\ \frac{\partial\mu}{\partial Q} \qquad \ldots.(2.26)$$

The frequency splitting may be observed in most liquids, besides the shifting of the frequency and the term $\left(\frac{\partial^2 V}{\partial Q_i\, \partial Q_j}\right)$. $Q_i\ Q_j$ is believed to be responsible for this feature. It is this term which couples the same vibrational mode of two different molecules i and j. The Raman band shape reflects the modulation of the oscillator force constant by intermolecular interactions. The $I_{iso}(\omega)$ reflects only the spherically symmetric average value of the potential, whereas $I_{aniso}(\omega)$ detects the angular dependence of the intermolecular potential. In view of these different dependences, the $I_{aniso}(\omega)$ and $I_{iso}(\omega)$ will not only exhibit different shapes, but their positions will also be shifted to different extents leading to a nonvanishing splitting factor

$$\delta\nu = \nu\ (\text{aniso}) - \nu\ (\text{iso}) \qquad \ldots.\ (2.27)$$

Although it has been shown by Wang and McHale[4,6] that the frequency splitting $\delta\nu$ can occur for any angular dependent

intermolecular interaction, we may limit our discussion to dipole-dipole coupling. The interaction leads to orientational order between molecules and causes a splitting of the vibrational mode into an in-phase and out-of-phase vibrations. The frequency of the completely polarized in-phase vibration is equal to the isotropic Raman line centre while the frequency of the depolarized out-of-phase vibration is nearly equal to the center of the VH band. The splitting factor for dipole-dipole coupling is given by the relation

$$\delta\nu = \nu\,(\text{out-of-phase}) - \nu\,(\text{in-phase})$$

$$\propto \left\langle \frac{K_{ij}}{R_{ij}^{3}} \right\rangle \left(\frac{\partial \mu}{\partial Q}\right)^{2} \qquad \ldots\ (2.28)$$

The angular brackets indicate an ensemble average which reflects the fact that for different relative orientations where the out-of-phase mode is active the anisotropic component of the band is shifted to various extents depending upon the magnitude of the orientational factor K_{ij}. Because of the fact that it is not possible to evaluate the factor $\left\langle \frac{K_{ij}}{R_{ij}^{3}} \right\rangle$ one has to be satisfied with the proportionality relationship,

$$\delta\nu \propto \left(\frac{\partial \mu}{\partial Q}\right)^{2} \qquad \ldots\ (2.29)$$

The quantity $\left(\frac{\partial \mu}{\partial Q}\right)^{2}$ is the square of the dipole moment derivative which is responsible for the infrared intensity of the vibrational band. Therefore $\delta\nu$ is proportional to the intensity of the IR band and this leads to the conclusion that the splitting will be large for vibrations which give

rise to strong IR bands. It has indeed been observed in many molecules.

2.2 Kubo lineshape and relaxation time

Kubo developed a general theory of relaxation processes that has been adapted to vibrational relaxation by several research workers[11-14]. Using this theory it can be shown that correlation functions that involve the process of "pure dephasing" are given by the following expression,

$$\phi_{pp}(t) = \exp\left[-\langle\omega^2\rangle \left\{ t\,\tau_c + \tau_c^2 \exp\left(\frac{-t}{\tau_c}\right) - \tau_c^2 \right\}\right] \quad \ldots\ (2.30)$$

The process of dephasing is orientation dependent unless the intermolecular potential is orientation independent (for example in case repulsive forces are predominant). The eqn. (2.30) can be modified in the two extreme cases of long and short times.

In case $t \ll \tau_c$ the oscillators vibrate with random phases in a "quasi-static" environment which has not had time to change. In this case the decay of $\phi_{pp}(t)$ is expected to follow the Gaussian distribution of environmental interactions. One obtains the following relation:

$$\phi_{pp}(t) \simeq \exp\left(-\tfrac{1}{2}\langle\omega^2\rangle t^2\right) \quad \ldots\ (2.31)$$

For $t \gg \tau_c$ i.e. if time is much longer than the correlation time of the perturbation, it is evident that $\phi_{pp}(t)$ will be represented by an exponential,

$$\phi_{pp}(t) = \exp(-\langle\omega^2\rangle \tau_c t) = \exp\left(-\frac{t}{\tau_p}\right) \quad \ldots(2.32)$$

where $(\tau_p)^{-1} = \langle\omega^2\rangle \tau_c$ $\ldots(2.33)$

Therefore depending upon the rate of the modulation process (due to the fluctuations of the intermolecular potentials) one may predict the band profile.

In the limit $\tau_c \langle\omega^2\rangle^{\frac{1}{2}} \gg 1$, known as slow-modulation limit, the perturbation effectively lasts for a long time and the phase memory of the oscillators is rapidly lost. The $\phi_{pp}(t)$ function therefore decays rapidly and has essentially Gaussian form with a small long time exponential tail.

For rapid modulation ($\tau_c\langle\omega^2\rangle^{\frac{1}{2}} \ll 1$) the perturbation due to fluctuations in the intermolecular potential rapidly decays and the phase memory of the oscillators is retained for longer times. $\phi_{pp}(t)$ therefore decays more slowly and hence the band profile significantly narrows and for time $t > \tau_c$ an exponential decay is observed. The band profile is obtained by the fourier transformation of eqn. (2.32); $\phi_{pp}(t) = e^{-t/\tau_p}$ and has the Lorentzian shape given as,

$$I(\Delta\omega) = \frac{1}{\pi}\left\{\frac{\gamma}{\Delta\omega^2 + \gamma^2}\right\}, \quad \ldots. (2.34)$$

where $\gamma = \langle\omega^2\rangle \tau_c$, is the bandwidth of the band under consideration. Since $\tau_c\langle\omega^2\rangle^{\frac{1}{2}} \ll 1$ it follows that $\gamma \ll \langle\omega^2\rangle^{\frac{1}{2}}$ and a "motional narrowing" is observed. However, at short times (high frequency displacements from the band centre) the $\phi(t)$ function will eventually reflect

a Gaussian distribution of intensity. It is necessary to retain the correct behaviour of band moments (because there is no definite second or higher moment for Lorentzian profile of the band).

Since τ_c represents a modulation time it is related to the time scale of the molecular fluctuations in the medium. The second moment measures the range of frequency distribution due to the various molecular interactions. The τ_c and $\langle\omega^2\rangle$ contain valuable information about the nature of the intermolecular potential.

2.3 Isotropic and anisotropic Raman bands

In case of the Raman spectra observed with the vertically polarized laser source, the parallel (I_{VV}) and perpendicular (I_{VH}) components (Fig. 2.2) of the scattered light are related[2,11] to the isotropic and anisotropic parts of the scattering tensor by,

$$I_{iso}(\omega) = I_{VV}(\omega) - 4/3\ I_{VH}(\omega) \qquad \ldots\ldots (2.35)$$

$$I_{aniso}(\omega) = I_{VH}(\omega), \qquad \ldots\ldots (2.36)$$

where $I_{iso}(\omega) = \frac{1}{2\pi}\int_{-\infty}^{\infty} \langle \alpha(0)\alpha(t)\rangle \exp(i\omega t)\, dt$ .... (2.37)

or inversely,

$$\langle \alpha(0)\alpha(t)\rangle = \int_{-\infty}^{\infty} I_{iso}(\omega) \exp(-i\omega t)\, dt \quad .... (2.38)$$

Similarly, the Fourier transform of the normalized $I_{VH}(\omega)$ band gives

$$\langle \mathrm{Tr}\,[\beta(o)\beta(t)] \rangle \langle \Omega(o)\Omega(t) \rangle = \int_{-\infty}^{\infty} I_{VH}(\omega) \exp(-i\omega t)\, dt, \qquad \ldots\ldots (2.39)$$

where β is the anisotropic part of the polarizability. The auto correlation function $\langle \Omega_i(o)\, \Omega_i(t) \rangle$ is usually known as the vibrational relaxation function, but it must be kept in mind that this function encompasses all non-orientational contributions to the decay of the total correlation function. This will include the various possible ways of vibrational relaxation and collision induced effects.

Although there may be some complicated factors that lead to problems in separating vibrational relaxation and the reorientational correlation functions, it has been shown that in case of polar Raman bands arising due to totally symmetric vibration, the vibrational and reorientational contributions may be separated and the bands for which the value of depolarization ratio, $\rho \approx 0$ there is no contribution from the anisotropic part of the scattering tensor.

2.4 Raman activity:

The expression for transition moment for Raman transitions is given as

$$\int \psi_n \propto E \psi_m \, d\tau = E \int \psi_n \propto \psi_m \, d\tau \qquad \ldots\ldots (2.40)$$

For considering selection rule we are concerned with $\int \psi_n \alpha_{ij} \psi_m \, d\tau$. The selection rule for Raman scattering[15-19] may be stated as: " A transition between states (Fig. 2.3) characterized by the wave functions ψ_n and ψ_m is forbidden in Raman scattering unless for at least one of the components α_{ij} of the molecular polarizability tensors (i or j = x,y or z) the product $\psi_n \alpha_{ij} \psi_m$ belongs to a representation whose structure contains the totally symmetric species". The component α_{ij} transforms in the same way as does the product of the transformations T_i and T_j and the species of the components of α or in some cases some suitable linear combination of them are normally given in the point group character tables. It is therefore easy to read the selection rules for normal mode of vibration of any species.

The polarizability α is a tensor of nine components. The electric polarizability is a function of normal coordinate and this may be expanded in a Taylor series with respect to the normal coordinates. We thus obtain

$$\alpha = \alpha_o + \left(\frac{\partial \alpha}{\partial Q_k}\right)_o Q_k + \text{higher terms} \quad .... \quad (2.41)$$

This expansion is for the kth normal mode. Here α_o is the polarizability at the equilibrium configuration of the molecule. $\left(\frac{\partial \alpha}{\partial Q_k}\right)_{Q_k=0}$ is the derived polarizability (which is also for the k th normal mode) at equilibrium configuration. The condition for the normal mode k to be Raman active is that $\left(\frac{\partial \alpha_{ij}}{\partial Q_k}\right)_{Q_k = 0} \neq 0$, where i or j = x, y or z. If any one of

the components α_{xx}, α_{yy}, α_{zz}, α_{xy}, α_{yz}, α_{zx} is non-zero the vibration will be Raman active. The polarizability tensor is a symmetric one for normal Raman effect and therefore only six components have to be taken into consideration.

2.5 Theory of Raman effect.

The intensity of scattered light for a Raman transition between two states i and f of a scattering system is given by[20],

$$I = 10^8 \frac{\pi^2}{\epsilon_0^2} (\tilde{\nu}_0 \pm \tilde{\nu}_{fi})^4 I_0 \sum_{\rho\sigma} [\alpha_{\rho\sigma}]_{fi} [\alpha_{\rho\sigma}]^*_{fi} \quad \ldots\ (2.42)$$

where I_0 is the intensity of the incident radiation of wavenumber $\tilde{\nu}$, $\tilde{\nu}_{fi}$ is the wavenumber associated with the Raman transition $f \leftarrow i$, ϵ_0 is the permittivity of free space, and $[\alpha_{\rho\sigma}]_{fi}$ is the $\rho\sigma$ th element of the transition polarizability tensor,

$$[\alpha_{\rho\sigma}]_{fi} = \frac{1}{hc} \sum_r \frac{\langle f|\mu_\rho|r\rangle\langle r|\mu_\sigma|i\rangle}{\tilde{\nu}_{ri} - \tilde{\nu}_0 - i\Gamma_r} + \frac{\langle f|\mu_\sigma|r\rangle\langle r|\mu_\rho|i\rangle}{\tilde{\nu}_{rf} + \tilde{\nu}_0 + i\Gamma_r} \quad \ldots\ (2.43)$$

Here $\langle f|\mu_\rho|r\rangle$ is the ρ th component of the transition dipole moment associated with the transition $f \leftarrow r$, μ_ρ is the dipole moment operator in the ρ direction, and $i\Gamma_r$ is a damping factor related to the lifetime of the state r. The summation is over all states r of the system, with the exclusion of i and f, the initial and final ones. The coordinate suffixes ρ and σ refer to the molecule-fixed cartesian

vectors x, y and z and it follows that the transition polarizability tensor is of second rank, possessing nine components, which may conveniently be represented in matrix form

$$\begin{vmatrix} \alpha_{xx} & \alpha_{xy} & \alpha_{xz} \\ \alpha_{yx} & \alpha_{yy} & \alpha_{yz} \\ \alpha_{zx} & \alpha_{zy} & \alpha_{zz} \end{vmatrix}$$

The nature of the Raman effect is determined by the initial and final eigenstates $|i\rangle$ and $|f\rangle$ and by the proximity of the wavenumber of the exciting radiation to that of any electronic transition of the system, i.e. the magnitude of $|\tilde{\nu}_{ri} - \tilde{\nu}_o|$. It is possible to distinguish electronic and vibrational Raman effects from each other if the eigenstates $|i\rangle$, $|f\rangle$ and $|r\rangle$ are factorized into electronic and vibrational parts and substituted into eqn. (2.43). The Kramers-Heisenberg dispersion formula provides detailed knowledge of the selection rules, band intensities and polarization properties of electronic Raman scattering.

In the adiabatic Born-Oppenheimer approximation, the eigenstates $|i\rangle$, $|f\rangle$ and $|r\rangle$ may be expressed as products of electronic and vibrational states and if the system is initially in the ground electronic state g, we may write:

$$\begin{aligned} |i\rangle &= |gm\rangle = |g\rangle|m\rangle, \\ |f\rangle &= |an\rangle = |a\rangle|n\rangle, \\ |r\rangle &= |ev\rangle = |e\rangle|v\rangle, \end{aligned} \qquad \ldots\ (2.44)$$

where $|a\rangle$ and $|e\rangle$ are excited electronic states and m, n and v represent vibrational quantum numbers. This enables the transition polarizability to be written in the form

$$[\bar{\alpha}_{\rho\sigma}]_{an,gm} = \frac{1}{hc} \sum_{ev} \left[\frac{\langle n|[\mu_\rho]_{ae}|v\rangle \langle v|[\mu_\sigma]_{eg}|m\rangle}{\tilde{\nu}_{ev,gm} - \nu_0 + i\Gamma_{ev}} + \frac{\langle n|[\mu_\sigma]_{ae}|v\rangle \langle v|[\mu_\rho]_{eg}|m\rangle}{\nu_{ev,an} + \nu_0 + i\Gamma_{ev}} \right]$$

.... (2.45)

$[\mu_\rho]_{ae}$ is the pure electronic transition moment, $\langle a|\mu_\rho|e\rangle$, associated with the electronic transition a,← e. Under the conditions for which the adiabatic - Born - Oppenheimer approximation is valid, the dependence of such an electronic transition moment on the normal coordinates of the system, Q_k, is small. It may be expressed as a rapidly converging Taylor series expanded around the equilibrium position, the Herzberg - Teller expansion

$$[\mu_\rho]_{ae} = [\mu_\rho]^0_{ae} + \frac{1}{hc} \sum_{s \neq e} \sum_k [\mu_\rho]^0_{as} \frac{h^k_{es}}{\tilde{\nu}_s - \tilde{\nu}_e} Q_k + \cdots$$

.... (2.46)

where $h^k_{es} = \langle e | \frac{\partial H}{\partial Q_k} | s \rangle_k = 0$

s being a second excited state. The zero superscripted transition moments refer to their values at the equilibrium position, defined by $Q_k = 0$ for all k. Higher order terms in the Taylor expression are normally sufficiently small to be neglected

Substitution in eqn. (2.45) and simplification of the resulting expressions taking into account that the electronic transition moments and the integral h^k_{es} do not, under the conditions for which Born-Oppenheimer approximation is valid, operate on the vibrational wavefunctions, we, therefore, may write,

$$[\bar{\alpha}_{\rho\sigma}]_{an,\ gm} = A + B + C + D, \qquad \ldots. \quad (2.47)$$

The expressions for the A,B,C,D terms are given in Appendix .. In the ideal limit of the normal, i.e. non-resonance, Raman effect the wavenumber of the exciting radiation is far from that of any region of electronic excitation, that is $\tilde{\nu}_0 << \tilde{\nu}_{ev,\ gm}$ for all ev, and the following approximations may be made:

(1) The denominators in the transition polarizability are large and insensitive to the vibrational quantum numbers m, n, v. Differences between the various $\tilde{\nu}_{ev,\ gm}$ may therefore be neglected.

(2) The variation of Raman intensity with excitation wavenumber is governed solely by the $\tilde{\nu}^4$ dependence.

(3) Since $(\tilde{\nu}_{ev,\ gm} - \tilde{\nu}_0)$ and $(\tilde{\nu}_{ev,\ an} + \tilde{\nu}_0)$ are much larger than the damping factor, $i\Gamma_{ev,}$ the latter may be neglected.

(4) A large number of states s will be contributing to the B,C and D terms such that it is virtually impossible to determine the relative magnitudes of each contribution. For this reason, in the non-resonance situation we express

the Taylor expansion as

$$[\mu\rho]_{ae} = [\mu\rho]^{\circ}_{ae} + \sum_{k} [\mu\rho]'_{ae} Q_k \qquad \ldots\ (2.48)$$

where $[\mu\rho]'_{ae}$ incorporates the vibronic coupling of g, a and e to other states. It is a corollary of assumption (1) that, since the states v represent a complete orthonormal set, the sums in A, B, C, D terms may be evaluated by invoking the closure theorem provided that the v dependence may be stated as

$$\sum_{v} |v\rangle\langle v| \equiv 1 \qquad \ldots\ (2.49)$$

and arises from the matrix product rule

$$\sum_{j} A_{ij} \; B_{jk} = (AB)_{ik} \qquad \ldots\ (2.50)$$

Introducing these approximations leads to the following simplified equations for the contributions to the transition polarizability:

$$A = \frac{1}{hc} \sum_{ev} \frac{[\mu\rho]^{\circ}_{ae}[\mu\sigma]^{\circ}_{eg}}{\tilde{\nu}_{eg} - \tilde{\nu}_0} + \frac{[\mu\sigma]^{\circ}_{ae}[\mu\rho]^{\circ}_{eg}}{\tilde{\nu}_{ea} + \tilde{\nu}_0} \quad n/m \qquad \ldots\ (2.51)$$

$$B + C = \frac{1}{hc} \sum_{e} \sum_{k} \left[\frac{[\mu\rho]'_{ae}[\mu\sigma]^{\circ}_{eg} + [\mu\rho]^{\circ}_{ae}[\mu\sigma]'_{eg}}{\tilde{\nu}_{eg} - \tilde{\nu}_0} + \frac{[\mu\sigma]^{\circ}_{ae}[\mu\rho]'_{eg} + [\mu\sigma]'_{ae}[\mu\rho]^{\circ}_{eg}}{\tilde{\nu}_{ea} + \tilde{\nu}_0} \right] \langle n|Q_k|m\rangle \qquad \ldots\ (2.52)$$

$$D = \frac{1}{hc} \sum_{e} \sum_{k,k'} \left[\frac{[\mu\rho]'_{ea}[\mu\sigma]'_{eg}}{\tilde{\nu}_{eg} - \tilde{\nu}_0} + \frac{[\mu\sigma]'_{ae}[\mu\rho]'_{eg}}{\tilde{\nu}_{ea} + \tilde{\nu}_0} \right] \langle n|Q_k Q_{k'}|m\rangle \qquad \ldots\ (2.53)$$

For vibrational Raman scattering the transition terminates in the ground electronic state and therefore we put a = g in the above equations. Since n and m then become vibrational quantum numbers of the same (i.e. ground) electronic state the vibrational overlap integral, $\langle n/m \rangle$, can only be non-zero if n = m, in which case it has the value unity. This is a consequence of the orthonormality of $/n\rangle$ and $/m\rangle$ if they belong to the same electronic state and it follows that the A term may contribute to Rayleigh scattering but not to vibrational Raman scattering. The integral $\langle n/Q_k/m \rangle$ is non-zero if $n = m \pm 1$, and has the value $[h(m+1)/8\pi^2 c\tilde{\nu}_k]^{\frac{1}{2}}$ for $n = m + 1$ and $[hm/8\pi^2 c\tilde{\nu}_k]^{\frac{1}{2}}$ for $n = m-1$. Thus the (B+C) term is responsible for Stokes and anti-Stokes fundamental vibrational Raman scattering. The D term is responsible for the first overtone ($k = k'$) and binary combination tone ($k \neq k'$) vibrational Raman scattering, but is usually so small compared to the (B+C) term, that overtones and combination bands are rarely observed in normal Raman scattering). Higher order overtone and combination bands would, of course, be controlled by the higher terms in eqn. (2.48). Examination of the (B+C) and D terms reveals that when a = g (as it must for vibrational Raman scattering) the magnitudes of these terms are unchanged when the coordinate suffixes ρ and σ are transposed. It therefore follows that for vibrational Raman scattering excited off resonance $\alpha_{\rho\sigma} = \alpha_{\sigma\rho}$, i.e. transition polarizability

tensor is symmetric about the leading diagonal and has only six independent components.

2.6 The intermolecular potential functions

A simple pair potential for atoms is the hard-sphere function in which the atom is modelled by a hard sphere of diameter d (Fig 2.4a). The potential will be zero for $R > d$ and infinity for $R < d$ with a discontinuity at $R = d$, where R is the distance between the centres of the two atoms or molecules. The hard sphere potential when introduced into statistical theories, reproduces qualitatively many of the properties of a fluid: the thermal conductivity and viscosity are two examples and the value of d can be chosen to give the best fit to such properties. The particular properties mentioned are primarily dependent on the repulsive part of the potential and for such properties the van der Waals attractive well is not much important and therefore hard sphere model can successfully explain them. It should however not be implied that the hardsphere potential is an accurate representation of the potential.

It isnecessary to use a potential which has a minimum so as to obtain a liquid-gas phase change. The simplest potential which possesses this property is a combination of square well attraction (Fig. 2.4b) with the hard-sphere repulsion. Unfortunately this potential is longway from being a realistic

potential and its use in theories of fluids has been very difficult.

The potential which has been the basic one for many studies of atomic fluids and which is also reasonably close to the real potentials (Fig. 2.4c) has the following form [21,22],

$$U = 4\varepsilon \left[\left(\frac{d}{R}\right)^{12} - \left(\frac{d}{R}\right)^{6} \right] \qquad \ldots\ldots (2.54)$$

It is called the Lennard-Jones (L-J) potential after its originator. Many times it is referred as 6-12 potential being a member of the family given as,

$$U = A\left[\left(\frac{d}{R}\right)^{m} - \left(\frac{d}{R}\right)^{n} \right], \quad m > n \qquad \ldots. (2.55)$$

where m and n are integers. These potentials are zero at $R = \infty$ and $R = d$ and have a minimum at $R_{min} = d \left(\frac{m}{n}\right)^{\frac{1}{m-n}}$

$\ldots\ldots (2.56)$

of depth $U_{min} = A\left[\left(\frac{n}{m}\right)^{\frac{m}{m-n}} - \left(\frac{n}{m}\right)^{\frac{n}{m-n}} \right]$ $\ldots\ldots (2.57)$

For the L-J potential,

$$R_{min} = 2^{1/6} d$$

$$U_{min} = -\varepsilon$$

For large values of R the L-J potential is asymptotic to an R^{-6} curve and therefore it has the correct form to reproduce the long-range dispersion energy between closed shell atoms and molecules. For $R < d$ the first term in the potential dominates and making this proportional to R^{-12} ensures a sharp rise in the repulsive branch of the curve. There is no physical significance in putting m = 12, but a mathematical advantage

is there in having m = 2n for the evaluation of certain integrals that enter the calculation of fluid properties.

A most commonly employed potential (Fig. 2.4d) contains the exponential term and is given by the following relation

$$U = -\frac{A}{R^6} + B \exp(-CR) \quad \ldots\ (2.58)$$

which is usually called as the (exp-6) potential. The merit of this function is that both the long-range attraction and short range repulsion are functions that are supported by theoretical analysis.

Let us now consider potential curves which have no discontinuities in their derivatives e.g. 6-exp or 6-12. The most common potentials of this kind now used are those of Kitaigorodsky[23], Hendrickson[24], Liquori et al.[25], Scott and Scheraga[26], and Flory et al.[27]. There exists about ten other independent procedures for obtaining parameters of the potential curve, but they are less reliable.

The universal potential of Kitaigorodsky[28]

$$V(R) = 3.5 \left[8600 \exp\left(-13 \cdot \frac{R}{R_o}\right) - 0.04 \left(\frac{R_o}{R}\right)^6 \right] \quad \ldots\ (2.59)$$

contains only one parameter, the equilibrium distance R_o. Ramachandran et al.[28] have shown that even with such limitations on the 6-exp potential parameters, conformational calculations of peptides especially sugars yield quite good results. As shown in the case of universal potential[35] it is most important to

choose the R_o equilibrium distance. If the choice is good it only remains to find two parameters for the 6-exp potential and one for 6-12 potential. Two sets of parameters were considered. A, B and C satisfying the Kitaigorodsky potential i-e. K_1 and K_2. The first set K_1 was found assuming that $V(R) = 0$ when R is equal to the sum of the van der Walls radii. The second set K_2 is found on the assumption that in that point the potential curve has its minimum. The values of the minimum contacts between nonbonded atoms are given[28] in the Table II.2 and the equilibrium distances for the universal potential of Kitaigorosky are given in the Table II.3.

In case of crystals the closet atoms belonging to different molecules are as a rule located at distances shorter than equilibrium ones. Scott and Scherega[26] and Flory et al.[27] obtained R_o by adding 0.2Å to the mean value of the intermolecular contacts found by Bondii (the difference is likely to be 0.3 - 0.4 Å). These authors derived the second parameter indispensable to their potentials from some experimental data based on the theory of dispersion forces. In the case of 6-12 potentials the constants found i.e. A and R_o are sufficient where A is the coefficient at R^{-6} in the 6-exp or 6-12 potential.

Table II.2 Values of Minimum contacts between Nonbonded Atoms[a]

Type of contact	Normal limits (Å)	Extreme limits (Å)
H...H	2.0	1.9
H...O	2.4	2.2
H...N	2.4	2.2
H...C	2.4	2.2
O...O	2.7	2.6
O...N	2.7	2.6
O...C	2.8	2.7
N...N	2.7	2.6
N...C	2.9	2.8
C...C	3.0	2.9

Table II.3 Equilibrium Distances for the Universal Potential of Kitaigorodsky[b]

Interaction	R_o (Å)		Interaction	R_o (Å)	
	K_1	K_2		K_1	K_2
H...H	2.66	2.40	N...CH_3	3.78	3.40
H...N	3.06	2.75	O...O	3.33	3.00
H...O	3.00	2.70	O...C	3.56	3.20
H...C	3.22	2.90	O...CH_3	3.72	3.35
C...CH_3	3.39	3.05	C...C	3.78	3.40
N...N	3.44	3.10	C...CH_3	3.94	3.55
N...O	3.39	3.05	CH_3...CH_3	4.11	3.77
N...C	3.61	3.25			

Another very important type of potential which has to be taken into consideration is H-bonding type. In case of hydrogen bonding the H atom is partly bonded to two electronegative atoms most commonly N, O or halogen atom. The hydrogen is more strongly bound to one atom than the other. The main contribution to the binding energy comes from the electrostatic energy between the dipolar A-H bond and a partial negative charge on the electronegative atom B. For the stronger complexes, however, there is a significant contribution arising from the overlap of orbitals of A-H bond with those of B. This interaction leads to a partial transfer of electrons from B to the A-H bond.

A potential well for hydrogen bond can be described by a parabola cut off at the point of intersection with the abscissa or a curve of the Morse potential type etc. It appears probable that the arbitrary configuration of the potential will affect but slightly the results of the calculation of optimum molecular conformation or packings. The coordinates of the potential well bottom are the only parameters of importance.

As an example we take the use of OH-O bonding. If we consider atom-atom potential model the dependence of the hydrogen bond energy on the OH-..O angle is affected automatically. The deflection of the angle from 180° at constant O-H and

H...O distance results in a sharp rise of energy due to O atom repulsion.

The hydrogen bond potential curves has been studied by Lippincott Schroeder and particularly by Reid.[2,9] The O-H...O potential was treated as a sum of the three components: O-H interaction, H...O interaction, and O...O interaction. Reid's potential has the form,

$$V(r,R) = D_o \left[1-\exp\left(\frac{-n(r-r_o)^2}{2r}\right)\right] + CD_o \left[1-\exp\frac{-n(R_o-r-r_o)^2}{2c(R_o-r)}\right] + \frac{259.5}{R_o^6} - 4.55 \times 10^6 \; e^{-4.8 R_o} \quad \ldots (2.60)$$

where R_o is the equilibrium O...O distance, r is the O-H distance and r_o is the H...O distance. The constants are empirical in nature.

2.6a. The interacting multipoles

The potential energy V can be expressed in different ways[22] so far as the charge distribution of the interacting molecules do not overlap. The alignment theory of Keesom considers molecular attractions as a direct interaction between static multipoles within the molecule. The Keesom interaction is important whenever the molecules have permanent dipole moments. The alignment effect in its simplest form can be expressed by the potential energy V which takes the form,

$$V = \frac{-\mu_1\mu_2}{R^3}\left[-2\cos\theta_1\cos\theta_2 + \sin\theta_1\sin\theta_2\cos(\phi_1-\phi_2)\right]$$

$$+ \frac{3}{2R^4}\{Q_1\mu_2[\cos\theta_2 + 2\cos\theta_1 \sin\theta_1 \sin\theta_2 \cos(\phi_1 - \phi_2) - 3\cos^2\theta_1 \cos\theta_2] + \mu_1 Q_2[\cos\theta_1 + 2\cos\theta_2 \sin\theta_2 \sin\theta_1 \cos(\phi_1 - \phi_2) - 3\cos^2\theta_2\cos\theta_1]\} + \frac{3}{4R^5} Q_1 Q_2 \{1-5\cos^2\theta_1 - 5\cos^2\theta_2 - 15\cos^2\theta_1 \cos^2\theta_2 + 2[4\cos\theta_1 \cos\theta_2 - \sin\theta_1 \sin\theta_2 \cos(\phi_1-\phi_2)]^2\}$$

$$+ \frac{1}{2R^5}\{O_1\mu_2[(12 - 20\cos^2\theta_1)\cos\theta_1 \cos\theta_2 + (15\cos^2\theta_1 - 3)\sin\theta_1 \sin\theta_2 \cos(\phi_1 - \phi_2)]$$

$$+ \mu_1 O_2[(12-20\cos^2\theta_2)\cos\theta_1 \cos\theta_2 + (15\cos^2\theta_2-3)\sin\theta_2 \sin\theta_1 \cos(\phi_1-\phi_2)]\}$$

$$+ \text{ terms of order } R^{-6} \text{ etc.} \qquad \ldots\ldots (2.61)$$

where μ_1, Q_1 and O_1 denote the dipole moment, quadrupole moment and octupole moment respectively of molecule 1 and similarly μ_2, Q_2 and O_2 denote the corresponding moments of molecule 2. The θ and ϕ are the polar co-ordinates of the molecular axis as shown in Fig. 2. 1d.

The mean value of V is zero if all orientations of molecule are equally probable. The Boltzmann distribution function however increases the weight of attractive orientations and this therefore gives a potential energy which may be an appreciable fraction of the van der Waal's interaction energy.

2.6b. Dipole-dipole interaction

The strength of a dipole-dipole interaction depends on the separation of the dipole centers and their relative orientations. In order to derive an expression for the energies

involved, it is necessary to calculate only the energy of interaction between all pairs of charges and then to sum the results. The potential energy of interaction for the head-to-tail configuration depicted in Fig. 2.1a. for two identical dipoles with their centers separated by a distance R is given by[30]

$$U_{tot} = \frac{\mu^2}{l^2}\left[\frac{2}{R} - \frac{1}{R+l} - \frac{1}{R+l}\right] \quad \ldots\ldots (2.62)$$

For the parallel configuration of two identical dipoles as shown in Fig. 2.1b, the potential energy is given as

$$U = \frac{2\mu^2}{l^2}\left[\frac{1}{(R^2 + l^2)^{\frac{1}{2}}} - \frac{1}{R}\right] \quad \ldots\ldots (2.63)$$

The length of the dipole as well as the strength of the dipole moment is needed for the calculation. However, if $l << R$ and the term $(R^2 + l^2)^{-\frac{1}{2}}$ is approximated as $R^{-1}(1-\frac{1}{2}\frac{l^2}{R^2})$ the energy of interaction (Fig. 2.1a) is given as

$$U = -\frac{2\mu^2}{R^3} \quad \ldots\ldots (2.64)$$

In a general situation given in the Fig. 2.1(c), the interaction energy assumes the form

$$U = -\frac{\mu^2}{R_{12}^3}(2\cos\theta_1\cos\theta_2 - \sin\theta_1\sin\theta_2) \quad \ldots\ldots (2.65)$$

The above formula, however, is for a configuration where the dipoles rotate in one plane (e.g. the plane of the paper). In a three dimensional configuration where the dipoles with their orientations shown in Fig. 2.1d and angles defined,

the interaction energy

$$U = -\frac{\mu^2}{R_{12}^3}\,(-2\,\mathrm{Cos}\theta_1\,\mathrm{Cos}\theta_2 + \mathrm{Sin}\theta_1\mathrm{Sin}\theta_2\mathrm{Cos}\phi_{12}) \quad \ldots\ (2.66)$$

The molecules in a liquid are in random motion due to the thermal energy kT and their interaction energy with the electric field is given as $\mu \cdot E$ which is negative. In order to calculate the extent to which molecules are directed by the electric field E, we find out the average value $\mu\overline{\mathrm{Cos}\theta}$ along the direction of the field E where μ is the dipole moment of the molecule and θ is the angle between the dipole and the electric field E. The average value is given by the relation,[30,31]

$$\mu\ \overline{\mathrm{Cos}\,\theta} = \frac{\mu \int_0^{\pi} \mathrm{Cos}\theta\ e^{\mu E \mathrm{Cos}\theta/kT}\ \mathrm{Sin}\theta\, d\theta}{\int_0^{\pi} e^{\mu E \mathrm{Cos}\theta/kT}\ \mathrm{Sin}\theta\, d\theta} \quad \ldots\ (2.67)$$

Substituting $\frac{\mu E}{KT} = a$ and $\mathrm{Cos}\ \theta = x$

we get $\mu\overline{\mathrm{Cos}\ \theta} = \mu \dfrac{\int_{-a}^{a} e^{ax}\, x\, dx}{\int_{-a}^{a} e^{ax}\, dx} = \mu\, L(a), \quad \ldots\ (2.68)$

Where $L(a) = \left(\mathrm{Cotha} - \frac{1}{a}\right)$ is called the Langevin function and has a limiting value of 1 which is also expected as the maximum value of $\mathrm{Cos}\,\theta$ is 1. The exponential in the expression for $\overline{\mathrm{Cos}\ \theta}$ can be developed in the following series

$$\overline{\mathrm{Cos}\,\theta} = \frac{\sum_{n=0,2,4\ldots} \frac{n a^n}{(n+1)!}}{\sum_{n=1,3,5\ldots} \frac{a^n}{n!}} = a\,\frac{1/3 + 1/30\ a^2 + \ldots}{1 + 1/6\ a^2 + \ldots} \quad \ldots\ (2.69)$$

For small values of a, the quadratic and higher terms may be neglected and therefore $\overline{\cos\theta}$ is linear in E.

$$\overline{\cos\theta} = \frac{a}{3} = \frac{1}{3}\frac{\mu E}{kT} \text{ if } a \ll 1 \qquad \ldots\ldots (2.70)$$

However, for larger values of a we must take into account other terms in the series development for L (a).

$$L(a) = \frac{1}{3}a - \frac{1}{45}a^3 + \frac{2}{945}a^5 \ldots\ldots (2.71)$$

The function L(a) is compared with $\frac{a}{3}$ for small values of a and its deviation has also been tabulated (Table II.4). It can be seen that for a = 0.2, the deviation is only 0.3%. The approximation $L(a) = \frac{1}{3}\cdot a$ may therefore be safely used as long as $a = \mu E/kT < 0.1$ or $E < \frac{0.1\,kT}{\mu}$. The strengths of the electric field at room temperature (300°K) may be calculated which will satisfy this condition for a particular dipole moment.

For μ = 4 Debye, the value $\frac{0.1\,kT}{\mu} = 3\times10^5 \frac{V}{cm}$

In usual dielectric measurements the electric field E is much smaller than $10^5 \frac{V}{cm}$ and therefore the equation $L(a) = \frac{a}{3}$ may be used.

The polarising influence of the electric field appears in the average of Cos θ and does not appear as an appreciable change in the direction of the individual dipole moments. Normally $\overline{\cos\theta}$ is much smaller than 0.01 which means that if we could think of a picture of the dipole vectors of a number

of molecules at the certain time, it would be imposible to see in that picture that the dipoles prefer a certain direction. Only an accurate measurement of the angles θ would show that the value of Cos θ differs slightly from the zero.

Table II.4 The comparison of the function L(a) with a/3

a	L(a)	a/3
0.1	0.0333	0.0333
0.2	0.0665	0.0667
0.5	0.1640	0.1667
1.0	0.3130	0.3333
2.0	0.5373	0.6667

2.6c. Van der Waals type of interactions

The van der Waals theory[32,33] of intermolecular attractions deals with a situation where the molecules are separated large enough so that the electronic orbitals do not overlap. Depending on the nature of the molecules which are interacting, the van der Waals type of interactions may be classified into three classes.

(a) Keesom forces: Keesom forces relate to the dipole-dipole interactions. The interaction potential between the two molecules of dipole moments μ_i and μ_j and at positions R_i and R_j, which tends to align both molecules is given by,

$$V_{or}(R_{ij}) = \mu_i \cdot \nabla_i \nabla_j |R_i - R_j|^{-1} \cdot \mu_j \quad \ldots\ (2.72)$$

This orientation is the parallel alignment of the two molecules and is adopted at very low temperatures when the molecules are nearly at rest. The interaction energy for such a system can be written as,

$$U_{or} = -\mu_i \mu_j \frac{\partial^2}{\partial r^2} r^{-1} \Big|_{R_{ij}} = -2\frac{\mu_i \mu_j}{R_{ij}^3}, \quad \ldots\ (2.73)$$

for thermal energy, $kT \ll \frac{\mu_i \mu_j}{R_{ij}^3}$. The averaging over all orientations of the interaction energy is required if $kT \gg \mu_i \mu_j / R_{ij}^3$ and the interaction energy may then be calculated. The resulting expression for the interaction energy may be written as,

$$U_{or} = -\frac{2\mu_i^2 \mu_j^2}{3\,kT\,R_{ij}^6} \quad \ldots\ (2.74)$$

where the orientational effect of both the dipoles have been considered leading to the doubling of the interaction energy. The orientation effect vanishes for molecules which do not possess permanent dipoles. Due to the thermal motion any alignment vanishes at high temperatures.

(2) Debye forces: Debye, in order to find the interaction which does not vanish with increasing temperature, pointed out that polar molecules not only align but also polarize each other. The induced dipole simultaneously rotates with the inducing dipoles and therefore the interaction energy is temperature independent. The interaction potential of the two dipoles μ_i and μ_j is

$$V_{ind}(R_{ij}) = -\tfrac{1}{2}\mu_i \cdot \nabla_i \nabla_j R_{ij}^{-1} \cdot \alpha_j \cdot \nabla_j \nabla_i R_{ij}^{-1} \cdot \mu_i \quad \ldots (2.75)$$

where α_j is the polarizability of molecule j.

If the molecule j also exhibits a permanent dipole μ_j, a potential similar to U_{ind} given above by eqn. (2.75), results by interchanging molecules i and j. At low temperatures, the permanent and the induced dipoles align along the joining vector R_{ij} to give an interaction energy

$$U_{ind} = -\frac{2(\alpha_j \mu_i^2 + \alpha_i \mu_j^2)}{R_{ij}^6} \quad \ldots . (2.76)$$

At high temperature all orientations contribute according to Boltzmann distribution, so that the interaction energy can be

written as,

$$U_{ind} = - \frac{(\alpha_j \mu_i^2 + \alpha_i \mu_j^2)}{R_{ij}^6} \quad \ldots\ldots (2.77)$$

With increasing temperature the induction effect decreases, but it does not vanish. Although, this effect explains the attractions even at high temperatures but fails to explain the attraction between non-polar molecules.

London (Dispersion) forces:

The existence of attractive forces as evident from the departures of all substances from the ideal gas law was a paradox for the classical physics. The explanation came through the quantum mechanical consideration as following. Everywhere in the space the quantized radiation is present and the photons are moving randomly. These moving photons are constantly scattered by any particle which are present so that the instantaneous dipoles are formed. These instantaneous dipoles are able to produce rapidly fluctuating fields which in turn polarize the other molecules. Consider that each instantaneous dipole $\mu_i^{inst.}$ of molecule i induces a dipole $\mu_j^{ind.}$ of molecule j. The interaction potential of both molecules is obtained by substituting the instantaneous dipole $\mu_i^{inst.}$ for μ_i into the eqn. 2.75 and averaging over the time

$$V_{dis}(R_{ij}) = - \tfrac{1}{2} \langle \mu_i^{inst.} \cdot \nabla_i \nabla_j R_{ij}^{-1} \cdot \alpha_j \cdot \nabla_j \nabla_i R_{ij}^{-1} \cdot \mu_i^{inst.} \rangle_{av}$$

$\ldots$ (2.78)

The coupling parameter between photons and molecules is the molecular polarizability α_i. The final expression for the dispersion forces can be expressed by,

$$U_{dis} = -\frac{3}{2} \frac{h\nu_i \, h\nu_j}{R_{ij}^6 h(\nu_i + \nu_j)} \alpha_i \alpha_j \quad \ldots\ldots (2.79)$$

Dispersion forces are often estimated based upon this simple formula, for the polarizabilities of most molecules are known. As to $h\nu_i$ and $h\nu_j$ it is found that energies corresponding to the ionization energies I_i and I_j often approximate them to a reasonable extent. The dispersion energy occurs between any two molecules and it increases with the increase in temperature. The relations between photon scattering and molecular interaction led to the name dispersion effect. This interaction is known as "London- van der Waals interaction" because the original quantum mechanical treatment was given by London. It is this dispersion type interaction which can explain the general additive attraction between arbitrary atoms or molecules. The orientation effect is not necessarily additive between three molecules and in many cases the third molecule may be repelled than attracted. The inductive effect is also greatly reduced when many molecules superimpose their polarizing field from different sides. It is for these reasons that orientation and induction effects are usually overshadowed by dispersion effects.

2.7 Diffusion properties of the molecular liquids

The molecular motions in a liquid are difficult to visualise as the molecules of a liquid are almost as close as in the crystalline solid. There is approximately 10% expansion on melting which leads to some looseness and randomness in the liquid structure[34]. The molecules of a liquid are in a potential well which is however, somewhat flattened one. This confinement is usually referred to as the "solvent cage effect". The molecule is considered as vibrating against the walls of the cage, that is against its immediate neighbours with occasional escape to the position adjacent to it. The solvent cage is depicted in the Fig. 2.5a where the molecules are shown as roughly spherical in shape. The cage model is supported by the successful treatment of diffusion in liquids in which the random diffusional motion of molecules in a liquid is taken to occur as a sequence of jumps from one position to another. The elementary jump distance s is about $2r_o$ where r_o is the radius of the molecule. The diffusion coefficient is given as

$$D = \frac{s^2}{2\tau} \qquad \ldots\ (2.80)$$

where τ is the average time between jumps, and it therefore has the value

$$\tau = \frac{s^2}{2D} \qquad \ldots\ (2.81)$$

If we treat the liquid as having a quasi-crystalline structure, with more or less definite molecular sites, it turns out that a somewhat more accurate treatment should give the relation

$$D = \frac{s^2}{6\tau} \quad \text{or} \quad \tau = \frac{s^2}{6D} \qquad \ldots\ (2.82)$$

For the small molecules a reasonable value of S which is taken as $2r_o$ is about 4Å. The solvent cage is a sufficiently loose one and the average vibrational energy is kT. Vibrations against the wall of the cage occur at intervals of h/kT or about 1.5×10^{-13} sec at 25°C. We may therefore conclude that the molecule in a solution vibrates about $2.5 \times 10^{-11} / 1.5 \times 10^{-13}$ or approximately 200 times against its immediate neighbours before escaping to a new position and new neighbours.

This picture is also applicable to solute molecules. The frequency with which two solute molecules A and B will by the process of diffusion accidently become neighbours may be obtained (Fig. 2.56). This process is known as encounter and the estimation of encounter frequencies is central to much of solution kinetics. However, the complicated structure of the liquid makes the problem quite difficult. Therefore, one may make the approximation that the molecules of the solvent and solute are of the same size and are also spherical in shape which then leads to about 12 nearest neighbours. On each jump the solute molecule finds about 6 new molecules. These considerations are of great value in studying the solute-solvent interactions.

2.8 Dielectric properties of materials.

The statistical mechanics provides a way of obtaining macroscopic quantities when the properties of the molecules and the molecular interactions are known[31]. In the statistical mechanical theories of dielectric constant, simplified models

are often used for the molecules and the intermolecular forces to make the calculations tractable. A molecule is normally represented by an ideal dipole and a scalar polarizability or by an ideal dipole in the centre of a dielectric sphere and the molecular interaction is taken to follow a hard-sphere or a Lennard-Jones potential. The system consists of a large number of molecules ($\simeq 10^{23}$) exerting long-range (dipole-dipole) forces on each other. The statistical-mechanical theories of dielectric constant start from the consideration that the polarization P is given by,

$$P = D - \epsilon_0 E, \qquad \ldots\ (2.83)$$

where $D = \epsilon_0 E$, in the dielectric material and P is also known as dipole density. The influence of higher multipole densities are neglected.

The polarization P may be divided into four categories depending upon the nature of the dipole moment which is established,

$$P = P_{or} + P_i + P_e + P_s \qquad \ldots\ (2.84)$$

The orientational polarization (P_{or}) is exhibited by the polar dielectrics and arises due to the orientation (rotation) of the dipoles in the direction of the electric field. The electric field introduces a certain amount of orderlines in the position of polar molecules which are in chaotic motion due to the

thermal energy associated with the molecules. The orientational polarization is therefore temperature dependent. This polarization (P_{or}) can appear only in gases, liquids and amorphous viscous bodies. The ionic polarization (P_i) arises due to the mutual displacement of ions and atoms. The time required for the process of ionic polarization is of the order of picoseconds. The electronic polarization occurs in all atoms or ions and is observed in all dielectric materials. The specific nature of the electronic polarization is that it occurs during a very brief interval of time (10^{-15} seconds). The space charge polarization (P_s) arises because of the presence of lower resistivity materials within the dielectric.

The induced dipole moment P of a polarized molecule is equal to the product of the polarizability (α) of the molecule and the intensity of the applied electric field E. However, the internal intensity of the field where the molecule exists surrounded by other polarised molecules is not equal to the external intensity of the field. The internal field also called the local field (E_{loc}) at any molecule is a geometrical sum of the external field (E_o) and the field E of dipoles created by the neighbouring molecules. This local field known as Lorentz field[31, 35-37] is given by

$$E_{loc} = E_o + 1/3 \frac{P}{\varepsilon_o} \qquad \ldots\ldots (2.85)$$

The polarization P in case of solids and liquids may be presented by the equation, $P = N \alpha E_{loc}$ .... (2.86)

where N is the number of molecules in a unit volume. The substitution of the value for E_{loc} leads to the formula for polarization as,

$$P = \frac{N\alpha . E_0}{1-N\alpha/3\epsilon_0} = \epsilon_0(K-1)E_0 \qquad \ldots\ (2.87)$$

Therefore the dielectric constant is a function of the density of the material through N and the polarizability.

$$K = 1 + N\alpha / (\epsilon_0 - N\alpha/3) \qquad \ldots\ (2.88)$$

The polarizability of the atoms (and molecules) of nonpolar matter in the CGS system of units is the magnitude of the order of the cube of the radius of the atoms. Therefore the magnitude,

$$4\frac{\pi}{3}\alpha = \frac{4\pi}{3} r^3 \qquad \ldots\ (2.89)$$

should represent the volume of the atoms or molecules.

The local microscopic field acting on a molecule will be a function of the macroscopic average field together with fields arising from its own induced dipole moment and those of neighbouring polarized molecules. The dipolar field intensity experienced by a neighbouring molecule will be of the order of $\mu/4\pi\epsilon_0 r^3$ where μ is the molecular dipole moment and r is a representative intermolecular spacing. In this way since $\mu = \alpha E$, then in order for $E_{loc} = E$ we must have

$$\frac{\alpha}{4\pi\epsilon_0 r^3} \ll 1 \qquad \ldots\ (2.90)$$

When the inequality of equation is not satisfied then $E_{loc} \neq E$. The local field acting on a specific molecule will be greatly influenced by the electric fields of other molecules. The local field E_{loc} may be calculated by considering the dielectric material to be composed of two regions, a small spherical region centered around the molecule for which the E_{loc} is to be calculated and the remaining part of the dielectric. The radius of the sphere is considered to be large in comparison with the dimensions of the dielectric material. The molecules within the spherical cavity are interacting like point parallel dipoles and the molecules outside the sphere are considered to form a continuous medium. The local field E_{loc} is given by,

$$E_{loc} = E_1 + E_2 \qquad \ldots\ (2.91)$$

where E_1 is the field intensity due to the material outside the sphere and E_2 is the field intensity due to dipoles inside the sphere. It can be shown than

$$E_1 = E + \frac{P}{3\epsilon_0} = \left(\frac{\epsilon+2}{3}\right)E \qquad \ldots\ldots\ (2.92)$$

where E is the externally applied electric field.

The calculation of E_2 is not so easy but it can be shown that if the molecules within the sphere form a simple cubic, fcc or bcc lattice about the central molecule of interest then $E_2 = 0$. This result also holds for a completely random arrangement of molecules within the sphere. For isotropic materials such as liquids $E_2 < E_1$ and to a good approximation

$$E_1 = \left(\frac{\epsilon+2}{3}\right)E \qquad \ldots\ (2.93)$$

so that one obtains

$$\frac{3(\epsilon-1)}{(\epsilon+2)} = \frac{N}{\epsilon_0}\alpha \qquad \ldots\ (2.94)$$

which on rearrangement leads to $\epsilon - 1 = \frac{N\alpha/\epsilon_0}{1 - N\alpha/3\epsilon_0}$ ....(2.95)

which predicts that as the density of the material approaches the value $N = \frac{3\epsilon_0}{\alpha}$, the permittivity tends to infinity so that a small applied field strength would result in an infinite polarization of the material. As no such effect is observed the equation is not valid. Onsager was the first to provide a satisfactory explation by replacing the cavity with one being of the same size as the molecule whose dipole moment μ is, assumed to occupy only a small region located at the centre of the molecule. According to this scheme, the local field takes the following form.

$$E_1 = \alpha E + \beta m \qquad \ldots\ (2.96)$$

where αE represents the cavity field and βm is the reaction field. The cavity field is that part of the local field that remains unaltered if the molecule in question has its dipole moment removed. The reaction field is the component of the local field that now results when the dipole moment is restored to the molecule. The dipole moment cannot contribute to its own local field directly but it can do so indirectly by inducing polarization in the neighbouring molecule which in turn modify the local field. This reaction field will have no orienting effect on the molecule since it will always be parallel to the

dipole moment μ. Following Onsager treatment, the local field is given by,

$$E_{loc} = \frac{3\epsilon E}{(2\epsilon+1)} + \frac{2(\epsilon-1)}{(2\epsilon+1)} \cdot \frac{N\mu}{3\epsilon_0} \quad \ldots\ (2.97)$$

The interaction terms corresponding to solute solvent interactions are usually calculated adopting Onsager's reaction field model which treats[38] the system as a rigid dipole moment μ at the centre of a spherical cavity of radius a immersed in a homogeneous (solvent) continuum with dielectric constant ϵ and refractive index n. The solvent acts on the solute molecule as an effective electric field, the reaction field F, arising from the orientation and inductive polarizations of the dielectric continuum by the solute dipole. The treatment is based on the expression for the reaction field, arising from both orientation and inductive polarizations of the solvent dielectric due to the solute's dipole:

$$F = \mu f_\epsilon, \quad \text{where} \quad f \equiv \frac{2}{a^3}\left(\frac{\epsilon-1}{\epsilon+2}\right) \quad \ldots\ (2.98)$$

The reaction field (F_{ind}) due solely to the induction polarization is given by a similar expression, with ϵ replaced by the square ofthe refractive index n (optical dielectric constant):

$$F_{ind} = \mu f_n, \quad \text{where} \quad f_n \equiv \frac{2}{a^3}\left(\frac{n^2-1}{2n^2+1}\right) \quad \ldots\ (2.99)$$

Thus, the effective field due to the orientation polarization, i.e. the contribution of the permanent solvent dipoles is:

$$F_{or} = F - F_{ind} = (f_\epsilon - f_n) = \frac{2}{a^3}\mu\left(\frac{\epsilon-1}{2\epsilon+2} - \frac{n^2-1}{2n^2+1}\right) \quad \ldots(2.10)$$

2.9 Effect of solvent on anisotropy shift

The anisotropy shift is related at least in a first approximation, to the permanent dipoles of the dissolved molecules[39]. Starting from this hypothesis and making the assumption of a coupling mechanism through transition dipoles McHale[6] derived theoretically the following expression for the anisotropy shift, $\delta\nu$:

$$\delta\nu = \frac{2\mu^2 (\partial\mu/\partial Q)_o^2}{25\,\pi^2\, c^2\, \nu_o\, KTd^3} \frac{No}{V_M}\, \phi\, S, \qquad \ldots\ (2.101)$$

where μ is the dipole moment, ν_o and Q are the wave number and the normal coordinate of the vibrational mode under consideration, d is the minimum intermolecular distance, No is Avogadro's number, V_M is the molar volume of the solute, and finally S is a screening factor for the interaction energy of two dipoles.

Actually S comprises two factors, S_p and S_t, related respectively to the interaction of permanent and transition[39] dipole. According to the dielectric model of Onsager - Frohlich, the first has the form[40]

$$S_p = \left(\frac{n^2 + 2}{2\epsilon + n^2}\right)^2 \epsilon \qquad \ldots\ (2.102)$$

where n is the refractive index of the solute and ϵ is the static dielectric constant of the medium. S_t has a similar form, except that ϵ is replaced by $\epsilon_\infty = n^2$, the dielectric constant at infinite frequency. Owing to the several approximations involved in the Onsager - Frohlich model, one should expect that the validity of eqn. (2.101) is limited to dilute solutions.

2.10 Simple and associated molecular liquids

The "simple liquids" may be considered as the liquids for which the orientation dependent interactions are smaller than the thermal energy kT[11]. This condition for dipolar intermolecular interactions may be given as (for identical molecules),

$$\mu^2 / R_{ij}^3 \ll kT, \qquad \ldots. (2.103)$$

where μ is the permanent dipole moment and R_{ij} is the intermolecular distance. The molecular interactions may be studied by determining the vibrational relaxation functions calculated from the isotropic part of the band profiles measured from spontaneous Raman scattering experiment. The parameters related to molecular interactions may, in case of Lorentzian band shape, be calculated using simple formulae given elsewhere.

The term "associated liquids" may be applied to liquids for which the orientation dependent intermolecular interactions are considerably greater than kT. The condition for non-random distribution of the molecules due to the effect of dipolar forces is fulfilled for strongly polar molecules. The influence of this effect on the isotropic part of the Raman band may be investigated by studying the solvent dependence of the line shape of the symmetric stretching vibration. The effects of resonant transfer of vibrational energy due to transition dipole-transition dipole interactions on the band shape are minimized as the solute molecules become separated.

There will, however, be an interaction between the polar molecules and the molecules of the solvent, and this interaction can be taken into account approximately using the form of the Lorentz local field given by eqn. (2.93). In this way eqn.(2.94) can easily be generalized to describe the permittivity of a mixture of molecules of various kinds.

References:

[1] D.W. Oxtoby, J. Phys. Chem. 87, 3028 (1983)

[2] J.G. Grasselli, M.K. Snavely and B.J. Bulkin, "Chemical Applications of Raman Spectroscopy" (Wiley, New York, 1981) p. 166.

[3] W. Schindler, T.W. Zerda and J. Jonas, J. Chem. Phys. 81, 4306 (1984).

[4] C.H. Wang and J. McHale, J. Chem. Phys. 72, 4039 (1980).

[5] J. Jonas, Acc. Chem. Res. 17, 74 (1984)

[6] J.L. McHale, J. Chem. Phys. 75, 30 (1981) and references therein.

[7] H.W. Kroto, "Molecular Rotation Spectra" (Wiley, London, 1975) p.2.

[8] D. Scheibe, J. Raman Spectrosc. 13, 103 (1982).

[9] A.M. Benson and H.G. Drickamer, J. Chem. Phys. 27, 1164(1957).

[10] R.R. Wiederhehr and H.G. Drickamer, J. Chem. Phys. 28, 311 (1958).

[11] J. Yarwood and R. Arndt in "Molecular Association", Vol.2, Ed. by R. Foster (Academic Press, London, 1979) p.267.

[12] S.M. George, H. Auweter and C.B. Harris, J. Chem. Phys. 73, 5573 (1980).

[13] B. Hegemann and J. Jonas, J. Chem. Phys. 79, 4683 (1983).

[14] T. Kato, J. Chem. Phys. 84, 3409 (1986).

[15] G. Herzberg, "Molecular Spectra and Molecular Structure, Part II - Infrared and Raman Spectra of Polyatomic Molecules" (Princeton, N, J, 1945).

[16] E.B. Wilson Jr., J.C. Decius and P.C. Cross, "Molecular Vibrations" (McGraw - Hill, New York, 1955).

[17] P. Gans, "Vibrating Molecules" (Chapman and Hall, London, 1975).

[18] G.M. Barrow, "Introduction to Molecular Spectroscopy" (MeGraw - Hill. International, Tokyo, 1964).

[19] L.A. Woodward, "Introduction to the Theory of Molecular Vibrations and Vibrational Spectroscopy" (Clarendon Press, Oxford, 1972).

[20] R.J.H. Clark and T.J. Dines, in"Advances in Infrared and Raman Spectroscopy", Vol.9, Ed. by R.J.H. Clark and R.E. Hester (Heyden, London, 1982) p. 282 and references therein.

[21] J.N. Murrell and E.A. Boucher, "Properties of Liquids and Solutions". (Wiley, Chichester, 1982) p. 31.

[22] H. Margenau and N.R. Kestner, "Theory of Intermolecular Forces" (Pergamon Press, Oxford, 1969)p. 1.

[23] A.I. Kitaigorodsky, Tetrahedron, 14, 230 (1961).

[24] J.B. Hendrickson, J. Amer. Chem. Soc. 83, 4537 (1961).

[25] P. De Santis, E. Giglio, A.M. Liquori and A. Ripamonti, Nature (London) 206, 456 (1965).

[26] R.A. Scott and H.A. Scheraga, J. Chem. Phys. 44, 8 (1966); 45, 2091 (1966).

[27] P.J. Flory, D.A. Brant and W.J. Miller, J. Mol. Biol. 23, 47 (1967).

[28] A.I. Kitaigorodsky, "Molecular Crystals and Molecules" (Academic Press, New York, 1973) pp. 388, 166 and references therein.

[29] C. Reid, J. Chem. Phys. 30, 182 (1959).

[30] R. Gabler, "Electrical Interactions in Molecular Biophysics" (Academic Press, New York, 1978) pp. 115, 156.

[31] C.J.F. Bottcher, "Theory of Electric Polarization", Vol. 1 (Elsevier, Amsterdam, 1973) pp. 161, 205.

[32] D. Langbein in "Springer Tracts in Modern Physics: Theory of van der Waals Attraction", Vol. 72, Ed. by G. Hohler (Springer - Verlag, Berlin, 1974) p.4.

[33] M. Karplus and R.N. Porter, "Atoms and Molecules"(Benjamin, California, 1970) p. 262

[34] A.W. Adamson," A Textbook of Physical Chemistry" (Academic Press, New York, 1973) p. 691.

[35] C. Kittel, "Introduction to Solid State Physics", (Wiley Eastern, New Delhi, 1976) p. 408.

[36] B. Tareev, "Physics of Dielectric Materials". (Mir Publishers, Moscow, 1975) p. 67.

[37] R. Pething, "Dielectric and Electronic Properties of Biological Materials" (Wiley, Chichester, 1979) p.3.

[38] N. Mataga and M. Ottolenghi in "Molecular Association", Vol.2. Ed. By R. Foster (Academic Press, London, 1979) p. 39.

[39] M.G. Giorgini, G. Fini and P. Mirone, J. Chem. Phys. 79, 639 (1983).

[40] P. Mirone, J. Chem. Phys. 77, 2704 (1982).

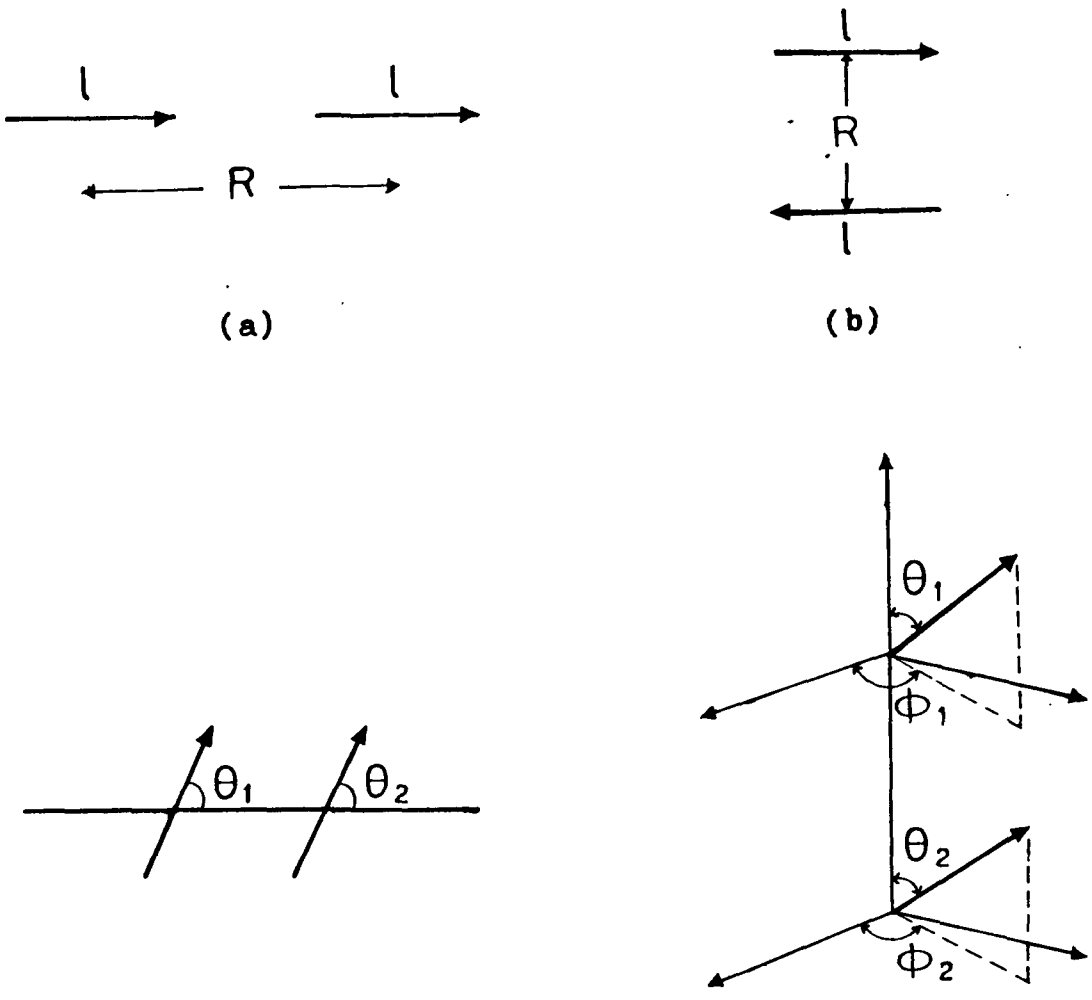

Fig 2.1 The orientational configuration of two dipoles: (a) Head to tail,(b) parallel, (c) Orientation of two dipoles with respect to a line passing through the dipole centres, (d) Generalized configuration of the pair of dipoles.

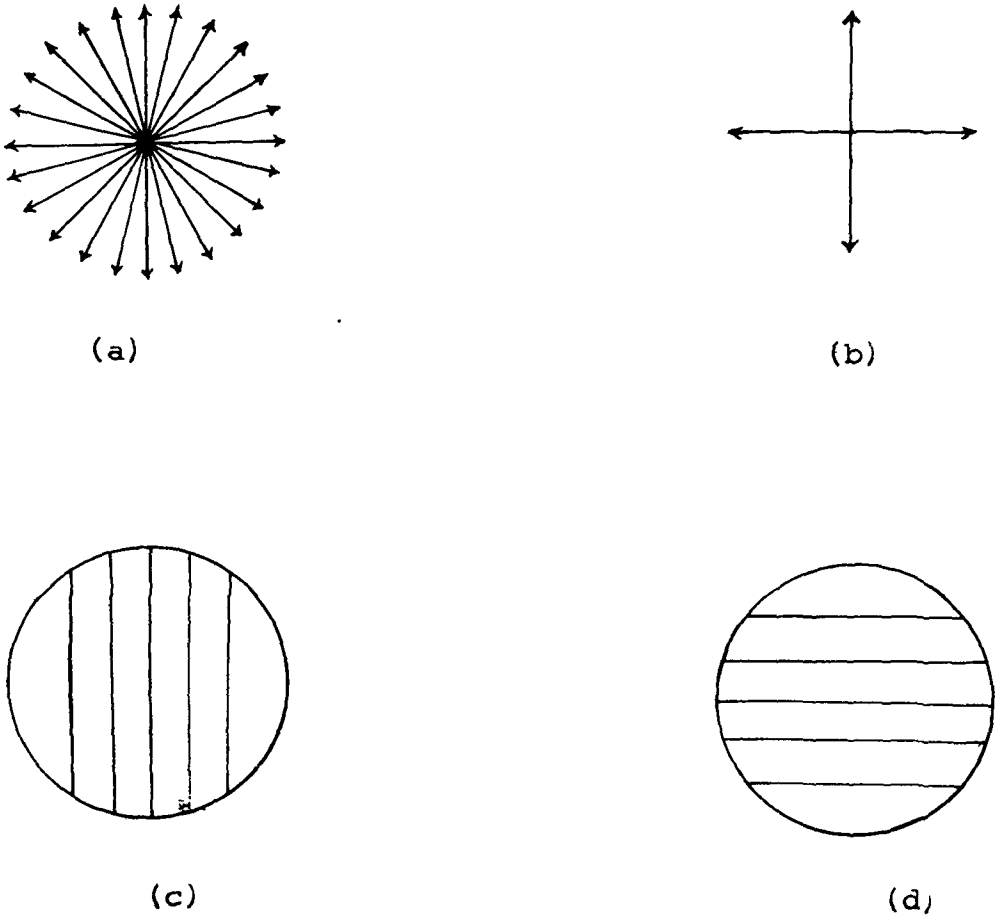

Fig. 2.2. End view of the scattered (unpolarized Raman radiation. The vibrations of the electric vectors are shown (a) unresolved, (b) resolved into linear vibrations perpendicular to each other, (c) Analyzer directed so that its vibrational direction is parallel to the laser electric field direction (E ∥ z). (d) Analyzer aligned with vibrational directions perpendicular to that of the electric field of laser.

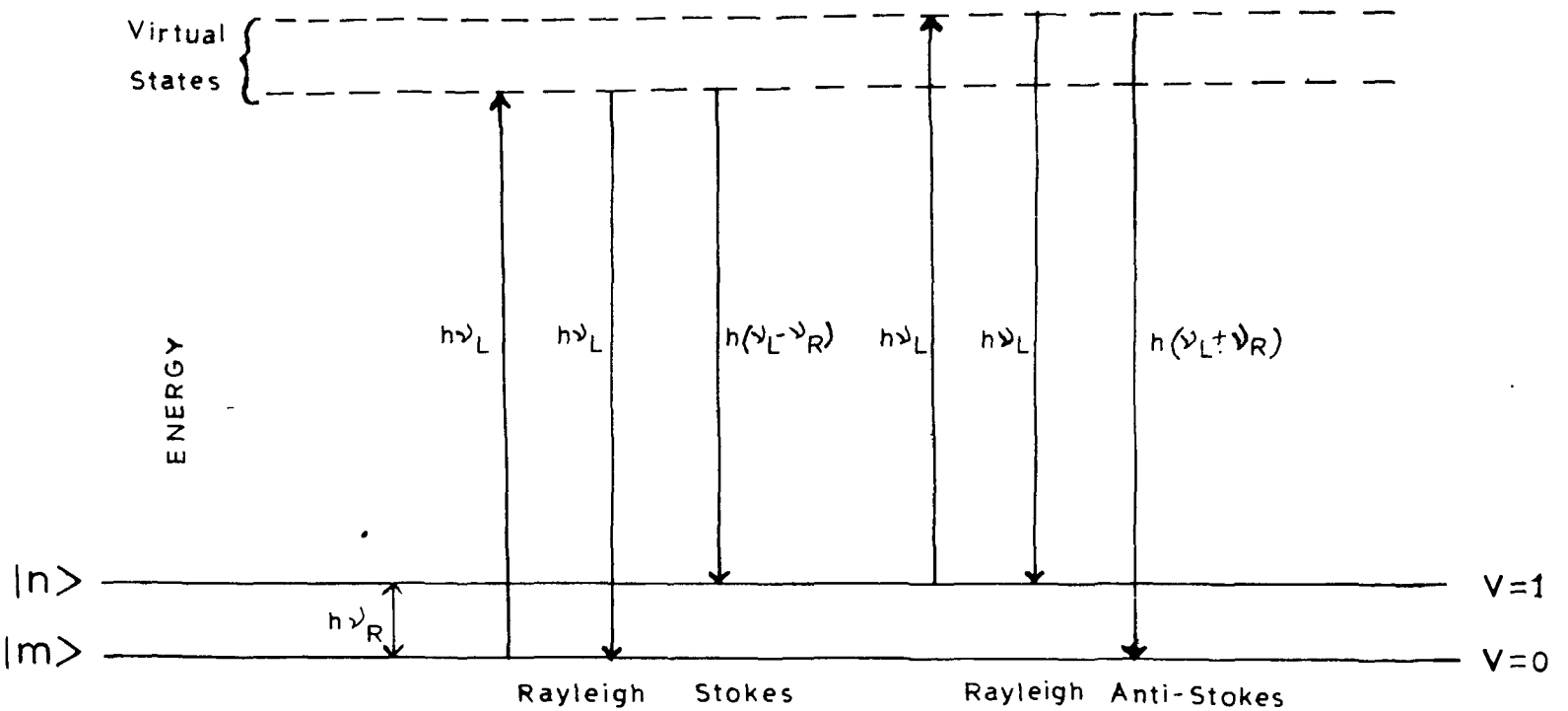

Fig. 2.3 Energy level diagram illustrating the fundamental processes of Raman scattering. The exciting line is of energy $h\nu_L$. Raman bands correspond to the energy $h(\nu_L - \nu_R)$ and $h(\nu_L + \nu_R)$.

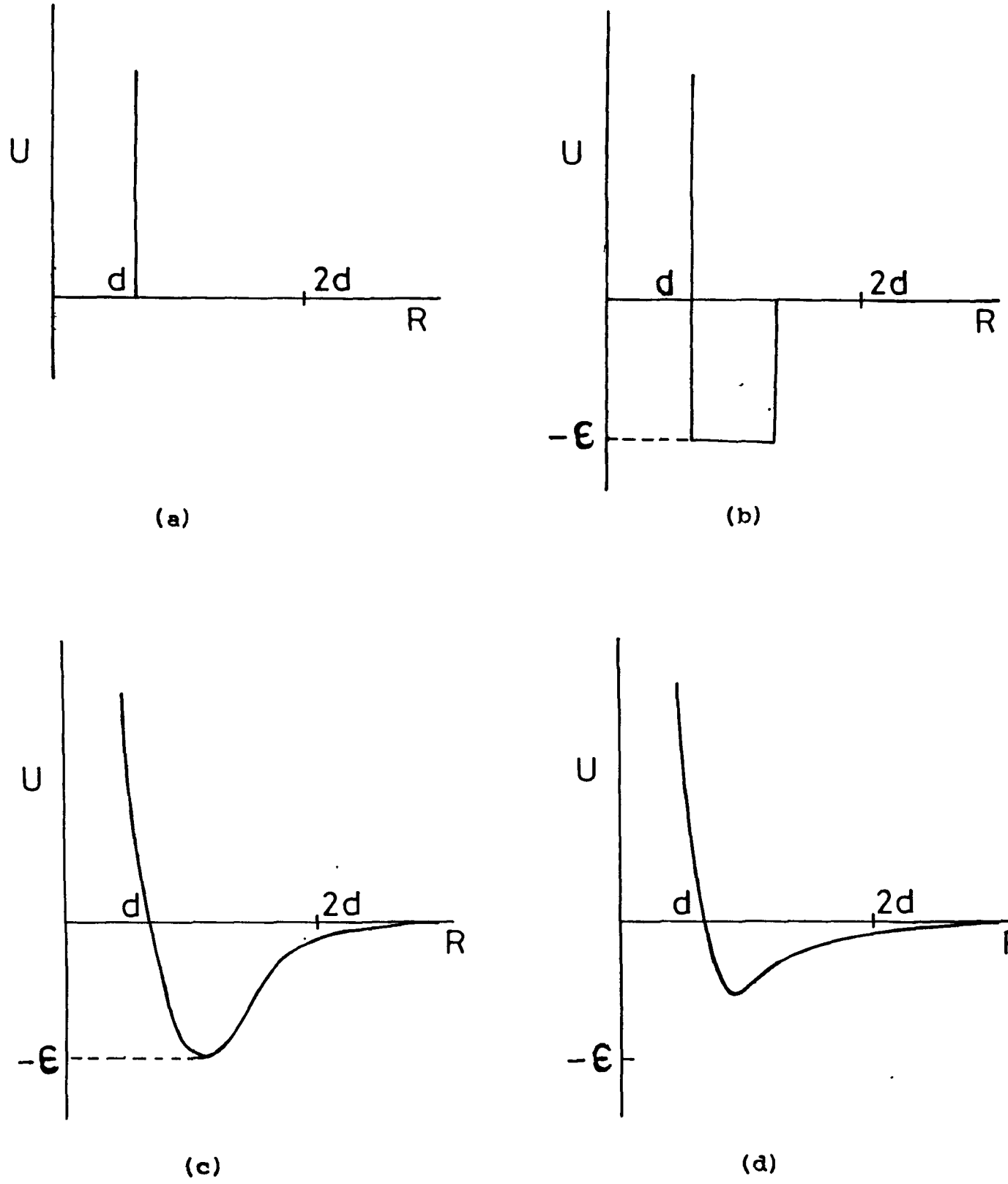

Fig. 2.4 A comparison of simple empirical potentials, (a) hard-sphere, (b) square-well, (c) Lennard-Jones, (d) (exp-6)

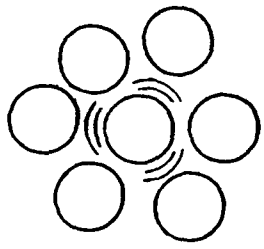

(a)

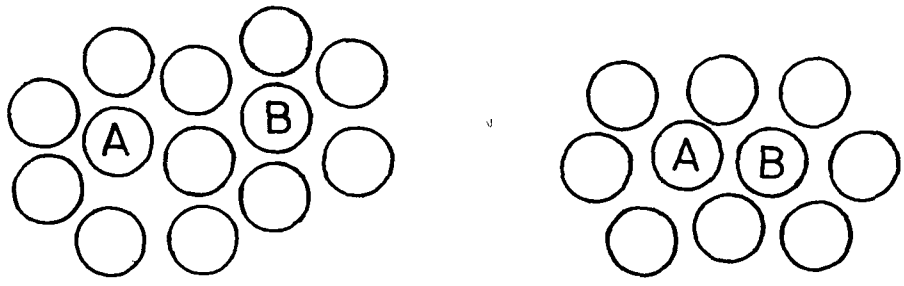

(b)

Fig. 2.5 (a) The solvent cage (b) Diffusional encounter between A and B molecules.

CHAPTER III

EXPERIMENTAL

3.1 Vibrational relaxation time measurement

The vibrational relaxation time can be obtained from the analysis of Raman band profiles of polarized and depolarized configurations, by calculating the intensity of the isotropic and anisotropic components using the standard relationships:

$$I_{iso}(\tilde{\nu}) = I_{vv}(\tilde{\nu}) - 4/3\, I_{VH}(\tilde{\nu}) \quad \ldots \quad (3.1)$$

$$I_{aniso}(\tilde{\nu}) = I_{VH}(\tilde{\nu}) \quad \ldots \quad (3.2)$$

The I_{VV} and I_{VH} components are defined as follows: Consider the laser light travelling along the Y direction and if X is the direction of observation then X - Y plane forms the scattering plane(Fig. 3.1). The direction of polarization of the laser light is normally taken perpendicular to this plane i.e. $\parallel$ Z direction. The scattered radiation is detected in two orientations by rotating the analyzer parallel to the direction of the incident radiation ($I_{ZZ} \equiv I_{VV}$) and perpendicular to the direction of the polarization of the incident radiation ($I_{ZY} \equiv I_{VH}$).

Assuming the band profile to be Lorentzian in shape the vibrational relaxation time (τ_v) can be calculated by the relation [1]:

$$\tau_v = (\pi c \Gamma_{iso})^{-1} \quad .... \quad (3.3)$$

where Γ_{iso} is the full width at half height (FWHH) of the isotropic component and c is the velocity of light. In order to accurately determine these quantities one must record the band profiles with as high spectral resolution as possible. The finite slit - width effect on the observed Raman linewidth was corrected according to the formula[2],

$$\delta_t = \delta_a \left[1 - \left(\frac{S}{\delta_a}\right)^2\right] , \quad ... \quad (3.4)$$

where δ_t is the corrected linewidth (FWHH), δ_a is the observed linewidth and S is the spectral slit - width.

3.2. Laser Raman experimental set up

The Raman scattering is a very weak phenomenon compared to Rayleigh scattering. Only a small fraction of photons are scattered by Raman scattering; so Raman lines are usually very weak ($\sim 10^{-6}$ of the intensity of the Rayleigh light). The majority of the scattered light is

similar to the original incident light in terms of photon energy. As the ratio of incident light to Raman scattered light sometimes exceeds 10^9, high spectral purity is needed to unveil weak Raman spectra. A double monochromator with high stray light rejection capability, good resolution and sensitive detection system with very low inherent noise is therefore required for Raman data collection. The small cross - section of the Raman scattering also demands a strong excitation source, preferably, a laser.

3.2a Source of excitation

In our laboratory Spectra - Physics model 165-09 Ar^+ laser, coherent radiation Innova - 90 K, Liconix model 4240 B He - Cd laser and Spectra - Physics model 365 dye laser, pumped with Ar^+ laser are available. In order to study the solvent dependence at very dilute concentrations, high powers are required. He- Cd laser with a power of about 80 mW (at 4416 Å) is suitable for neat liquids but for dilute solutions no remarkable spectra with good S/N ratio could be obtained. Since high powers were available with the 4880 Å and 5145 Å laser lines from Ar^+ laser only these two lines were used as the excitation source. The important characteristics of the Ar^+ laser are described below:

(a) Noise light control RMS, 10 Hz - 2 MHz 0.2%.

(b) Noise current control RMS, 10Hz - 2 MHz 1%.

(c) Stability light control in any 30 minute period after 2 hour warm up $\pm$ 0.5%.

(d) Stability current control in any 30 minute period after 2 hour warm up $\pm$ 3%.

(e) Frequency stability 60 MHz /^{o}C

(f) Beam diameter 1.25 mm at $1/e^2$ points for 514.5 nm.

(g) Beam divergence (full angle) 0.69 miliradian at 514.5 nm.

(h) Polarization - vertical.

The Raman spectrometer was a commercial one purchased from Spex industry, USA and the salient features of this spectrometer are described below:

3.2b. The double monochromator

The 1403 Spex Ramalog has a 0.85 - m focal length double monochromator with an aperture f/7.8 that selectively passes radiation on the basis of frequency of radiation. The discrimination of the spectrometer is a measure of the stray light inthe monochromator. Due to the low intensity of the Raman light it is esseatial that the level of the stray light is as low as possible. For this reason a double monochromator is always preferable to a single one because the stray light intensity in the former is reduced to about

the square root of that in the latter. To drive the spectrometer through the spectral region it has been provided with the DATAMATE - DM 1. The double monochromator (Fig. 3.2) has holographic gratings of 1800 gr/mm blazed at 5000 Å and there are four slits on it to pass the radiation. The entrance and exit slits primarily function to control resolution, while the two centre slits are responsible for blocking stray light from entering the second half of the monochromator. Slits may be set between 3 μm and 3 mm by twisting the barrel of micrometer atop the housing (1 div = 1 μm). On the entrance housing is a graduated push - pull slide to open the slit height to 0.2, 1 and 2 cm, or to position 3 Hartmann 1.2 mm apertures. The two central slits may be opened an additional 2 mm through an external control. Due to the double dispersion, this results in a 10 mm wide image at the exit slit.

The fundamental grating equation[3] as applied to Czerny - Turner mount (Fig 3.3) is

$$d (\sin \alpha + \sin \beta) = m \lambda \quad , \qquad \ldots\ldots \qquad (3.5)$$

where m = order, λ = wavelength, d = grating spacing, α = angle of incidence and β = angle of diffraction. In case of 1403 instrument this formula may be expressed as:

$$2d \sin \theta \cos \varphi = m\lambda \quad , \qquad \ldots \qquad (3.6)$$

where $\varphi = 10^{o}$; hence $\cos \varphi = 0.984$.

θ = grating rotation measured from zero, its position at the direct image, and the following relations hold:

$$\alpha = \theta + \varphi \ , \ \beta = \theta - \varphi \qquad \ldots \quad (3.7)$$

The theoretical resolving power of the grating is given as,

$$R_T = \lambda / d\lambda = \nu / d\nu = 2 \sin\theta \cos \varphi \ \frac{W}{\lambda} = mN, \qquad \ldots \quad (3.8)$$

where λ = wavelength, ν = wavenumber, N = total number of grating grooves, W = width of grating ruling and m = Order of diffraction.

These expressions are wavelength dependent , though if resolution is expressed as $\Delta\nu$, it is independent of the wavelength or frequency observed.

There are two factors which mainly influence the resolution. The first one is source of radiation; since resolution is a linear function of grating width (i.e. optical path difference), it deteriorates if the source illuminates less than the full width of the grating. As a consequence, the source or condensing lens should fully illuminate the collimating mirror. The second factor is the slit width; the slits seem to be the most important part of the spectrometer. The mechanical slit width is not the thing to be taken into account, instead one should think in terms of spectral band pass (spectral slit width). The band pass is a

function of reciprocal linear dispersion, which, in turn, depends on the wavelength, the grating constant, the focal length of the instrument and the spectral order. The spectral slit width

$$S = w\, D^{-1} = w \left[f \frac{d\theta}{d\lambda} \right]^{-1}, \qquad \ldots \quad (3.9)$$

where D^{-1} is the reciprocal linear dispersion, w is the mechanical slit width, f is the focal length of the collimator and $d\theta/d\lambda$ is the angular dispersion (rad / nm^{-1}). The linear dispersion is given by

$$D = \frac{\Delta x}{\Delta \lambda} = f \frac{d\theta}{d\lambda} \qquad .. \quad (3.10)$$

For example at 19435 cm^{-1} (5145 Å) the reciprocal linear dispersion for 1403 spectrometer (1800 gr/mm grating) is 10 cm^{-1}/mm. Thus a 50 μm slit will give a spectral band pass or slit width

$$S = 50 \times 10^{-3}\,mm \times 10\,cm^{-1}/mm = 0.5\ cm^{-1}$$

The tracking of a double monochromator refers to the angular coincidence of the two gratings as they are rotated. In 1403 instrument it is always such that wavelength settings in both halves of the spectrometer are better than the specified 1 cm^{-1} over 10000 cm^{-1} from 4000 - 9000 Å . With slits at 20 - 20 - 20 - 20 microns as compared to slits at 20 - 20 - 20 - 100 microns, total throughput is reduced to about 60%, but relative throughputs at various wavelengths are

hardly affected. The stability of the spectrometer is quite good over a one hour period. No measurable intensity change will occur if at least one of the slits is opened to 100 microns. If the exit slit is opened the double dispersion of the spectrometer is sacrificed. On the other hand, if an intermediate slit is opened the double dispersion is retained. In laser Raman spectroscopy the instrument is often slitless in effect because the focussed image is of the order of 50 microns at the entrance slit. Therefore widening of the entrance slit beyond 50 microns may have very little effect. The intermediate slits should be kept open wide enough to overcome the effects of wavelength drift. A minimum value of 100 microns in an environment without particularly good temperature and humidity control is advisable. In general, the intermediate slits should be at least 20% wider than the entrance and exit slit settings. The slit setting should be varied from scan to scan until the optimum balance of throughput and resolution are achieved.

The increasing of the height of a straight slit decreases the resolution. As the height of the slits is increased the ends of the entrance slit begin to pass portions of adjoining wavelengths. The effect of resolution is analogous to increasing the slit width. Therefore the height of the straight slits should be limited when maximum resolution is

required. The maximum throughput is attained whenever the source subtends at least as large a solid angle at the slit as does the collimating mirror in the spectrometer. In case of photoelectric detection, the detectors integrate energy over the entire irradiated area and as a consequence the total flux can be increased simply by increasing the slit height or width. In most cases this will increase flux at the detector as a quadratic function. When using photoelectric detection the combinations of slit widths and grating order can often pay large dividends in throughput.

The Table III.1 gives the approximate spectral band passfor 1800 gr/mm gratings in a 1403 spectrometer.

Table III.1. The relationship between the mechanical slit width and the spectral slitwidth for different excitation wavelengths

Spectral slitwidth (cm^{-1})	Mechanical slit width (μ)	
	For 5145 A excitation	For 4880A excitation
0.5	40	35
1.0	80	70
2.0	160	140
5.0	400	350

3.2c Collection of scattered radiation

A standard sampling platform is supplied with the Spex 1459 illuminator. The 1431B liquid cell of 1 ml. capacity with 1431 M holder was used for holding the sample. The sample is illuminated (Fig. 3.4) with laser radiation and then the laser focus control is adjusted until the brightest image is observed at the sample. The image of the sample scattered radiation is deflected on the target. The imaging of the scattered radiation on the entrance slit of the spectrometer is done by an elliptical collection mirror (f/ 1.4). The image is centered on the cross hairs with the lateral adjustments and focus adjustment is turned until the sharpest image is achieved. By rotating the swing away mirror counter-clockwise the sample scattered radiation is allowed to pass into the spectrometer. The signal is now peaked photoelectrically between the focus and lateral adjustment until the signal from the detector is maximum. In order to increase the scattering and collection efficiency spherical mirrors may be mounted above and behind the sample in the 1459 illuminator. Both mirrors increase the amount of scattered radiation that reaches the spectrometer entrance slit and therefore also increase the signal from the detector.

Two optical elements may be interposed in the beam, an analyzer and a scrambler, before it reaches the entrance slit. The analyzer is based on birefringence and

total reflection or on dichroism. The scrambler is a wedge of birefringent material. The two components of polarized light passing through it will be thrown out of phase as with a $\lambda/2$ plate. The retardation will vary from place to place and is not exactly $\lambda/2$; hence the emerging radiation will be depolarized. It cancels variations in spectrometer response that results from polarization dependent efficiencies.

The laser output is polarized perpendicularly, whereas the Raman radiation from the sample is depolarized. The analyzer interposed in pathway may transmit the light either perpendicularly polarized or parallel polarized, depending on the orientation of the analyzer. In both the cases the same scrambler is employed in front of the entrance slit of the monochromator to depolarize the radiation.

3.2d. The polarized and depolarized components of scattered light

In order to measure the depolarization ratio accurately, the polarization of the exciting laser beam is kept constant and the analyzer is placed after the sample.[4] Suppose the polarization of the laser beam is parallel to the Z axis (Fig. 3.1) and the direct transmission of the analyzer is turned from Y to Z direction to measure I_{VH} and

I_{VV} respectively. The intensity of the I_{VH} component is proportional to

$$I_{VH} \propto 3\,\gamma'^2 \qquad .. \qquad (3.11)$$

and that of I_{VV} component is proportional to

$$I_{VV} \propto (45\,\bar{\alpha}'^2 + 4\,\gamma'^2) \qquad ... \qquad (3.12)$$

where the factors $\bar{\alpha}'^2$ and γ'^2 are defined by the derivatives of the polarizability as,

$$\bar{\alpha}' = 1/3 \, (\alpha'_{xx} + \alpha'_{yy} + \alpha'_{zz}) \qquad .. \qquad (3.13)$$

$$\gamma'^2 = \tfrac{1}{2} [(\alpha'_{xx} - \alpha'_{yy})^2 + (\alpha'_{yy} - \alpha'_{zz})^2 + (\alpha'_{zz} - \alpha'_{xx})^2 + 6(\alpha'^2_{xy} + \alpha'^2_{yz} + \alpha'^2_{zx})] .. (3.14)$$

Since the constant factor is same for the fixed experimental conditions, the depolarization ratio is

$$\rho = \frac{I_{VH}}{I_{VV}} = \frac{3\,\gamma'^2}{45\bar{\alpha}'^2 + 4\gamma'^2} \qquad .. \qquad (3.15)$$

If the Raman scatter is known for the directions X and Z, its intensity in any direction φ of the X-Z plane may be calculated from

$$I(\varphi) = I_x \cos^2 \varphi + I_z \sin^2 \varphi \qquad .. \qquad (3.16)$$

The angle dependent intensities after the analyzer are:

$$I_{VH}(\varphi) \propto 3\gamma'^2 \qquad .. \qquad (3.17)$$

$$I_{VV}(\varphi) \propto (45\bar{\alpha}'^2 + 4\gamma'^2)\cos^2\varphi + 3\gamma'^2 \sin^2\varphi$$

$$= (45\bar{\alpha}'^2 + \gamma'^2)\cos^2\varphi + 3\gamma'^2 \qquad ... \qquad (3.18)$$

The observed depolarization ratio is

$$\rho_{obs} = \int_0^{\varphi} I_{VH}(\varphi)\, d\varphi / \int_0^{\varphi} I_{VV}(\varphi)\, d\varphi \qquad .. \qquad (3.19)$$

We may approximate ρ_{obs} by,

$$\rho_{obs} = \rho + \rho(1-\rho)\varphi^2/3 \qquad .. \qquad (3.20)$$

For $\rho << 0.75$, $\rho(1-\rho)\varphi^2/3$ is of the order of magnitude of ρ. Thus the measured depolarization ratio ρ_{obs} will be larger than the true depolarization ratio, ρ.

If an angle $\varphi = 10^{c}$ (= 0.175 rad) is need to measure a depolarization ratio of $\rho = 0.01$, in the case of highly polarized band, this method will produce a systematic error of

$$(1-\rho^2)\varphi^2/3 \simeq 10^{-4} \text{ or } 1\%$$

However, if a completely depolarized band is to be measured for which the depolarization ratio is $\rho = 0.75$, the systematic error by using the same collecting angle $\varphi = 10^{o}$ will be

$$0.19 \times 10^{-2} \text{ or } 0.3\%.$$

Therefore we see that measured depolarization ratio is always larger than the theoretically expected value.

3.2e. Photon counting detection

The detection system consists of a RCA C31034 - 02, 11-stage QUANTACON type photomultiplier tube (PMT) with S - 20 response in the photon counting mode. The C31034 - 02 is designed specifically for use at reduced temperatures e.g. - 30^{o}C. Cooling reduces the dark count caused by the thermionic emission to ~ 10 cps. The supply voltage is adjusted to provide a current amplification of ~ 10^{6}. Spex DATAMATE - DM1 is used for scanning the spectrometer and also for the acquisition of the data. The central processing unit (CPU) of the DATAMATE is a 8-bit microprocessor based ROM. The data can be processed in real time to subtract away background, take ratios, integrate or convert to logarithm for absorption states. DATAMATE photon counting results are expressed as and normalized to counts/sec. The DATAMATE also supplies HV (0-2000 volts D.C. - ve) to PMT. The HV is CPU selectable in 10 volts increment. The output current is variable from 0 to 2 mA. The linearity is better than 0.01% over full range. The noise level is 0.015% peak to peak at full load. The input in photon counting - DAM mode is -ve going pulse 0.1 mV amplitude or greater. The gain of the amplifier is 400 and

the rise time is 10 nsec. The pulse pair resolution is < 25 nsec. The discriminator is internally adjustable from 5 mV to 200 mV. The maximum count rate for photon counting is 25×10^6 Hz. The linearity and accuracy of the output data (Y-axis) is 0.3% full scale and resolution is one part in 4000.

3.3. Sample handling

In order to record spectra with good signal - to noise ratio, the cells should be clean and free from grease and finger-prints, as these can cause a considerable increase in fluorescent background of the spectrum and from air bubbles which increase the scatter of laser beam, thereby reducing the excitation efficiency and increasing the amount of laser radiation reaching the monochromator. The outside of the cell should be wiped with a tissue moistened with chloroform or acetone toremove as much dirt as possible before use.

Although the best signal - to - noise (S/N) ratio in the spectrum of a liquid is obtained when it is contained in a capillary cell, this method does not give good polarization results. The cell relies for its high efficiency on the multiple reflection of the Raman light from the walls, thus bringing a large proportion of it to collector lens. These multiple reflections, however, lead to the light becoming

depolarized to a considerable extent. This means that the measured value of the depolarization ratio, ρ , may be significantly different from the theoretically predicted value.

3.4. Resolution check

The resolution of the Raman spectrometer is checked by observing the symmetric stretching vibration, ν_1, of carbon - tetrachloride (CCl_4). There are so many Raman lines because of various naturally occuring isotopes of chlorine. CCl_4 containe 75.53% ^{35}Cl and 24.47% ^{37}Cl. Thus the naturally occuring CCl_4 is a mixture of $C^{35}Cl_4$, $C^{35}Cl_3{}^{37}Cl$, $C^{35}Cl_2{}^{37}Cl_2$, $C^{35}Cl^{37}Cl_3$ and $C^{37}Cl_4$. Resolving such closely spaced Raman bands requires a high resolution Raman spectrometer. If the resolution is not good A(462.4 cm^{-1}) and B(459,3 cm^{-1}) bands tend to overlap (Fig 3.5). One may measure the intensity at positions 1 and 2 to check the conditions of the spectrometer.

3.5. Calibration

The calibration of the spectrometer was done by using plasma lines from the Ar^+ laser in the neighbourhood of the Raman bands. The frequencies from standard measurement of the wavelengths of the Ar^+ laser plasma emission lines,[5] corrected to frequencies in vacuo were used for the calibration

purposes. The Ar^+ laser wavelengths and frequencies are given in Table III.2. Since for excitation purposes only 4880Å and 5145Å lines were used the plasma lines indicated in the table III.2. were used for calibration purposes.

Table III.2. The Ar^+ laser lines and their frequencies

Laser source	Wavelength (Å)	Frequency (cm^{-1}_{vac})
Argon ion laser lines	4579.36	21,830.99
	4657.95	21,462.66
	4726.89	21,149.64
	4764.88	20,981.02
	4879.86	20,486.68
	4965.09	20,135.00
	5017.17	19,926.00
	5145.27	19,429.91
Argon ion plasma lines	4932.8	20,267
	5287.0	18,909
	5305.8	18,842
	5397.8	18,521
	5403.0	18,503
	5496.0	18,190
	5559.0	17,984
	5607.0	17,830
	5650.7	17,692

3.6. Infrared spectral measurements

The infrared spectra were recorded using Perkin-Elmer model 983 IR spectrophotometer which consists of F 4.2 monochromator. It has four gratings and nine filters. The screen readout consists of digital display of wavenumbers, ordinate value, resolution, slitwidths and scan time. These parameters depend upon the mode number which may vary from mode 1 to 7. In order to study noncoincidence effect these spectral measurements are required as they give the idea about the transition dipole moment.

****

REFERENCES

1 K. Fukushi and M. Kimura, J. Raman Spectrosc. 13, 9 (1982).

2 K. Tanabe, Spectrochim. Acta, 40A, 437 (1984)

3 H.A. Strobel, "Chemical Instrumentation", (Addison - Wesley, Mass., 1973) pp 320 - 327.

4 C.D. Allemand, Applied Spectrosc, 24, 348 (1970).

5 J. Loader, " Basic Laser Raman Spectroscopy" (Heyden, London, 1970) pp. 31-35.

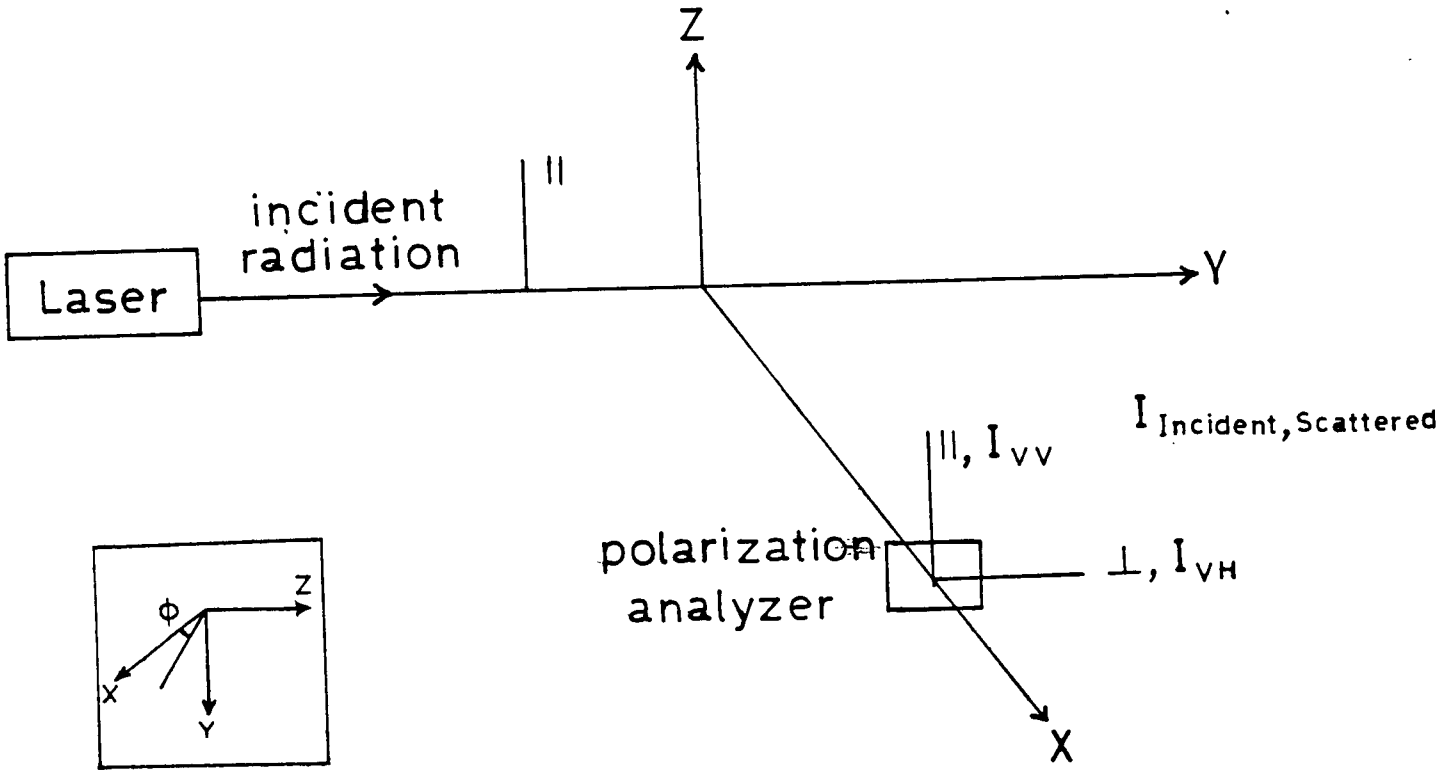

Fig. 3.1 Basic scattering diagram showing plane polarized ($\| z$) incident radiation detected at 90° geometry. The I_{VV} and I_{VH} represent the polarized (z axis $\|$) and depol.(x,y plane, $\perp$) Raman spectral components. The inset shows the angle of observation ϕ.

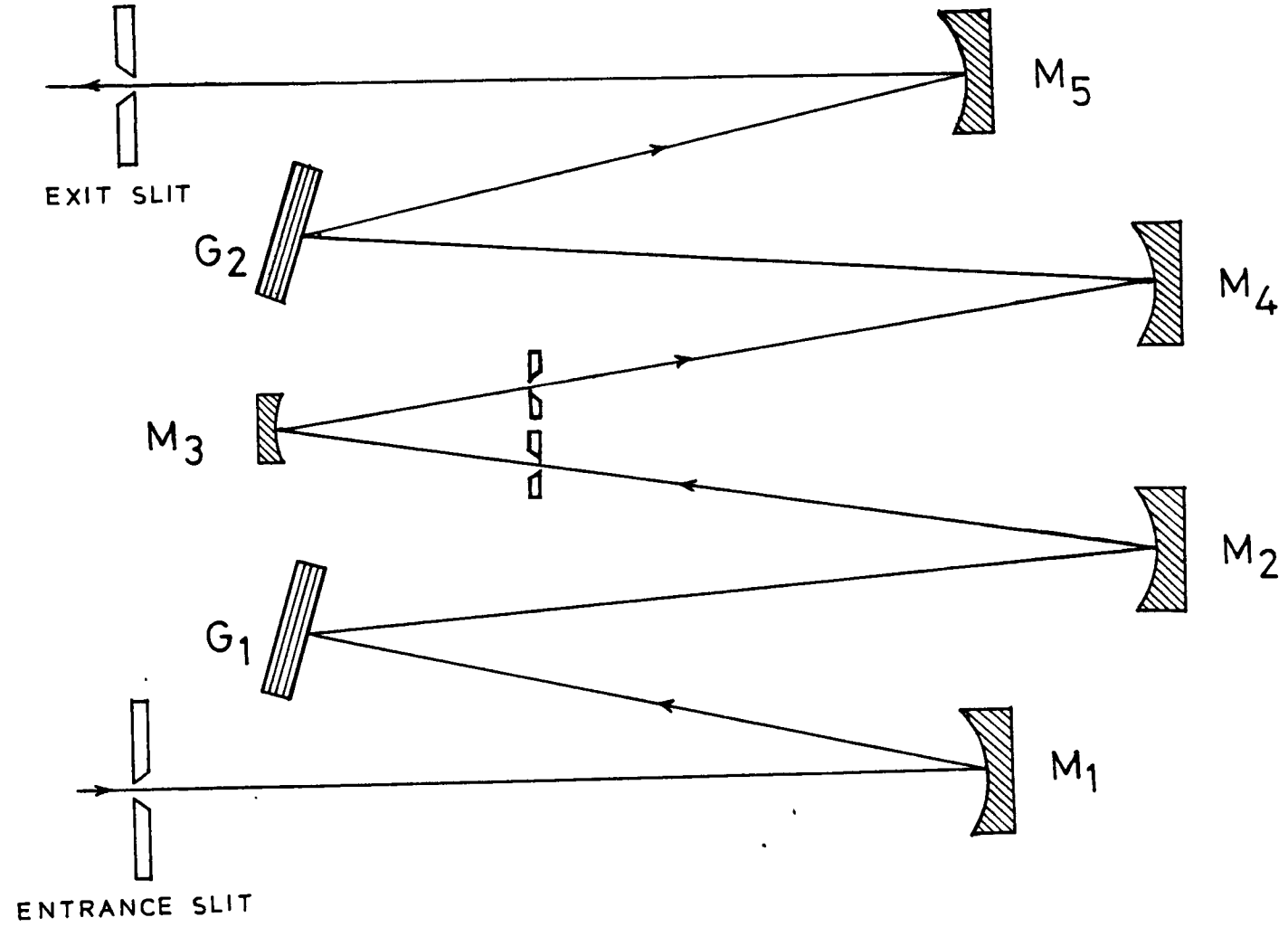

Fig. 3.2 The optical diagram of the double monochromator of spex 1403 Raman spectrometer

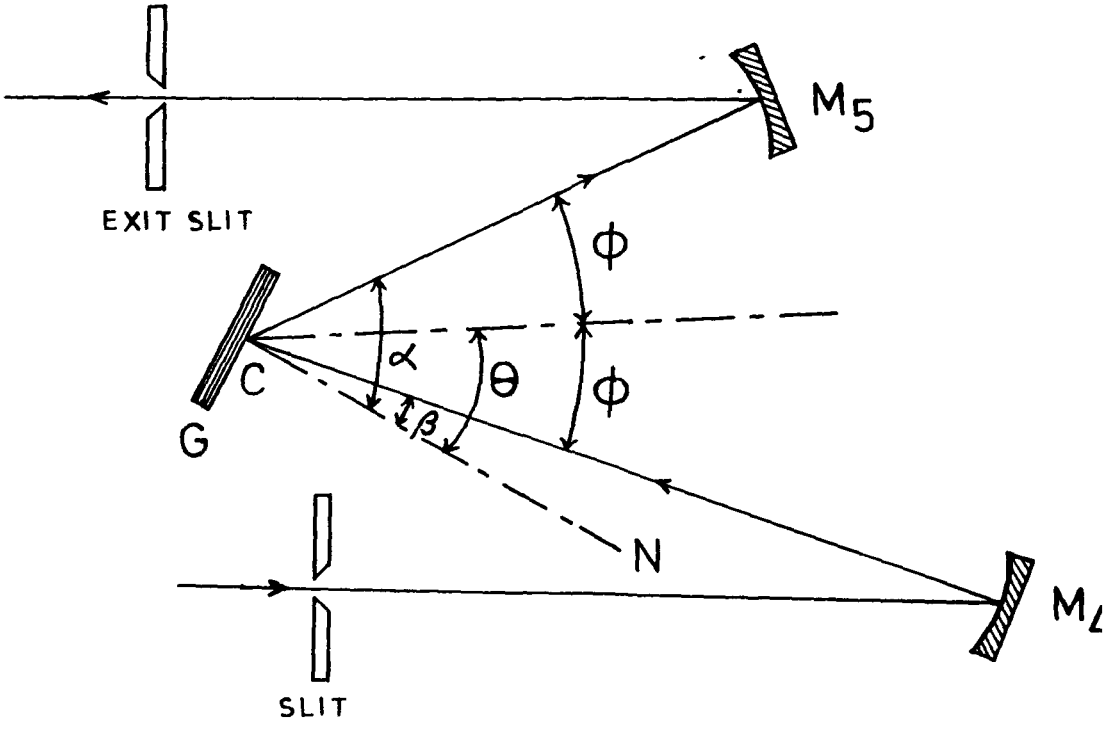

Fig. 3.3 The Czerny-Turner grating monochromator. To scan the grating is pivoted about point C and the angle ϕ is fixed.

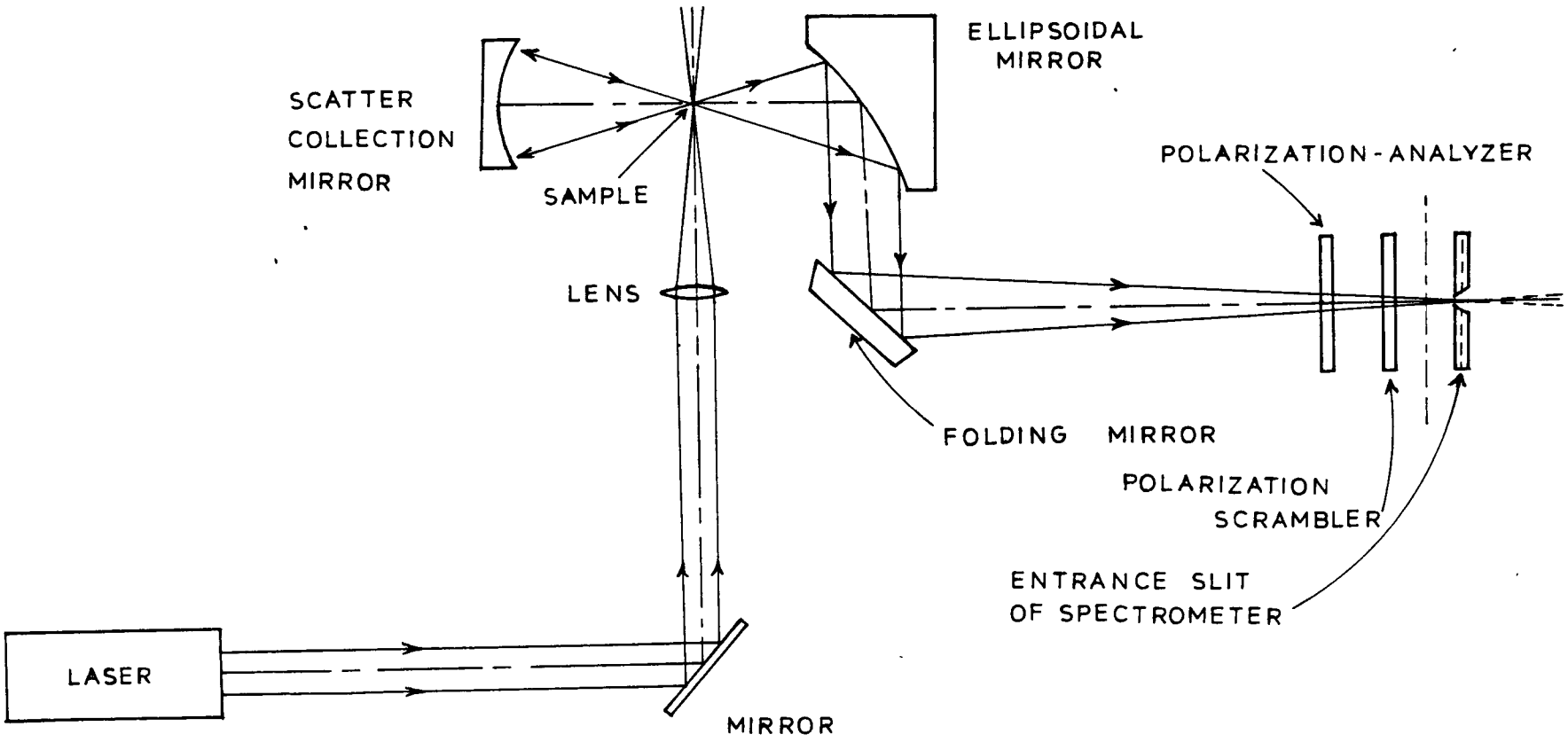

Fig. 3.4 The sample mounting, illumination, and the collection system geometry for the Raman scattered radiation.

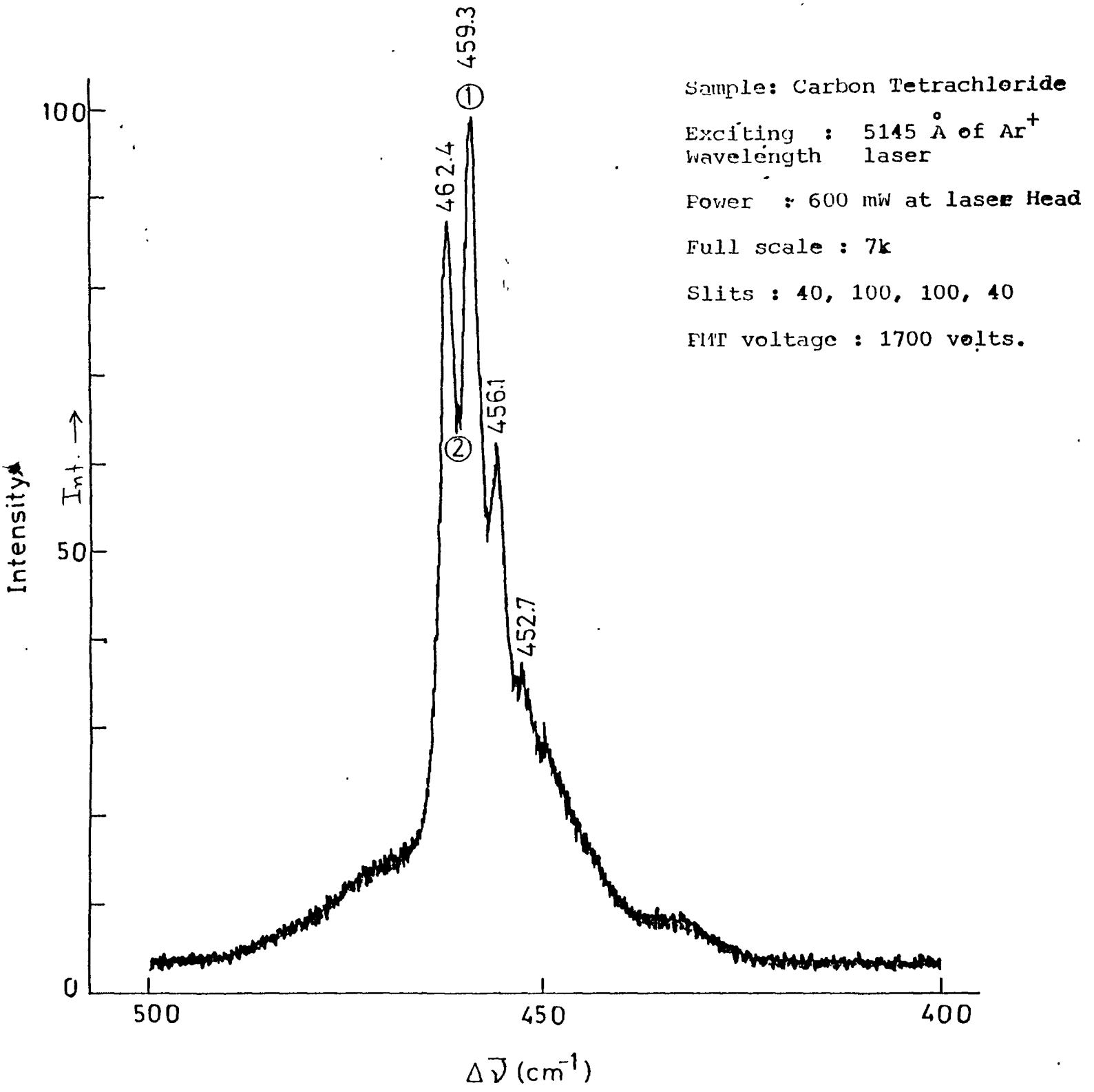

Fig. 3.5 The Raman spectrum of liquid carbon tetrachloride exhibiting well resolved peaks for the isotopic species.

CHAPTER IV

CHAPTER IV

VIBRATIONAL RELAXATION AND NONCOINCIDENCE EFFECT IN LIQUID N,N-DIMETHYLACETAMIDE*

ABSTRACT

The Raman linewidth and the non-coincidence effect in N,N-dimethylacetamide (DMA) molecule have been studied and explained in terms of molecular attraction parameters. The transition dipole-transition dipole (TD-TD) interaction is probably the predominant mechanism responsible for non-coincidence effect. The line broadening of the isotropic component is explained on the basis of dispersion type of interactions.

---

* Paper based on this work is to appear:

A. Purkayastha and K. Kumar, Spectrochim. Acta A (in press).

CHAPTER IV

4.1 Introduction

The isotropic and anisotropic components of the Raman spectrum of a liquid contain information about vibrational relaxation and reorientational motions. The analysis of the Raman spectrum of several molecular liquids indicate that the peak frequencies of the isotropic and anisotropic components of totally symmetric modes do not coincide. According to a model[1-3], which considers angular dependent intermolecular force, the neighboring molecules are oriented and form aggregates with a lifetime longer than the vibrational period. In case of polar modes, vibrational resonance coupling due to transition dipole-transition dipole (TD-TD) interactions may be the most important mechanism for perturbation of the vibrations. However inductive forces and dispersion forces etc. may also be important. The difference between the peak frequencies are expected to give information on the intermolecular forces and liquid structure.

The vibrational relaxation and reorientational motion have been studied for C=O stretching modes of few aldehydes and ketones[4,5]. Although noncoincidence effect has been observed for N,N-dimethylformamide[1], this important class of molecular liquids with strong interactions have not been investigated carefully from the point of view of relaxation

mechanism. In order to understand the mechanism of vibrational relaxation and reorientational motion in these biophysically important molecular systems, the N,N-dimethylacetamide (DMA) molecule (Fig. 4.1) was chosen. This molecule is free from hydrogen bonding in pure liquid and has a high dielectric constant and dipole moment. The measurements were made in the pure liquid and in solvents of varying dipole moment and dielectric constant as a function of concentration. These studies may be of considerable significance in understanding the mechanism of binding of small molecules to proteins particularly the Enzyme-substrate interactions. The interpretation of the experimental data has been carried out using molecular attraction parameters and simple theoretical models.

4.2 Experimental

The N,N-dimethylacetamide (DMA) and the solvents CCl_4, C_6H_6, $CHCl_3$ and CH_3CN were commercially available products and were used without further purification. Raman spectral measurements were made for the amide I band of DMA in the pure liquid and in solvents CCl_4, C_6H_6, $CHCl_3$ and CH_3CN. The experiments were performed using Spex Ramalog 1403 double monochromator with datamate and Spectra Physics model 165 Ar^+ laser as excitation source. The 5145 $\AA$ line was used with maximum power of about 1W. The polarization measurements were made by changing the orientation of the analyzer placed in the

scattered beam. The slit width was ~ 1 cm^{-1}. The accuracy of measurements is believed to be $\pm$ 1 cm^{-1}. Despite the small depolarization ratio ($\rho \simeq .15$) the isotropic line intensity was obtained using the usual formula $I_{iso}(\omega) = I_{VV}(\omega) - \frac{4}{3} I_{VH}(\omega)$. The infrared spectrum of liquid film of DMA was recorded using Perking Elmer 983 Infrared Spectrophotometer.

4.3 Results and Discussion

The information about vibrational relaxation and molecular reorientation processes can be obtained by the analysis of line-shapes of the isotropic and anisotropic components of Raman band of a liquid. The vibrational phase relaxation leads to broadening of the isotropic Raman lineshape[6,7]. In case of well separated vibrational transition when there is no overlapping with any other transition or hot bands there are three primary sources of line broadening. The first one is life-time broadening which is because of the finite lifetime of a quantum state. However in case of liquids where this broadening may be estimated, it generally makes a rather small contribution to the linewidth. It is therefore not considered here further. The second contribution to vibrational phase relaxation may be referred to as pure dephasing or environmental broadening. It arises from the fact that the vibrational frequency of a molecule is perturbed by its interaction with other molecules and therefore has a component $\Delta\omega_i(t)$, which fluctuates with time. If one considers the freezing of the environment at a particular time one would

observe a distribution of frequency shift and therefore a broadened lineshape. This is referred to as the static limit. However the time dependence of the environment is important and therefore the line is atleast partially "motionally narrowed" from the static limit.

The isotropic Raman lineshape may be quantitatively given by the fourier transform of the vibrational co-ordinate autocorrelation function, $\langle Q_i(t)\, Q_i(0)\rangle$, where the angular brackets define an ensemble average. The vibrational co-ordinate Q at a time t differs from $Q_i(0)$ by a phase factor $\exp[-i\{\phi_i(t)-\phi_i(0)\}]$. If we represent the fluctuations in frequency due to environment by $\Delta\omega_i(t)$ and define a characteristic time τ_c (the bath relaxation time) then the relationship between $\Delta\omega_i$ and τ_c is given by

$$\tau_c \equiv \int_0^\infty \frac{\langle \Delta\omega_i(t)\, \Delta\omega_i(0)\rangle}{\langle \Delta\omega_i^2\rangle}\, dt, \qquad \ldots.(4.1)$$

where $\langle \Delta\omega_i(t)\ \ \Delta\omega_i(0)\rangle$ is the autocorrelation function of $\Delta\omega_i$. The nature of lineshape depends on the relative magnitudes of the two characteristic frequencies $\langle \Delta\omega_i^2\rangle^{\frac{1}{2}}$ and τ_c^{-1}. When $\langle \Delta\omega_i^2\rangle^{\frac{1}{2}} \tau_c >> 1$, we have the static limit, while when $\langle \Delta\omega_i^2\rangle^{\frac{1}{2}} \tau_c << 1$ we have the rapid modulation limit where the line is narrowed to a Lorentzian with full width at half height (FWHH) given by,

$$\text{FWHH} = \langle \Delta\omega_i^2\rangle\, \tau_c \qquad \ldots.(4.2)$$

The third contribution to vibrational line broadening is resonant transfer or excitonic broadening which appears in pure liquids and decreases on dilution. When two identical molecules come together the energy levels which were earlier degenerate are likely to split with one moving higher and the other moving lower. Whenever a large number of molecules are brought together this split level takes the shape of an excitonic band. The resonant transfer contribution may be studied by isotropic substitution or by making use of solvents.

If it is possible to separate the vibrational degrees of freedom from bath degrees of freedom because of the separation in frequencies, the vibrations will respond almost adiabatically to the changes in environment. The coupling potential V [eqn. (2.1)] expressed in Taylor series as a function of normal co-ordinate is very small compared to H_o, the Hamiltonian for the vibrational degrees of freedom ($V \ll H_o$). Therefore the first order perturbation calculation for the energy difference (leading to frequency difference) between the ground and first excited states can be performed. The expression obtained is given by[3,7,8],

$$E = \left(\frac{\partial V}{\partial Q}\right)_o \left(\langle 1/Q/1\rangle - \langle 0/Q/0\rangle\right) + \tfrac{1}{2}\left(\frac{\partial^2 V}{\partial Q^2}\right)_o \left(\langle 1/Q^2/1 - 0/Q^2/0\rangle\right) + \left(\frac{\partial^2 V}{\partial Q_i \partial Q_j}\right)_o \left(\langle 1/Q/0\rangle\right)^2 + \ldots\ldots \quad \ldots.(4.3)$$

The main interaction term that couples the fundamentals of the νth mode of two molecules i and j can be written as

$$\Delta E_{res} = \frac{\partial^2 V_{ij}}{\partial Q_i \partial Q_j} \; Q_{o1i} \; Q_{o1j}, \qquad \ldots\ldots (4.4)$$

where $Q_{o1} = \langle 1/Q/0 \rangle$ is the expectation value of the normal co-ordinate in the transition state. Since for DMA the dipole moment $\mu = 3.82$ D, the dipole-dipole interaction predominates in the liquid phase. Considering only pair interactions and the first order term the frequency shift is expressed as

$$\Delta\nu \propto \left(- \frac{F_{\alpha\alpha\alpha}}{F_{\alpha\alpha}} \mu \frac{\partial \mu}{\partial Q}\right)\left(\frac{K_{ij}}{R_{ij}^3}\right) \qquad \ldots\ldots (4.5)$$

Since it is impossible to evaluate the average $(K_{ij}/R_{ij}3)$ for DMA, we will simplify eqn. (4.5) to the proportionality relation.

$$\Delta\nu \propto F_{\alpha\alpha\alpha} \mu \frac{\partial \mu}{\partial Q} \qquad \ldots (4.6)$$

The coupling potential may originate from various interactions such as dipole-dipole, transition dipole-transition dipole, quadrupole-quadrupole, hydrogen bonding etc. The angular dependent intermolecular force modifies the force constants of the harmonic oscillator, yielding an anisotropic frequency distribution and Raman bandshapes reflect the modulations. The isotropic Raman scattering process samples the average of this frequency distribution, while the anisotropy of the frequency distribution is detected by depolarized Raman scattering. The first spectral moments of the two scattering spectral components are necessarily different giving rise to a nonvanishing splitting

factor $\delta\nu = \nu(\text{aniso}) - \nu(\text{iso})$. As discussed by Mirone et.al.[1] and Döge and co-workers[5,9] we assume dipole-dipole coupling to be responsible for the interactions leading to orientational order between the DMAmolecules. This causes a splitting of the vibrational mode into an in-phase and out-of-phase vibrations. The frequency of the completely polarized (in-phase) vibration corresponds to the line centre of the isotropic component whereas the frequency of the depolarized (out-of-phase) vibration is nearly equal to the center of the VH band. In case transition dipole-transition dipole (TD-TD) interaction is the main coupling mechanism[9] eqn. (4.4) reads

$$(\Delta E_{\text{TD-TD}})_{\text{Res}} = \hbar\omega_{ij} = \left(\frac{\partial\mu}{\partial Q}\right)^2 Q_{01}^2 \langle K_{ij}/R_{ij}^3 \rangle, \quad \ldots (4.7)$$

where R_{ij} is the intermolecular distance and K_{ij} is a function of the mutual orientation of the molecules i and j. For point dipoles the orientation factor K_{ij} is,

$$K_{ij} = -2 \cos\theta_i \cos\theta_j + \sin\theta_i \sin\theta_j \cos\phi_{ij}, \quad \ldots. (4.8)$$

where θ_i is the angle between the dipole moment vector of molecule i and the ij vector which connects molecules i and j. ϕ_{ij} is the angle between the perpendicular components of the dipole moments of the molecules i and j.

Although it is impossible to evaluate the value $\langle \frac{K_{ij}}{R_{ij}^3} \rangle$ for DMA molecules, in case of dilute solutions when separation becomes large and $\frac{\mu^2}{R_{ij}^3} \ll kT$, one may substitute the average

value of the orientation factor and get the following expression[5] for TD-TD interactions,

$$\delta\omega = \frac{2\mu^2}{3\,KT\,\omega_o R_{ij}^6}\left(\frac{\partial\mu}{\partial Q}\right)^2 \qquad \ldots\ (4.9)$$

McHale[10] has obtained the expression for the first moment as:

$$M_\lambda^{(1)} = \omega_o + \frac{N}{2m\omega_o}\langle V_{ij}^{(2)}\, P_n\,(\mathrm{Cos}\,\theta_{ij})\rangle_B, \qquad \ldots\ (4.10)$$

where n = o when λ = iso, n = 1 when λ = IR and n = 2 when λ = aniso. $V_{ij}^{(2)} = \left(\frac{\partial^2 V_{ij}}{\partial Q_i \partial Q_j}\right)$ is the interaction of two transition dipoles and the bath averages over positions and orientation are governed by the interaction of permanent dipole moments. The averaging of $\langle V_{ij}^{(2)} P_n\,(\mathrm{Cos}\,\theta_{ij})\rangle_B$ requires a knowledge of the potential of the liquid as a function of all the molecules in the solvent system. These terms are however, impossible to treat adequately. If all molecular orientations were equally probable, a straightforward integration over $d\Omega_i\, d\Omega_j = \mathrm{Sin}\,\theta_i\, d\theta_i\, d\varphi_i\, \mathrm{Sin}\,\theta_j\, d\theta_j\, d\varphi_j$ causes the average $\langle V_{ij}^{(2)} P_n(\mathrm{Cos}\,\theta_{ij})\rangle_\Omega$ to vanish and no concentration dependence of the first moments is expected. However, the existence of $V_{ij}^{(2)}$, precludes the possibility of all orientations being equally probable. For molecules with large permanent dipole moments, the dipole-dipole interactions (U_{or}) is the dominant term in the long-range part of the intermolecular potential. We will consider this term to be the main term responsible for positional and orientational pair correlations so that the averages

$\langle\ \rangle_B$ can be performed. In this approximation we have

$$\langle V_{ij}^{(2)}\ P_n\ (\mathrm{Cos}\ \theta_{ij})\rangle_B = \frac{\int_d^\infty \int_0^{2\pi}\int_0^{\pi}\int_0^{2\pi}\int_0^{\pi} r^2\, dr\, d\alpha_i\, d\alpha_j\ e^{-\frac{U_{or}}{kT}}\ V_{ij}^{(2)}\ P_n\ (\cos\theta_{ij})}{\int_0^\infty \int_0^{2\pi}\int_0^{\pi}\int_0^{2\pi}\int_0^{\pi} r^2\, dr\, d\alpha_i\, d\alpha_j\ e^{-\frac{U_{or}}{kT}}} \qquad \ldots\ldots (4.11)$$

This approach of averaging over intermolecular distance and orientations is expected to yield only approximate results. In order to simulate short range repulsion, the lower limit on the integral over r is taken to be non-zero. It is valid to expand exponential $\exp(-U_{or}/kT) \sim 1 - \frac{U_{or}}{kT}$. The results of performing the integration are then;

$$\langle V_{ij}^{(2)}\rangle_B = -\frac{2}{3}\ \frac{\mu^2 \left(\frac{\partial\mu}{\partial Q}\right)_o^2}{\epsilon^2\, kT\, d^3 V} \qquad \ldots\ldots (4.12)$$

$$\langle V_{ij}^{(2)}\ \mathrm{Cos}\,\theta_{ij}\rangle_B = 0 \qquad \ldots\ldots (4.13)$$

$$\langle V_{ij}^{(2)}\ P_2\ (\mathrm{Cos}\,\theta_{ij})\rangle_B = -\frac{2}{75}\ \frac{\mu^2 \left(\frac{\partial\mu}{\partial Q}\right)_o^2}{\epsilon^2\, kT\, d^3 V} \qquad \ldots\ldots (4.14)$$

Here V is the sample volume.

In the transition dipole coupling model, the splitting $\delta\omega = \omega_{aniso} - \omega_{iso}$ is predicted to be

$$= \frac{8\mu^2 \left(\frac{\partial\mu}{\partial Q}\right)_o^2}{25\, m\, \omega_o\, kT\, d^3\, V_M}\ \frac{N_o\, \phi}{\epsilon^2}, \qquad \ldots\ldots (4.15)$$

where N_o is the Avogadro's number, ϕ is the volume fraction of

the solute, m is the effective mass for the mode, ω_o is the vibrational frequency of the isolated molecule, d is the minimum intermolecular distance and V is the molar volume of the solute. The term $1/\epsilon^2$ may be considered as the screening factor and substituting S, we have,

$$\delta\omega = \frac{8\mu^2 \left(\frac{\partial M}{\partial q}\right)^2}{25\, m\, \omega_o\, kT\, d^3\, V_M} N_o \phi S \qquad \ldots\ldots (4.16)$$

According to Giorgini et. al.[11] the screening factor S comprises two factors, S_p and S_t, related to the interaction of permanent and transition dipoles. Following the dielectric model of Onsager - Frohlich, the first term[12] $S_p = \left(\frac{n^2 + 2}{2\epsilon + n^2}\right)^2 \epsilon$ and the second term $S_t = \frac{(n^2 + 2)^2}{9\, n^2}$ which comes after substituting $\epsilon = n^2$. Here ϵ is the dielectric constant of the medium and n is the refractive index of the solute.

Since several approximations are involved in the Onsager - Frohlich model (e.g. the dielectric is treated as a continuum, polarizability being isotropic and the dipoles are point like) one may expect that the validity of the eqn. (4.16) is limited to dilute solutions. This model has been tested for the carbonyl stretching vibration of acetone, acetophenone etc. in several mixtures of known dielectric constant. With one or two exceptions, this explanation holds even in the high concentration range.

The expression (4.16) may be modified to read as following when the permanent dipole interactions are considered,

$$\delta\nu \frac{(2\epsilon + n^2)^2}{\epsilon} = \frac{2\mu^2 \left(\frac{\partial \mu}{\partial q}\right)_0^2}{25\pi^2 c^2 \nu_0 \, kT \, d^3} \frac{N_0}{V_M} \phi \, (n^2 + 2)^2 \quad \ldots (4.17)$$

One may therefore plot the graph of,

$\delta\nu \frac{(2\epsilon + n^2)^2}{\epsilon}$ as a function of ϕ which has been found to be almost linear by Giorgini et. al. for acetone, acetophenone etc.

The quantity $\left(\frac{\partial \mu}{\partial q}\right)_0^2$ is proportional to infrared band intensity and for DMA molecule the infrared band corresponding to the Raman band under study (amide I band) is very strong which indicates that splitting factor for DMA molecule should be quite large and it is indeed so, the anisotropy shift being 13 cm^{-1} in neat liquid (Fig. 4.2).

The Raman spectra of DMA molecule (Fig. 4.2) show that the I_{VV} component of the amide I band in pure liquid has a clear shoulder whereas the anisotropic part, I_{VH} is almost symmetric with its peak shifted to higher wavenumbers. The difference between the maximum frequencies of I_{VV} and I_{VH} is of the order of 13 cm^{-1}. This difference in maximum frequency may be interpreted as the effect of resonant transfer (due to TD-TD interactions) on the band shape.

In Fig. 4.3 the trends in the amide I band of DMA are shown as a function of different concentrations of solvents CH_3CN, $CHCl_3$, CCl_4 and C_6H_6.

The values of the isotropic and anisotropic peak frequencies, FWHH and the vibrational relaxation time (τ_v) for various

solutions are given in Tables IV.1 - IV.4. The experimental data for these mixtures can be explained in the following way:

With increasing concentration of CH_3CN, the isotropic frequency first increases and later it remains almost constant. The anisotropic frequency on the other hand, decreases continuously and ultimately coincides with the isotropic frequency.

In $CHCl_3$ - DMA system the maximum frequency of the isotropic part shifts to lower wavenumbers upto 50% concentration of solvent compared with the pure liquid. With increasing concentration of solvent (more than 50%) this shift decreases due to the effect of decoupling. The maximum of the anisotropic component shifts linearly towards lower wavenumbers. The anisotropy shift tends to vanish on very high dilution of DMA in $CHCl_3$.

In CCl_4 and C_6H_6 solvents there is a relatively slow increase of the isotropic and anisotropic maximum frequencies with the increasing solvent concentration. But the curve of concentration dependent maximum shift is not linear. The anisotropy shift in these solvents decreases very slowly which shows that dipole-dipole interactions in DMA are broken only at very high solvent concentration.

In all the above systems it has been seen that the anisotropy shift decreases as the concentration of the solvent is increased. In CH_3CN the anisotropy shift vanishes at about 80% dilution. $CHCl_3$ may form hydrogen bonds with the C = O

group. This gives rise to a large shift relative to the gas phase frequency. As a result maximum frequency of the isotropic component shifts towards lower wavenumbers compared with the pure liquid frequency. Due to the effect of decoupling one may however expect the shift into the opposite direction. Although in CCl_4 and C_6H_6 solvents the anisotropy shift decreases slowly with dilution in the beginning, on higher dilution there is rather strong changes of the anisotropy shift.

All these results therefore support the assumption that the anisotropy shift is an effect due to resonance coupling since it decreases with dilution whatever may be the solvent.

In order to test the validity of eqn. (4.17) in case of DMA, the quantity $\delta\nu\,(2\epsilon + n^2)^2\,\epsilon^{-1}$ was plotted against φ. The variations are shown in Figs. 4.4 and 4.5 for polar and non-polar solvents respectively. The linear variation of the quantity $\delta\nu(2\epsilon + n^2)^2\,\epsilon^{-1}$ as a function of φ is indicative of the validity of the eqn. (4.17) within the approximations.

The van der Waals type of attractions deal with a situation where interacting particles are separated by a distance such that electronic orbitals do not overlap[13,14]. The intermolecular interaction energy may consist of the terms mainly related to dipole-dipole, dipole-induced dipole and instantaneous dipole-induced dipole type of interactions.

The dipole-dipole interactions are expected to be important for polar solvents. The interaction energy between

two molecules or atoms of dipole moments μ_i and μ_j is given by the expression $U_{D.D} = -\frac{1}{\epsilon^2} \frac{2\mu_i^2 \mu_j^2}{3kT} \frac{1}{R_{ij}^6}$ for $kT > \frac{\mu_i \mu_j}{R_{ij}^3}$ ...(4.18)

where R_{ij} is the distance between the point dipoles, kT is the thermal energy and ϵ is the dielectric constant of the medium.

The dipole-induced dipole type of interaction energy is dependent upon the induced dipole moments and the energy associated with this interaction is given by the expression,

$$U_{D-ID} = -\frac{1}{\epsilon^2} (\alpha_i \mu_j^2 + \alpha_j \mu_i^2) \frac{1}{R_{ij}^6} \quad \ldots\ (4.19)$$

where α_i and α_j are the polarizabilities of the molecules i and j. (See Table IV.5 for molecular parameters).

The dispersion interactions between two molecules involve the polarizabilities of the interacting molecules and is attractive for all orientations. The dispersion energy, U_{dis}, as given by London dispersion model is

$$U_{dis} = -\frac{3}{2} \frac{1}{n^4} \frac{\alpha_i \alpha_j}{R_{ij}^6} \frac{I_i I_j}{I_i + I_j} = -\frac{F(n,I)}{R_{ij}^6} \quad \ldots\ (4.20)$$

where I_i and I_j are the ionisation potentials of the molecules i and j respectively, n is the refractive index of the medium, and the dispersion energy parameter $F(n,I) = \frac{3}{2} \frac{1}{n^4} \alpha_i \alpha_j \cdot \frac{I_i I_j}{I_i + I_j}$

The above three interactions are supposed to play a role in the FWHH of isotropic component (Γ_{iso}) of the Raman band. The isotropic linewith (Γ_{iso}) is related to the vibrational relaxation time by the following expression,

$$\tau_v = (\pi c \Gamma_{iso})^{-1} \quad \ldots\ (4.21)$$

Their relative contributions may be calculated by using the above expression (Eqn.4.18-4.20). The calculated values are given in Table IV.6. It is clear from the values for U_{D-D}, U_{D-ID} and U_{dis} that in all the solvents CH_3CN, $CHCl_3$, CCl_4 and C_6H_6 the dispersion energy is greater than the dipole-dipole interaction energy and dipole-induced dipole (induction) interaction energy. It is interesting to note that the role of dipole-dipole interaction energy or induction energy in case of even polar solvents is much less as compared to dispersion energy. It is mainly due to the presence of ϵ^2 and n^4 terms in various interaction energies. For solvents of high dielectric constants, the dispersion energy is going to play an important role in intermolecular interactions. The variation of Γ_{iso} as a function of dispersion energy in different solvents (at 90% solvent concentration) is shown in Fig. 4.6. It is very clearly a straight line and therefore the experimental data are well explained by considering only the contribution from dispersion forces. The dispersion forces therefore play the most important role in line broadening mechanism for the isotropic component of the amide I band of DMA molecule. This is a new and important finding of the present investigation.

References:

[1] G. Fini and P. Mirone, J. Chem. Soc. F. Trans. II 70, 1776 (1974).

[2] P. Mirone and G. Fini, J. Chem. Phys. 71, 2241 (1979).

[3] C.H. Wang and J. McHale, J. Chem. Phys. 72, 4039 (1980).

[4] J. Yarwood and R. Arndt, in "Molecular Association", Vol. 2, Ed. by R. Foster, (Academic Press, London, 1979) p. 267.

[5] D. Scheibe, J. Raman Spectrosc. 13, 103 (1982).

[6] D.W. Oxtoby, J. Phys. Chem. 87, 3028 (1983).

[7] F. Seifert, K.L. Oehme, G. Rudakoff, W. Hölzer, W. Carius and O. Schrötter, Chem. Phys. Letts. 105, 635 (1984).

[8] W. Schindler, T.W. Zerda and J. Jonas, J. Chem. Phys. 81, 4306 (1984) and references therein.

[9] G. Döge, R. Arndt and J. Yarwod, Mol. Phys. 52, 399 (1984)

[10] J.L. McHale, J. Chem. Phys. 75, 30 (1981).

[11] M.G. Giorgini, G. Fini and P. Mirone, J. Chem. Phys. 79, 639 (1983).

[12] P. Mirone, J. Chem. Phys. 77, 2704 (1982).

[13] D. Langbein in "Springer Tracts in Modern Physics: Theory of van der Waals Attraction", Vol. 72, Ed. by G. Hohler (Springer - Verlag, Berlin, 1974) p. 4.

14 K. Kumar, M.C. Bindal, P. Singh and S.P. Gupta, Int. J. Quant. Chem. 20, 123 (1981).

15 J. Timmermans, "Physico-Chemical Constants of Pure Organic Compounds", Vol.2 (Elsevier, Amsterdam, 1965).

16 "CRC Handbook of Chemistry and Physics", Ed. by R.C. Weast, 58th Edition (CRC Press, 1977-78).

17 K.M.C. Davis, in"Molecular Association", Vol.1, Ed. by R. Foster (Academic Press, London, 1975) p.168

18 "Physical chemistry of Organic Solvent Systems", Ed. by A.K. Covington and T. Dickinson (Plenum Press, London, 1973).

19 C.G. Gray and K.E. Gubbins, "Theory of Molecular Fluids", Vol.1 (Clarendon Press, Oxford, 1984) p.577.

Table IV.1. DMA - CH_3CN system

% DMA	Peak frequency $\Delta\bar{\nu}$ (cm^{-1})		Anisotropy shift $\delta\nu$ (cm^{-1})	FWHH Γ_{iso} (cm^{-1})	$\tau_v = (\pi c \Gamma_{iso})^{-1}$ (psec)
	Isotropic	Anisotropic			
90	1637	1650	13	27	0.39
80	1638	1648	10	27	0.39
70	1639	1647	8	27	0.39
60	1640	1647	7	27	0.39
50	1641	1647	6	26	0.40
40	1641	1646	5	25	0.42
30	1642	1645	3	24	0.44
20	1642	1643	1	23	0.46
10	1642	1642	0	22	0.48

Table IV.2. DMA- $CHCl_3$ system

% DMA	Peak frequency $\Delta\tilde{\nu}$ (cm^{-1})		Anisotropy shift $\delta\nu$ (cm^{-1})	FWHH Γ_{iso} (cm^{-1})	$\tau_v = (\pi c \Gamma_{iso})^{-1}$ (psec)
	Isotropic	Anisotropic			
90	1635	1648	13	31	0.34
80	1634	1647	13	32	0.33
70	1633	1645	12	34	0.31
60	1633	1643	10	34	0.31
50	1632	1642	10	33	0.32
40	1633	1640	7	32	0.33
30	1633	1639	6	32	0.33
20	1634	1638	4	31	0.34
10	1636	1637	1	30	0.35

Table IV.3 DMA - CCl_4 system

% DMA	Peak frequency $\Delta\bar{\nu}$ (cm^{-1})		Anisotropy shift $\delta\nu$ (cm^{-1})	FWHH Γ_{iso} (cm^{-1})	$\tau_v = (\pi c \Gamma_{iso})^{-1}$ (psec)
	Isotropic	Anisotropic			
90	1636	1648	12	25	0.42
80	1637	1648	11	26	0.41
70	1638	1648	10	27	0.39
60	1639	1648	9	28	0.38
50	1640	1649	9	29	0.37
40	1640	1649	9	30	0.35
30	1642	1650	8	30	0.35
20	1643	1650	7	31	0.34
10	1645	1651	6	31	0.34

Table IV. 4. DMA - C_6H_6 system

% DMA	Peak frequency $\Delta\tilde{\nu}$ (cm^{-1})		Anisotropy shift $\delta\nu$ (cm^{-1})	FWHH Γ_{iso} (cm^{-1})	$\tau_v = (\pi c \Gamma_{iso})^{-1}$ (psec)
	Isotropic	Anisotropic			
90	1637	1649	12	23	0.46
80	1638	1649	11	24	0.44
70	1639	1649	10	24	0.44
60	1640	1650	10	25	0.42
50	1641	1651	10	25	0.42
40	1642	1651	9	26	0.41
30	1644	1652	8	26	0.41
20	1646	1653	7	26	0.41
10	1648	1654	6	26	0.41

Table IV. 5. Molecular Parameters

Molecule	Refractive Index (n)	Dielectric Constant (ϵ)	Dipole Moment μ/Debye	Polarizability $\alpha/10^{-24}$ cm^3	Ionisation Potential (eV)
Acetonitrile	1.34154[a]	37.5[c]	3.913[e]	4.46[e]	12.2[b]
Chloroform	1.4459[b]	4.7[c]	1.04[e]	8.95[e]	11.42[b]
Carbon Tetrachloride	1.45704[a]	2.2[c]	0	10.39[e]	11.47[b]
Benzene	1.49859[a]	2.3[c]	0	10.5[e]	9.24[b]
N,N-Dimethylacetamide	1.4380[b]	37.8[d]	3.81[b]	8.83[f]	8.81[b]

a) Reference [15], b) Reference [16], c) Reference [17], d) Reference [18],

e) Reference [19], f) Calculated using formula $\alpha = \frac{3}{4\pi} \cdot \frac{M}{N_0 \rho} \cdot \frac{n^2 - 1}{n^2 + 2}$

where M is molecular weight, N_0 is Avagadro's number, ρ is density and n is refractive Index.

Table IV.6. Calculated values of parameters related to D-D, D-ID and dispersion energies for various solvents

Molecular System	$(2\mu_i^2\mu_j^2)/(\epsilon^2 3kT)$ $/10^{-60}$ (ergs-cm^6) at T = 300°K	$(\alpha_i\mu_j^2+\alpha_j\mu_i^2)/\epsilon^2$ $/10^{-60}$ (ergs-cm^6)	$\frac{3}{2n^4}\cdot\frac{I_iI_j}{I_i+I_j}\cdot\alpha_i\alpha_j$ $/10^{-60}$ (ergs-cm^6)
DMA-CH_3CN	2.55	0.11	149.43
DMA-$CHCl_3$	11.44	6.31	216.03
DMA-CCl_4	0	31.16	243.67
DMA-C_6H_6	0	28.81	199.18

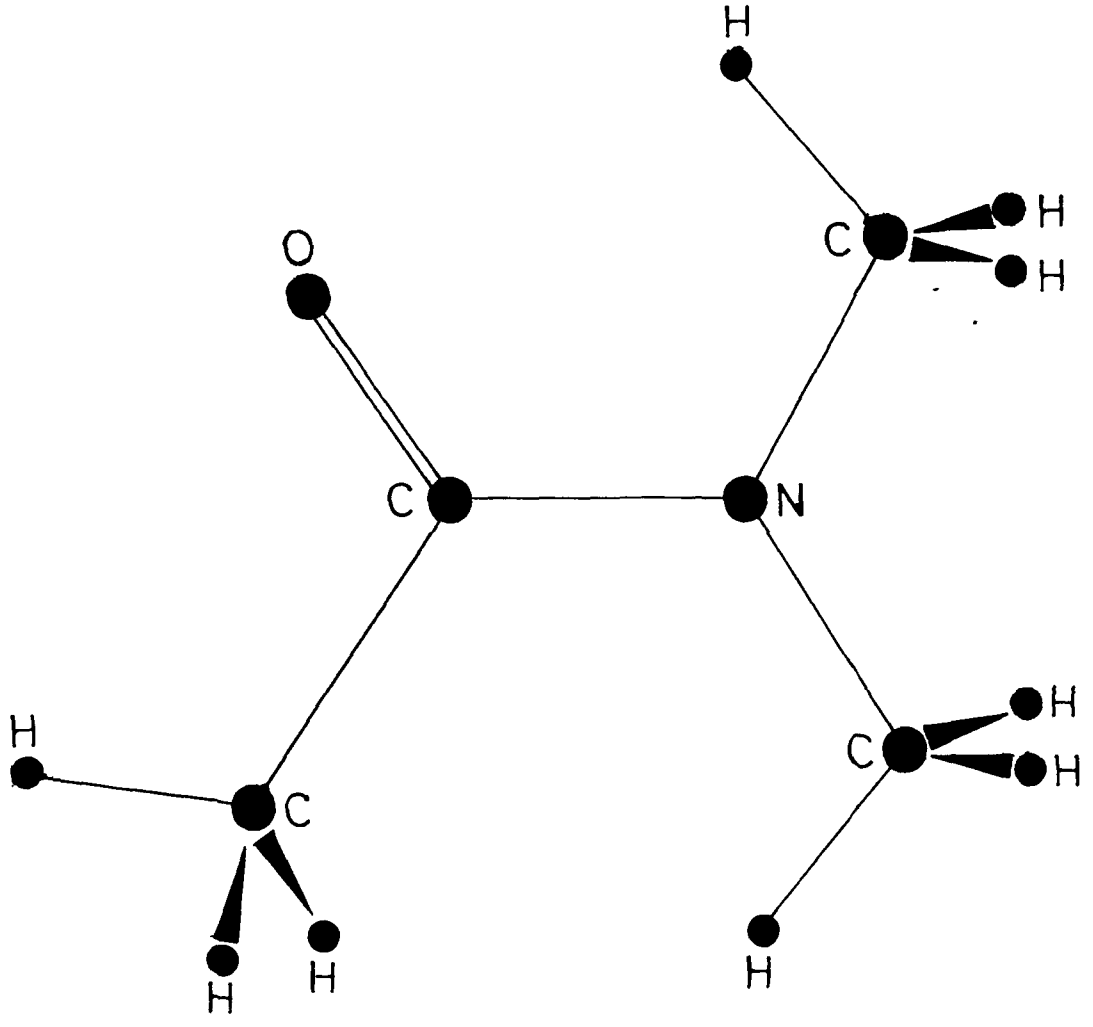

Fig. 4.1 The structure of N,N-Dimethylacetamide molecule

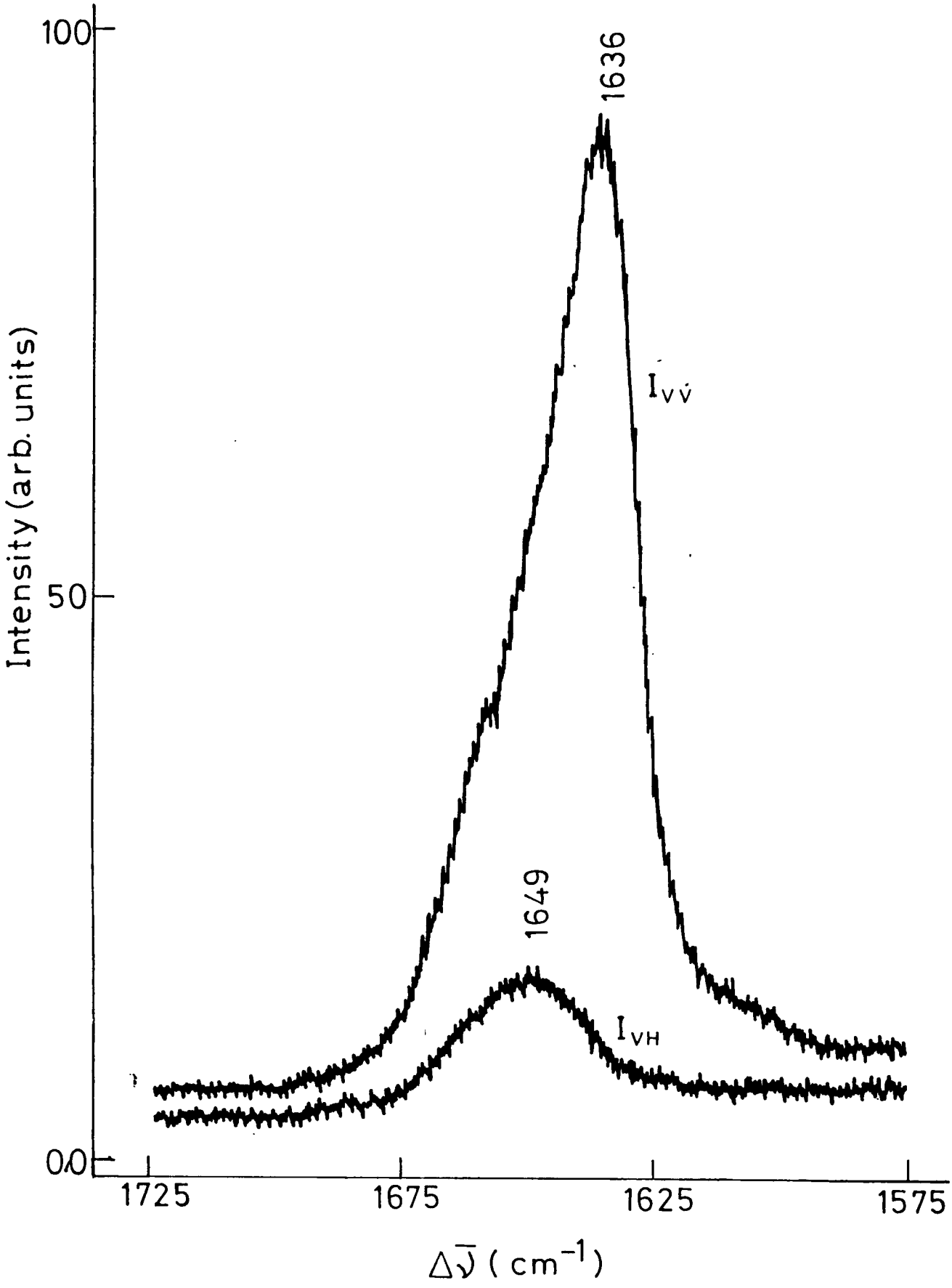

Fig.4.2 The laser Raman spectrum of DMA molecule in the amide I band region.

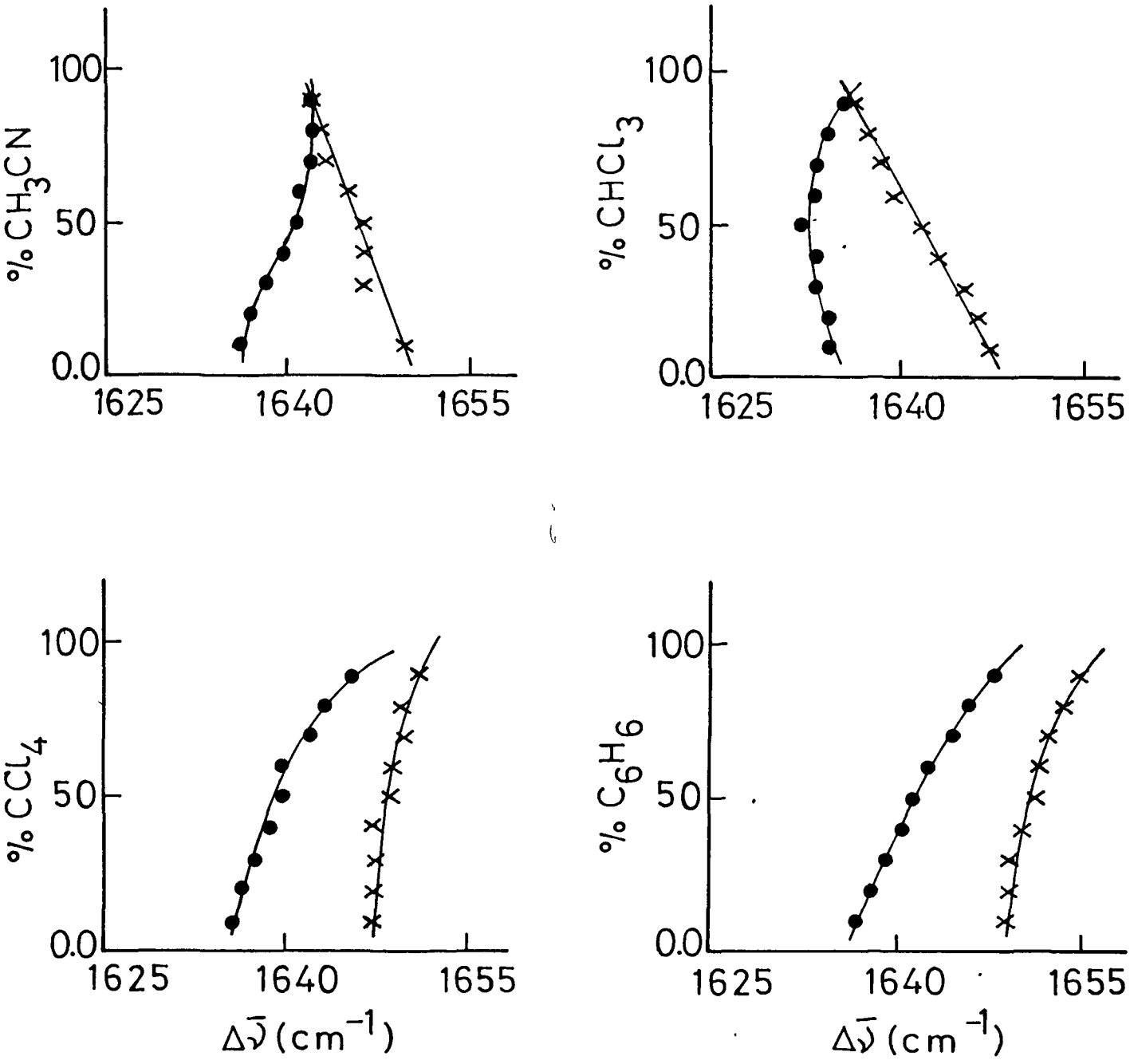

Fig. 4.3 The variation of isotropic (•) and anisotropic (x) maximum frequencies as a function of solvent(s) concentration.

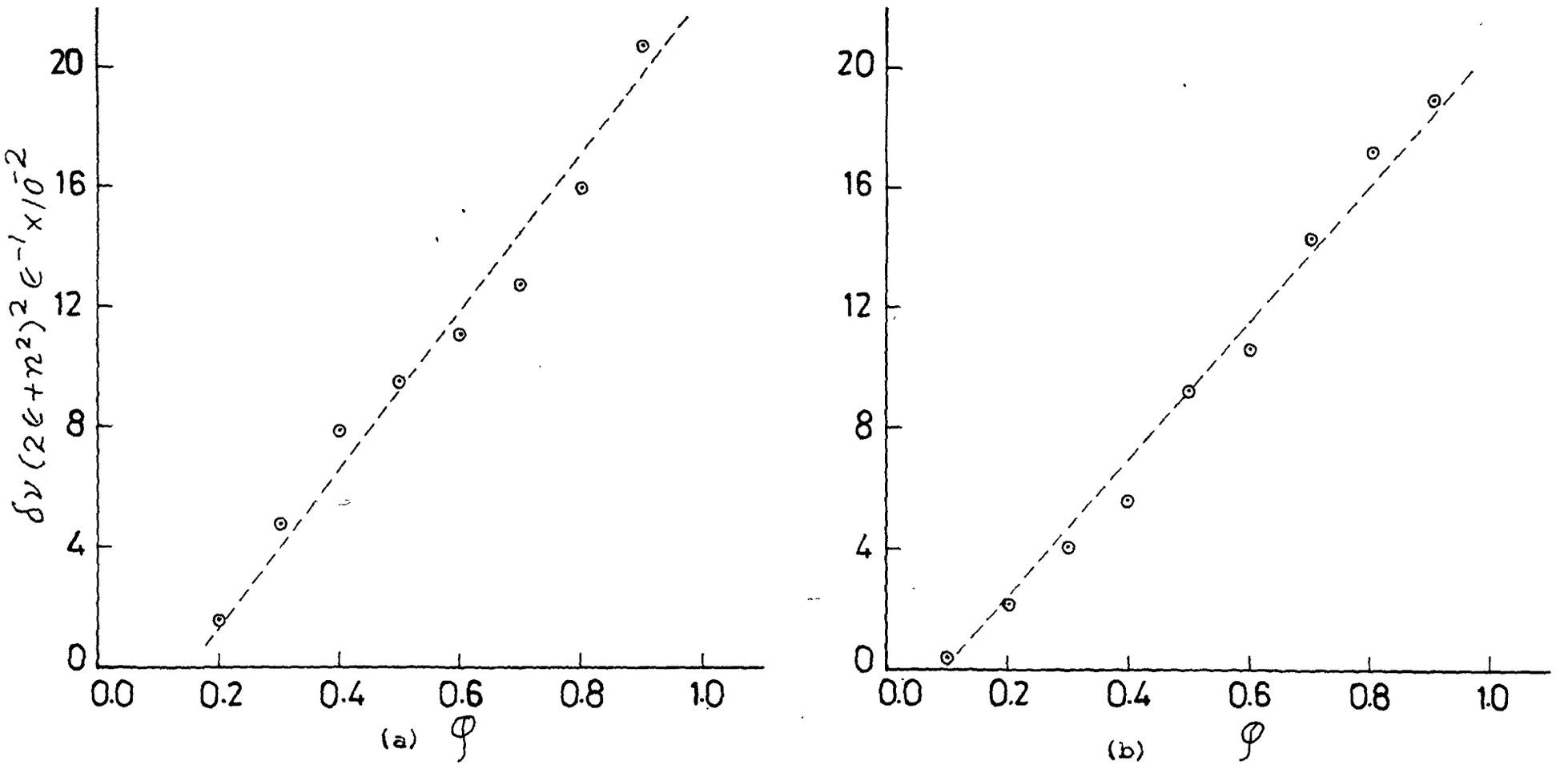

Fig. 4.4 The variation of $\delta\nu(2\epsilon + n^2)^2\,\epsilon^{-1}$ as a function of volume fraction φ for the amide I band of DMA in (a) CH_3CN and (b) $CHCl_3$

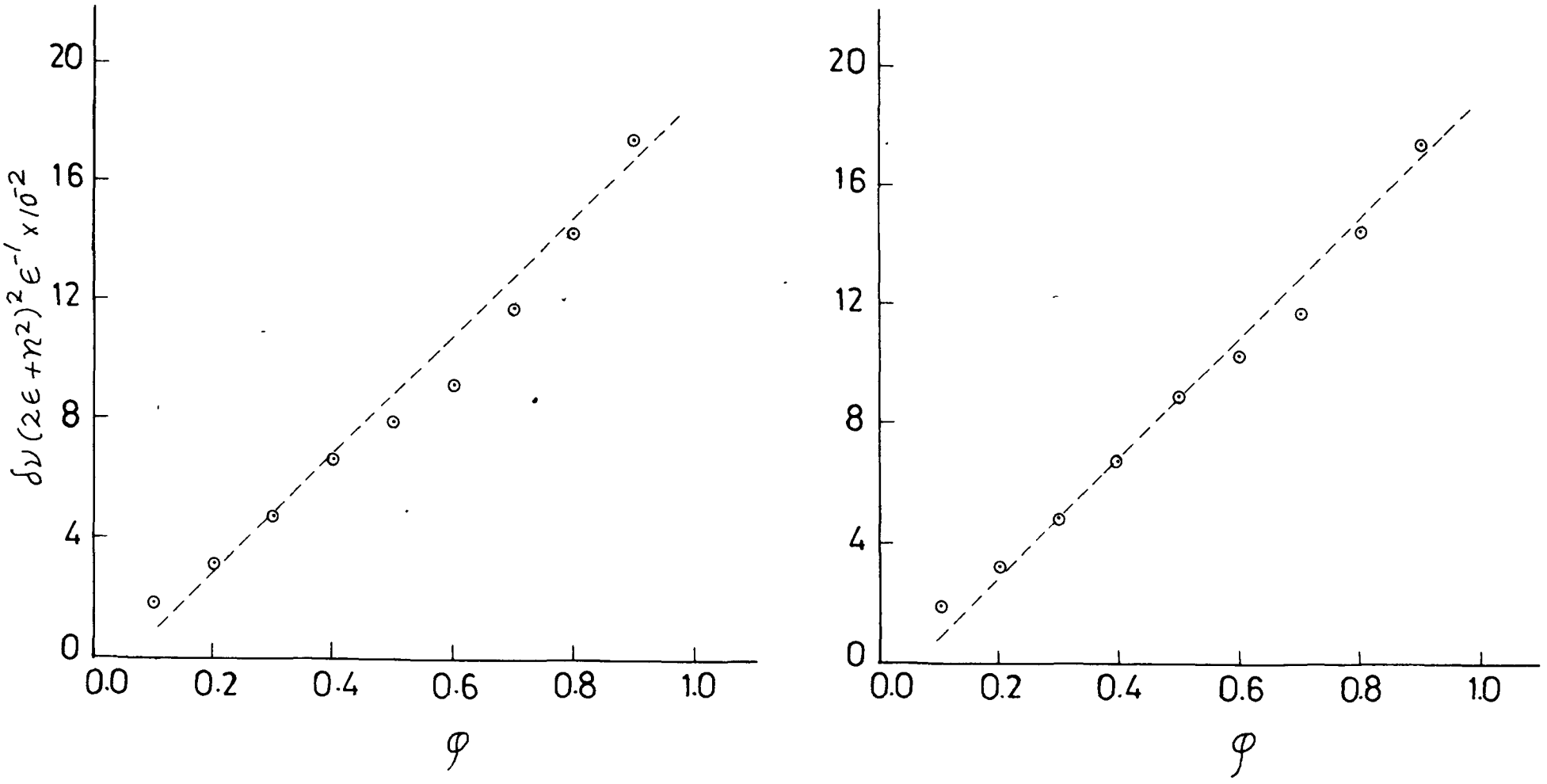

Fig. 4.5 The variation of $\delta\nu(2\epsilon + n^2)^2 \epsilon^{-1}$ as a function of volume fraction φ for the amide I band of DMA in (a) CCl_4 and (b) C_6H_6.

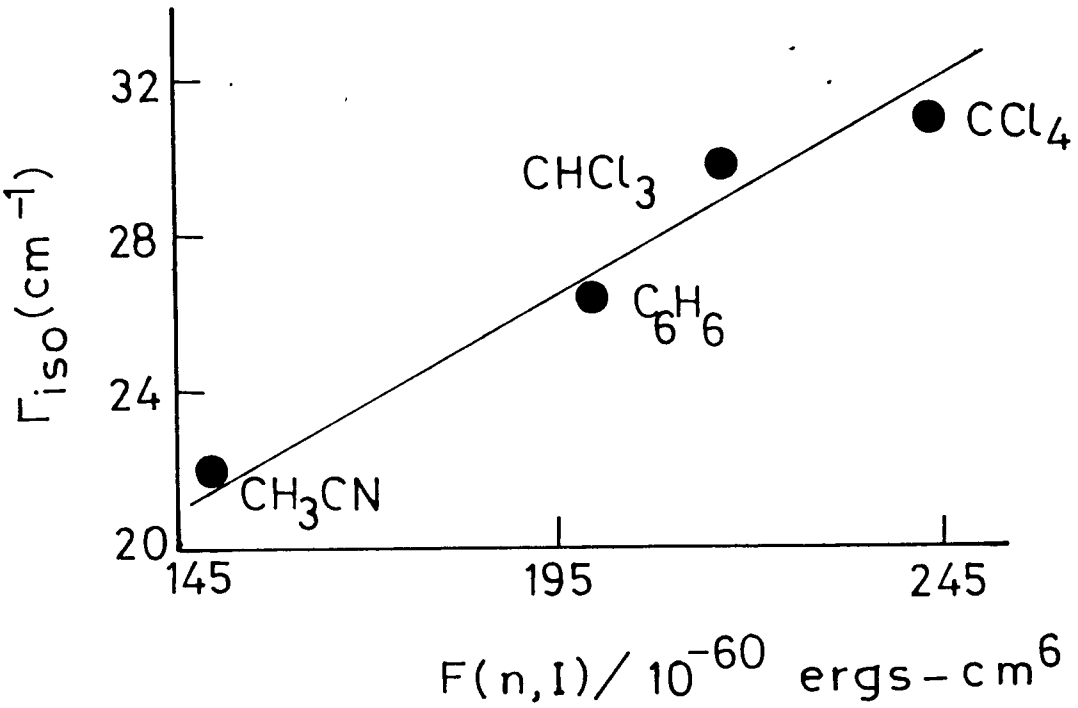

Fig. 4.6 The variation of Γ_{iso} as a function of dispersion energy parameter, F (n,I).

CHAPTER V

CHAPTER V

VIBRATIONAL RELAXATION AND NONCOINCIDENCE EFFECT IN LIQUID N,N-DIMETHYLFORMAMIDE*

ABSTRACT

The Raman band of the amide I mode of vibration of N,N-dimethylformamide (DMF) has been studied in neat liquid and as a function of solvent(s) concentration. The non-coincidence effect (anisotropy shift) is explained in terms of transition dipole-transition dipole interactions. The effect of solvent concentration on linewidth has been studied. The vibrational relaxation rate has been shown to be linearly dependent upon the product of the density, viscosity and a dispersion energy dependent term.

---

* Part of this work has been accepted for presentation: A. Purkayastha and K. Kumar, Symposium on Quantum Electronics (1985).

CHAPTER V

5.1 Introduction

In recent years considerable progress has been made towards a deeper understanding of the vibrational relaxation and molecular reorientation in liquids on the basis of theoretical and experimental work.[1-5] It is well known that laser Raman scattering experiments provide much information about local structure and molecular motions in liquids. A considerable amount of information about vibrational relaxation and reorientational motion can be obtained by analyzing the experimentally measured lineshapes of the isotropic and anisotropic components of the Raman spectrum of a molecular liquid.[6-9] Moreover the microscopic environment affects the behaviour of a vibrational mode of a reference molecule. In a liquid mixture the lineshape of the reference mode is influenced by the concentration fluctuations of the environment.

In few liquids the peak frequencies of the isotropic and anisotropic bands differ from each other. The difference in peak positions may sometimes be more than 10 cm^{-1}.[4,10-13] This noncoincidence effect has been interpreted as due to the coupling between vibrations of neighboring molecules with strongly polar modes by intermolecular dipole interactions in the liquid phase.[4,11,13] Although several papers have been devoted to this subject, a systematic analysis of the solvent

dependence of noncoincidence effect and vibrational linewidth is lacking. The present paper reports Raman data for N,N-dimethylformamide (DMF) in neat liquid and in solvents of varying dielectric constant and dipole moment.

N,N-dimethylformamide [Fig. 5.1] was chosen as an example of a liquid with large dipole moment (3.82 D) and rather strong intermolecular interactions. Amides are important because of their high dielectric constant and their biological applications. The effect of solvent on the noncoincidence between the isotropic and anisotropic components of the amide I band of DMF was studied by Fini and Mirone[10] and Giorgini et al.[12] However the vibrational relaxation and molecular reorientation in DMF have not been reported and the effect of solvent has also not been studied on the relaxation parameters. The dependence of relaxation times on hydrodynamic properties viz. viscosity and the molecular forces is an important area to be taken into consideration. We have therefore undertaken a detailed investigation of the vibrational lineshape as a function of the hydrodynamic parameter, viscosity (η) and dispersion energy parameter which are expected to play a major role in the line broadening mechanism. In the present investigation we have tried to interpret the variation of vibrational relaxation time in terms of both the above mentioned parameters and the results are presented. A theoretical model has also been developed to explain the experimental data.

5.2 Experimental

The sample of DMF and the solvents CH_3CN, $CHCl_3$, CCl_4 and C_6H_6 were obtained commercially and were used without further purification. Raman measurements were made for the amide I band of DMF in various solvents as a function of solvent concentration. The experiments were performed with a Spex Ramalog 1403 double monochromator equipped with datamate. The 5145A° and 4880A° laser lines from Spectra Physics model 165 Ar^+ laser were used as exciting source with a power of $\sim$ 900 mw. The slit width employed was ~ 4 cm^{-1} for all recorded spectra. In order to register the I_{VV} and I_{VH} components of the scattered Raman radiation an analyzer was placed in the path of the scattered radiation. The isotropic line shape was determined from the usual expression $I_{iso}(\omega) = I_{VV}(\omega) - \frac{4}{3} I_{VH}(\omega)$ which gives information about the spherically symmetric part of intra-and intermolecular forces. The anisotropic lineshape can be obtained directly from $I_{VH}(\omega)$ component and it gives the knowledge about the anisotropic forces and molecular reorientation. The finite slit width effect on the observed linewidth was corrected by the usual formula (3.4). The accuracy of measurements is believed to be $\pm$ 1 cm^{-1} for Raman spectral measurements. The Infrared spectra were recorded as a thin film of liquid between the two KBr plates using Perkin-Elmer 983 Infrared Spectrophotometer.

5.3 Results and Discussion

The isotropic Raman lineshape is dependent upon the vibrational phase relaxation and for well separated vibrational transition there are various sources of line broadening. The three primary sources are considered to be the life time broadening, environmental broadening (pure dephasing) and the resonance transfer. The explanation for vibrational phase relaxation requires the knowledge of the potential energy functions. The coupling potential V between the vibrations and bath which may arise due to dispersion interactions, dipole-dipole interactions, multipole interactions, repulsive forces etc., may be expanded in Taylor's series in vibrational coordinate Q_i [Eqn. 2.1]. In this expression the term $\frac{1}{2} \sum_{ij} \frac{\partial^2 V}{\partial Q_i \partial Q_j}$ takes care of the coupling between the fundamentals of the same mode in the two molecules i and j. This term allows the resonant energy transfer from one mode to another.

The transition dipole-transition dipole interactions cause resonance energy transfer between oscillators on adjacent molecules[14]. The transition moment for transitions between state /0> and /1> is

$$\mu'_{10} = \left(\frac{\partial \mu}{\partial Q}\right)_0 \langle 1/Q/0 \rangle \qquad \ldots (5.1)$$

where $\left(\frac{\partial \mu}{\partial Q}\right)_0$ is related to the infrared intensity data. The intermolecular potential V_{ij} is assumed to be given by,

$$V_{ij} = -\frac{\mu'_{10}}{R_{ij}^3} K_{ij} = -\left(\frac{\partial \mu}{\partial Q}\right)_0 \langle 1/Q/0 \rangle \frac{K_{ij}}{R_{ij}^3} \qquad \ldots\ldots (5.2)$$

where K_{ij} describes the relative orientations of the coupled oscillators and R_{ij} is the intermolecular distance. The interaction energy between the two transition dipoles is given as

$$\Delta E = - \left(\frac{\partial \mu}{\partial Q}\right)_o^2 \frac{\hbar}{4\pi\nu_o} \left\langle \frac{K_{ij}}{R_{ij}^3} \right\rangle \qquad \ldots (5.3)$$

In case of DMF molecule also it is very difficult to calculate the quantity $\left\langle \frac{K_{ij}}{R_{ij}^3} \right\rangle$ therefore the anisotropy shift ($\delta\nu$) is given by the proportionality relation

$$\delta\nu \propto \left(\frac{\partial \mu}{\partial Q}\right)^2 \qquad \ldots . (5.4)$$

The quantity $\left(\frac{\partial \mu}{\partial Q}\right)^2$ is proportional to the infrared absorption coefficient and therefore has to be proportional to infrared band intensity. Since the infrared absorption band for the amide I band of DMF is quite strong, the anisotropy shift $\simeq 14$ cm^{-1} [Fig. 5.2] in DMF molecules may be associated with large dipole moment derivatives.

The observed band shape also depends on a modulation time τ_c which depends on the rate of relative reorientational motions of the surrounding molecules.

The dipole-dipole interactions give rise to spectral broadening because for an anharmonic oscillator, the time average of the dipole moment in the two states $|0\rangle$ and $|1\rangle$ is different. This means that the interaction of the vibrating molecules with the surrounding permanent dipoles influences the energy of the transition $1 \leftarrow 0$. The dipole moment difference for the fundamental mode ($v = 1 \leftarrow o$) $\Delta_{01}\mu$

depends on the extent of both the mechanical and electrical anharmonicity and is given by the expression

$$\Delta_{01}\mu = \left(\frac{\partial \mu}{\partial Q_i}\right)_0 \left[\langle 1/\omega/1\rangle - \langle 0/\omega/0\rangle\right] + \frac{1}{2}\left(\frac{\partial^2 \mu}{\partial Q_i^2}\right)_0 \left[\langle 1/Q^2/1\rangle - \langle 0/Q^2/0\rangle\right] \quad \ldots (5.5)$$

The isotropic-anisotropic separation of the amide I (mainly C=O stretching) stretching band of DMF was measured at several concentrations in different mixtures of CH_3CN, $CHCl_3$, CCl_4 and C_6H_6 [Fig. 5.3]. The Raman spectra for a polar (CH_3CN) and a nonpolar (C_6H_6) solvent are shown in Fig. 5.4 and Fig. 5.5 respectively. The solvents cover a wide range of dielectric constant (ϵ). In order to test the validity of equation (4.17) the quantity $\delta\nu\,(2\epsilon+n^2)^2\,\epsilon^{-1}$ was plotted against ϕ and it is shown in Figs. 5.6 and 5.7. The screening factor S_t does not vary much[12] over the whole composition range in the mixtures and its omission or inclusion does not significantly modify the agreement with the experimental data.

It appears that the graphs of $\delta\nu\,(2\epsilon+n^2)^2\,\epsilon^{-1}$ are linear with ϕ within the experimental uncertainty. Thus it seems that the concentration dependence of the noncoincidence effect is explained at least as a first approximation, by the simple dielectric model of Onsager-Frohlich. Alternatively one could think that the agreement of the experimental results with the predictions of the dielectric model even in the high concentration range could result from the fortuitous cancellation

of errors resulting from the different approximations. The assumption of point dipoles should be fair for not too small molecules since the dipole length i.e. the distance between the centers of gravity of the positive and negative charges is at least one order of magnitude smaller than the molecular dimensions. The hypothesis that $\delta\nu$ depends linearly on the concentration is supported by its behaviour in mixtures of liquids having nearly identical dielectric constant, where it is reasonable to expect that the dielectric properties do not vary significantly with the composition.

The general correlation function may be expanded[14] in terms of the frequency moments of the experimental intensity distribution. The normalised moments are given as

$$M_n = \frac{\int_{band} (\omega-\omega_o)^n \, I(\omega-\omega_o) \, d\omega}{\int_{band} I(\omega-\omega_o) \, d\omega} \qquad \ldots\ (5.6)$$

where ω_o is a suitably chosen band origin. The zeroth moment (M_o) is the total integrated intensity of the band and M_1 is equal to the frequency at the maximum. The second moment M_2 is indicative of the width of the band. In case of vibrational correlation function it may be represented as $(M_2)_v$. This second moment is related to the vibrational relaxation time (τ_v) in case of rapid modulation limit, using Kubo model for lineshape. It is given by the expression

$$\tau_v^{-1} = (M_2)_v \, \tau_c \qquad \ldots\ (5.7)$$

For reorientational/translational motions depending mainly on long range dipolar interactions τ_c is directly proportional to the dynamic viscosity. Since the second moment is directly proportional to the liquid density the relation for the vibrational relaxation rate at a constant temperature is given as

$$\tau_v^{-1} \propto \rho\eta \qquad \ldots\ (5.8)$$

The current theories on vibrational dephasing predict the following behaviour for these two parameters under different experimental condition.

(1) Variation of $(M_2)_v$ in pure liquid: increases with increasing density at constant temperature.

(2) Variation of τ_c in the pure liquid and in mixtures:
(a) for long range dipolar interactions τ_c is proportional to at constant temperature. (b) for short range repulsive forces τ_c is proportional to $1/\eta$.

(3) Variation of $(M_2)_v$ in mixtures: (a) for band broadened by resonant transfer of vibrational energy: decrease on isotopic dilution, (b) for band broadened by dipolar interaction: decrease on dilution in a non-polar solvent and increase on dilution by solvent with a higher dipole moment. (c) for band broadened by a specific interaction: decrease by dilution with a solvent in which interaction is smaller or is removed.

To interpret the experimental results of a study of the vibrational relaxation of a particular band in the pure liquid

it is therefore useful to perform dilution studies in various solvents with the aim of changing the type of interaction of the active molecules with their neighbours. In this way one can expect to get information about the interactions that influence the band shape in the pure liquid.

The variation of the linewidth (Γ_{iso}) as a function of dispersion energy parameter has been studied for DMA molecule as mentioned in Chapter IV. It has also been studied for DMF molecule and the relationship is found to be almost linear (Fig. 5.8) as in case of DMA molecule. Now that the relationship with dispersion forces is established, we therefore considered it worthwhile to include the dispersion force parameter in the vibrational relaxation time relationship as it is related to the Γ_{iso} by the relation (4.21). We therefore tried to correlate the parameter $\left(\frac{n^2-1}{2n^2+1}\right)$ in conjunction with $\rho\eta$ so that a relation with all these parameters may be obtained. This parameter has been chosen because the Lorentz's reaction field is given by the expression[15]

$$E = \frac{2\mu}{a^3}\left(\frac{n^2-1}{2n^2+1}\right) \qquad \ldots\ (5.9)$$

where μ is the dipole moment of the solute molecule and a is the radius of the spherical cavity and n is the refractive index of the medium. The dipole moment in the reaction field expression (eqn. 5.9) is corresponding to the solute molecule and is therefore constant when only solvent is changed. The parameter $\left(\frac{n^2-1}{2n^2+1}\right)$ is thus solvent dependent.

It was seen that the parameter $\rho\eta\left(\frac{n^2-1}{2n^2+1}\right)^{-1}$ is best fitting with the linewidth (Γ_{iso}). This relationship has some resemblance[16] with the dielectric relaxation time and the dielectric constant parameter where instead of n^2 the permittivity of the medium(ϵ) is used. The relation $\epsilon = n^2$ is to be used for high frequencies $\sim 10^{14}$ Hz. We have therefore obtained an empirical relationship

$$\tau_v^{-1} \propto \rho\eta\left(\frac{n^2-1}{2n^2+1}\right)^{-1} \quad \ldots\ldots (5.10)$$

The linewidths (FWHH) for the amime I band of DMF in various solvents at varying concentrations were obtained and their variations are shown in Fig. 5.9. The values of τ_v^{-1} as calculated (Table V.1) using the formula (4.21) are plotted as a function of the parameter $f(\rho, \eta, n) = \left(\frac{n^2-1}{2n^2+1}\right)^{-1}\rho\eta$ This variation is shown in Fig. 5,10. The almost linear dependence of τ_v^{-1} in case of three solvents (CH_3CN, $CHCl_3$ and CCl_4) is clearly indicative of the validity of the expression and the assumptions involved in deriving it. The data points correspond to the 90% solvent and the molecular parameters for the solvent molecules are used for correlation. The fractional positive charge[17] on the nitrogen atom of the amide group may interact with the π-delocalized electron cloud of the benzene ring and may lead to the line broadening. This is in addition to the dispersion forces and therefore the data point for benzene solvent may not lie on the straight line which is representing mainly the dispersion force dependence. Thus vibrational relaxation time (τ_v) is shown to be a function

of the product of the hydrodynamic and dispersion force parameters. It is a very important and new information obtained for the first time in the present investigation.

References

[1] D. Scheibe, J. Raman Spectrosc. 13, 103 (1982)

[2] D.W. Oxtoby, J. Phys. Chem. 87, 3028 (1983).

[3] E.W. Knapp, J. Chem. Phys. 81, 643 (1984).

[4] W. Schindler, T.W. Zerda and J. Jonas, J. Chem. Phys., 81, 4306 (1984).

[5] G. Döge, R. Arndt and J. Yarwood, Mol. Phys., 52, 399 (1984).

[6] E.W. Knapp and S.F. Fischer, J. Chem. Phys. 74, 89 (1981).

[7] T. Bien and G. Doge, J. Raman Spectrosc. 12, 82 (1982).

[8] E.W. Knapp and S.F. Fischer, J. Chem. Phys. 76, 4730 (1982).

[9] V.F. Kalasinsky and T.S. Little, J. Raman Spectrosc. 14, 253 (1983).

[10] G. Fini and P. Mirone, J. Chem. Soc. F. Trans. II, 70, 1776 (1974).

[11] C.H. Wang and J. McHale, J. Chem. Phys., 72, 4039 (1980).

[12] M.G. Giorgini, G. Fini and P. Mirone, J. Chem. Phys., 79, 639 (1983).

[13] A. Purkayastha and K. Kumar, Spectrochim. Acta A, in press.

[14] J. Yarwood and R. Arndt in "Molecular Association", Vol.2, Ed. by R. Foster (Academic Press, London, 1979) and references therein pp.267-312.

[15] N. Mataga and M. Ottolenghi in "Molecular Association" Vol.2, Ed. by R. Foster (Academic Press, London, 1979) p.41.

[16] S. Bone, J. Eden, P.R.C. Gascoyne and R. Pething, J. Chem. Soc. F. Trans.I, 77, 1729 (1981).

[17] J.S.Dhull and D.R. Sharma, J. Phys. D 15, 2307 (1982).

[18] J. Timmermans, Physico - Chemical constants of pure organic compounds, Vol. 2 (Elsevier, Amsterdam , 1965)

[19] CRC Handbook of Chemistry and Physics Ed. by R.C. Weast., 58th Edition, (CRC Press, 1977-78).

Table V. 1. Molecular parameters and the function $f(\rho, \eta, n)$ for various solvent molecules.

Solvent	Refractive index n	Density (gm/c.c.) ρ	Viscosity (c poise) η	$f(\rho, \eta, n) = \left(\frac{n^2-1}{2n^2+1}\right)^{-1} \rho\eta$
CH_3CN	1.34154[a]	0.77656[a]	0.345[b]	1.54
C_6H_6	1.49859[a]	0.87369[a]	0.564[b]	2.18
$CHCl_3$	1.4459[b]	1.4798[a]	0.542[b]	3.80
CCl_4	1.45704[a]	1.58429[a]	0.843[b]	6.24

[a] Reference [18]

[b] Reference [19]

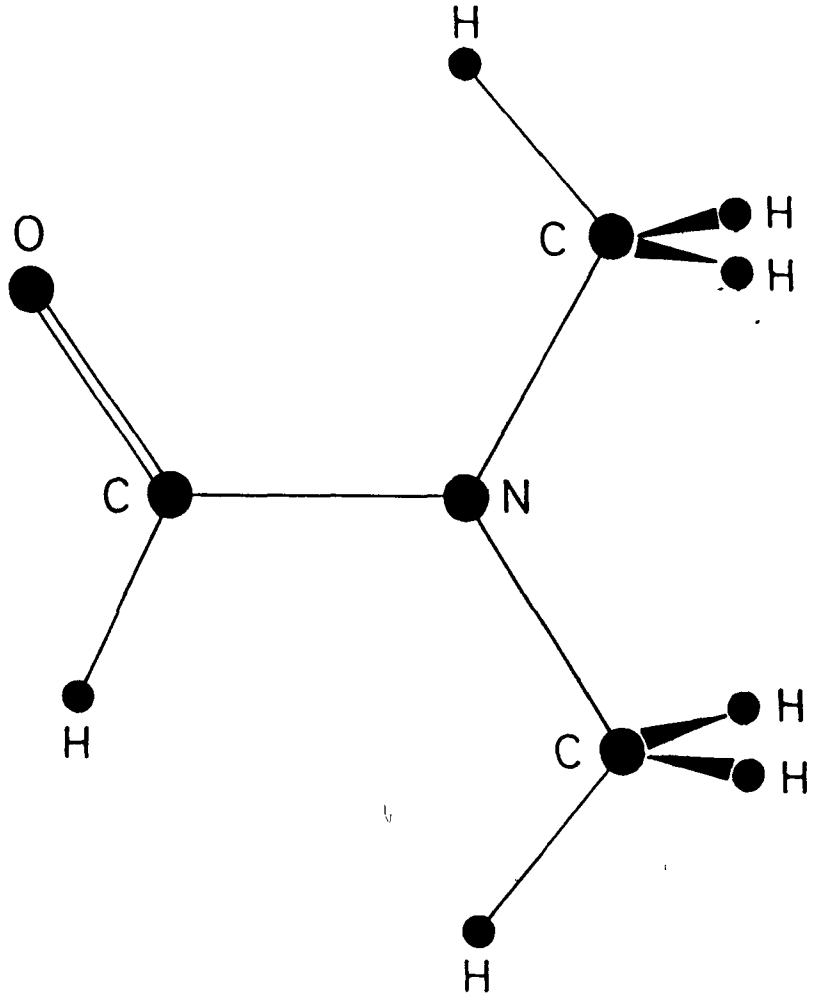

Fig. 5.1 The structure of N,N-Dimethylformamide molecule

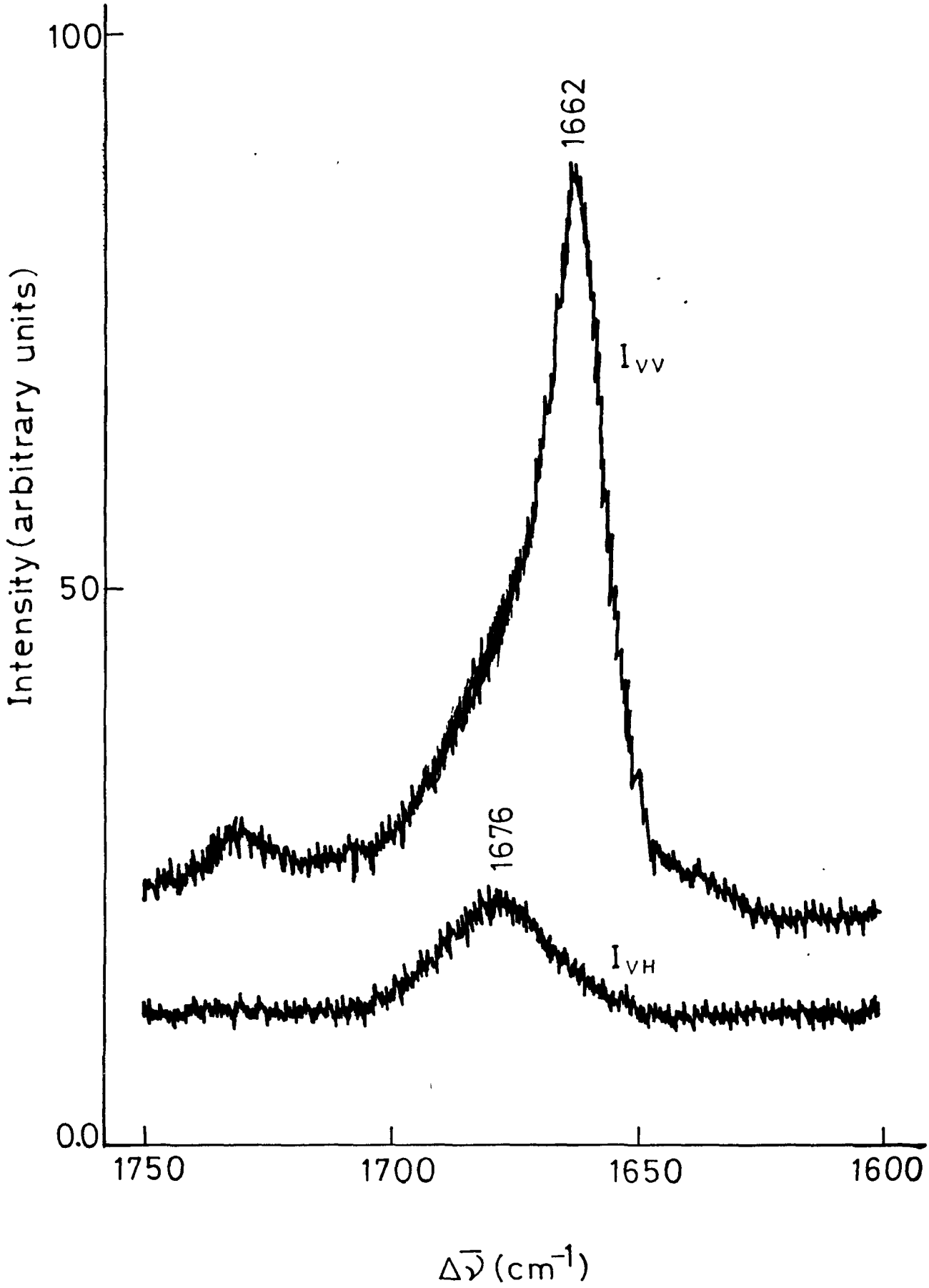

Fig.5.2 The laser Raman spectrum of DMF molecule in the amide I band region.

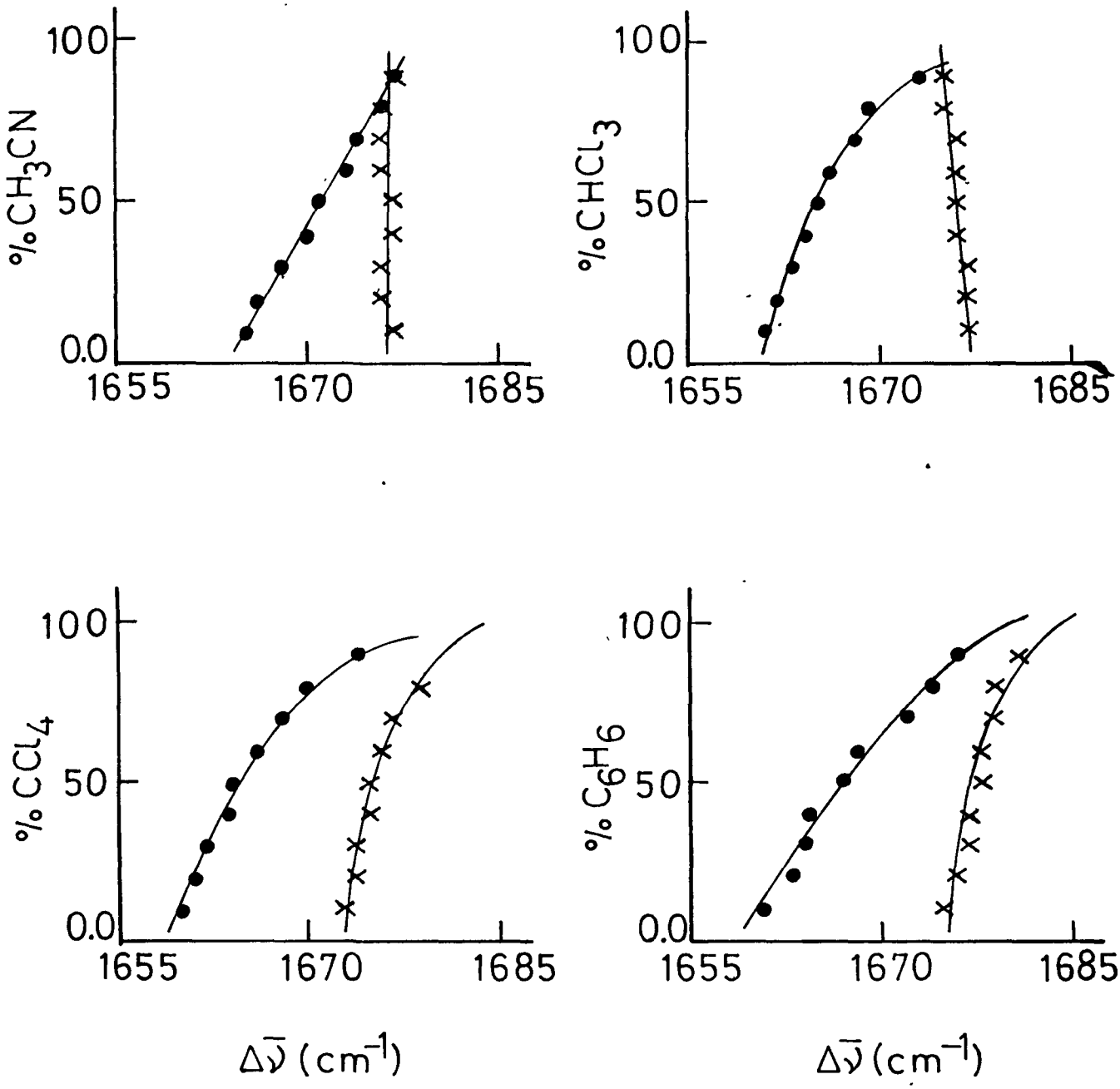

Fig. 5.3 The variation of isotropic(•) and anisotropic(×) maximum frequencies as a function of solvent(s) concentration.

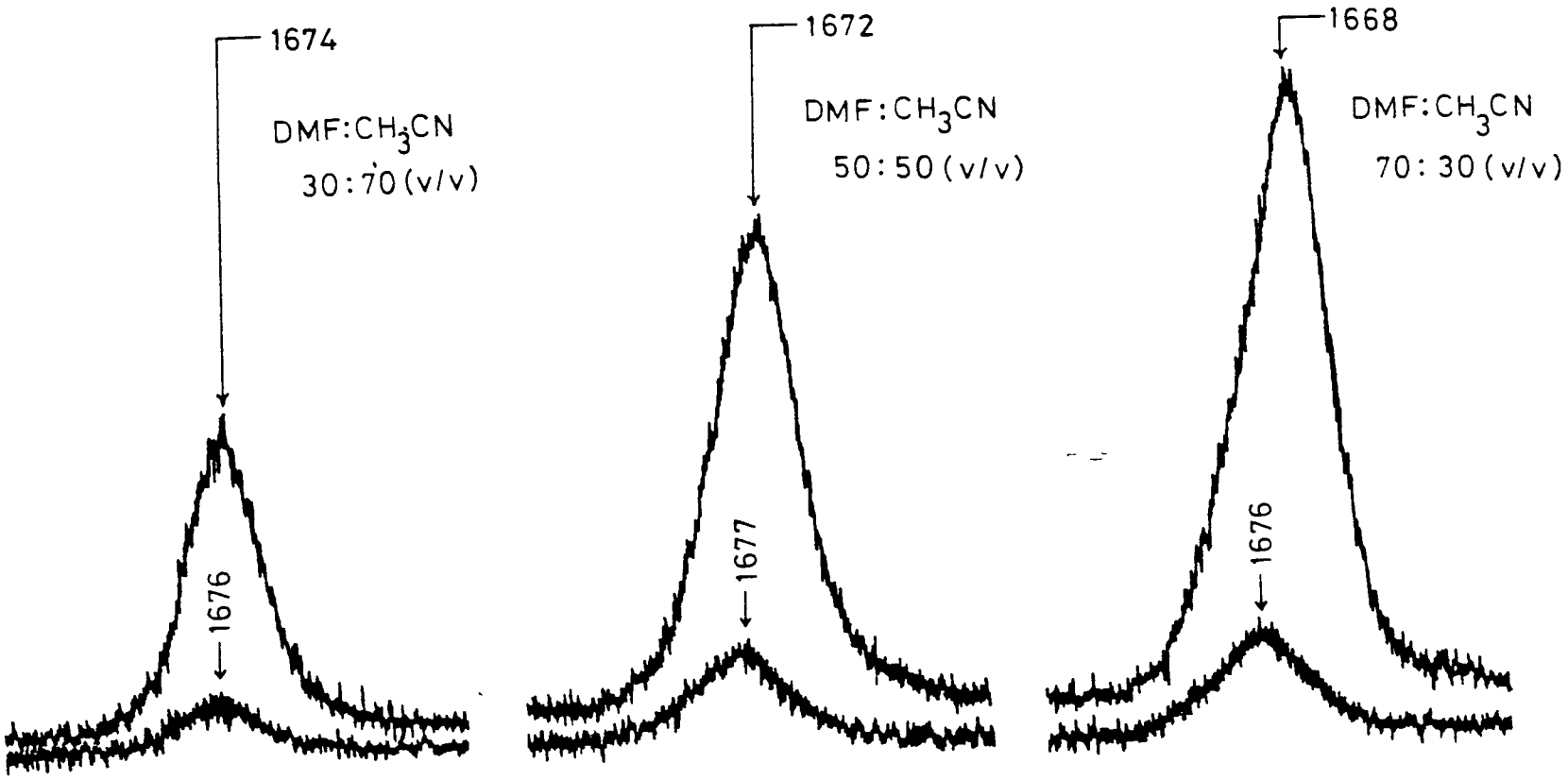

Fig. 5.4 The Raman spectrum showing amide I band of DMF in varying concentration of the solvent CH_3CN.

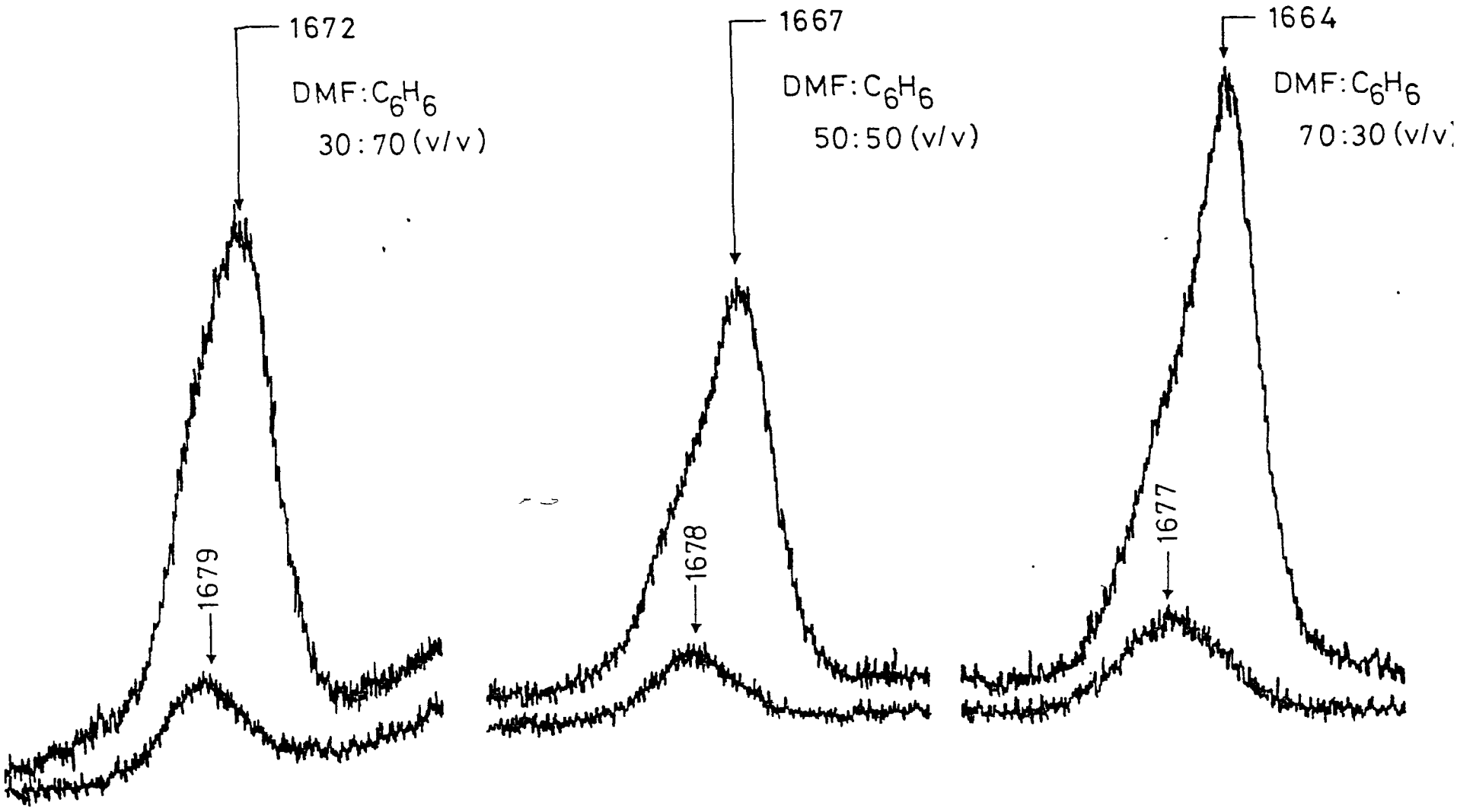

Fig. 5.5 The Raman spectrum showing amide I band of DMF in varying concentration of solvent C_6H_6. The spectrum of 30:70 composition is at a different scale than the other two compositions.

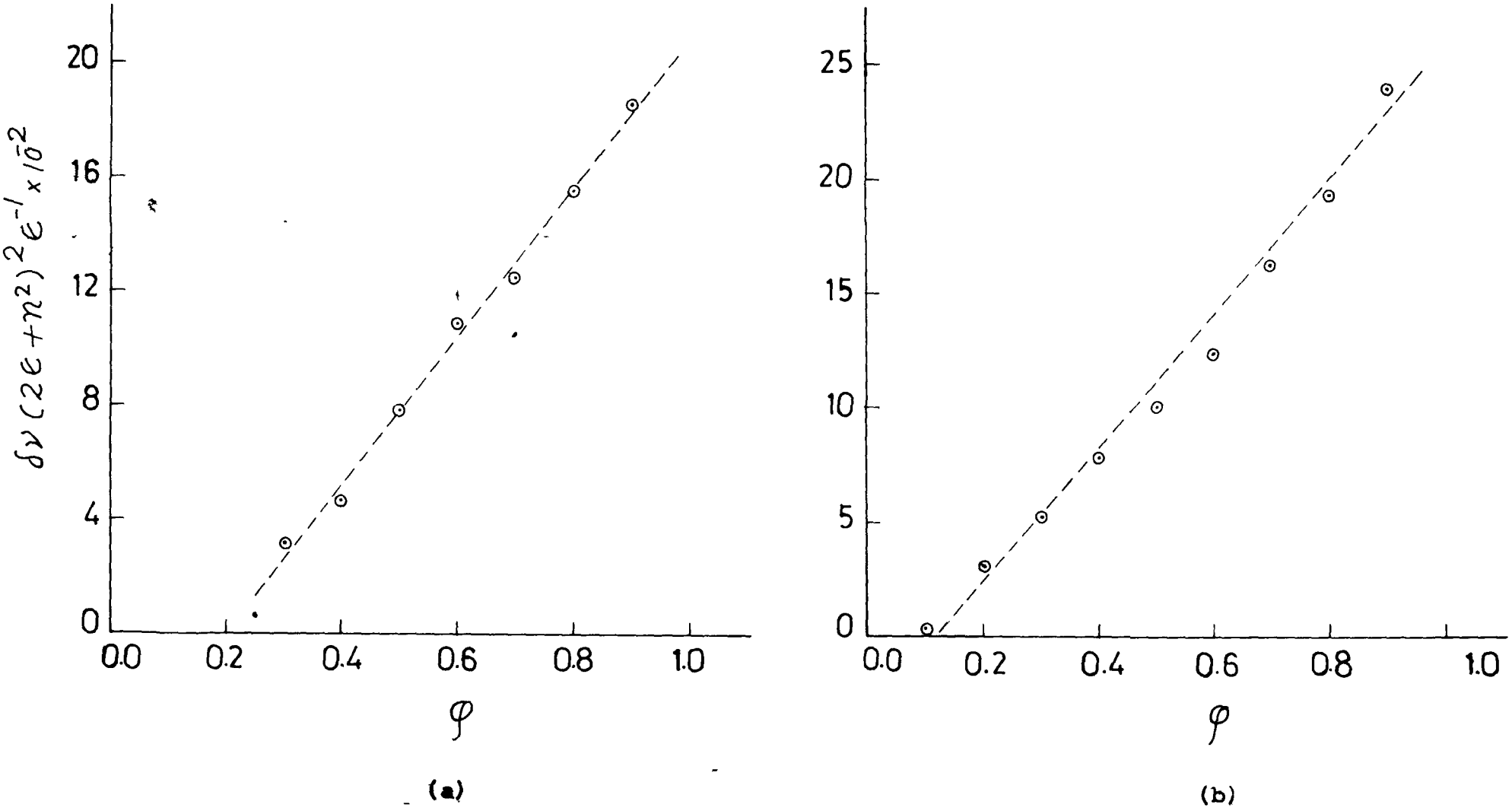

Fig. 5.6 The variation of the parameter $\delta\nu(2\epsilon + n^2)^2\ \epsilon^{-1}$ as a function of volume fraction φ of solute in solvents (a) CH_3CN, (b) $CHCl_3$.

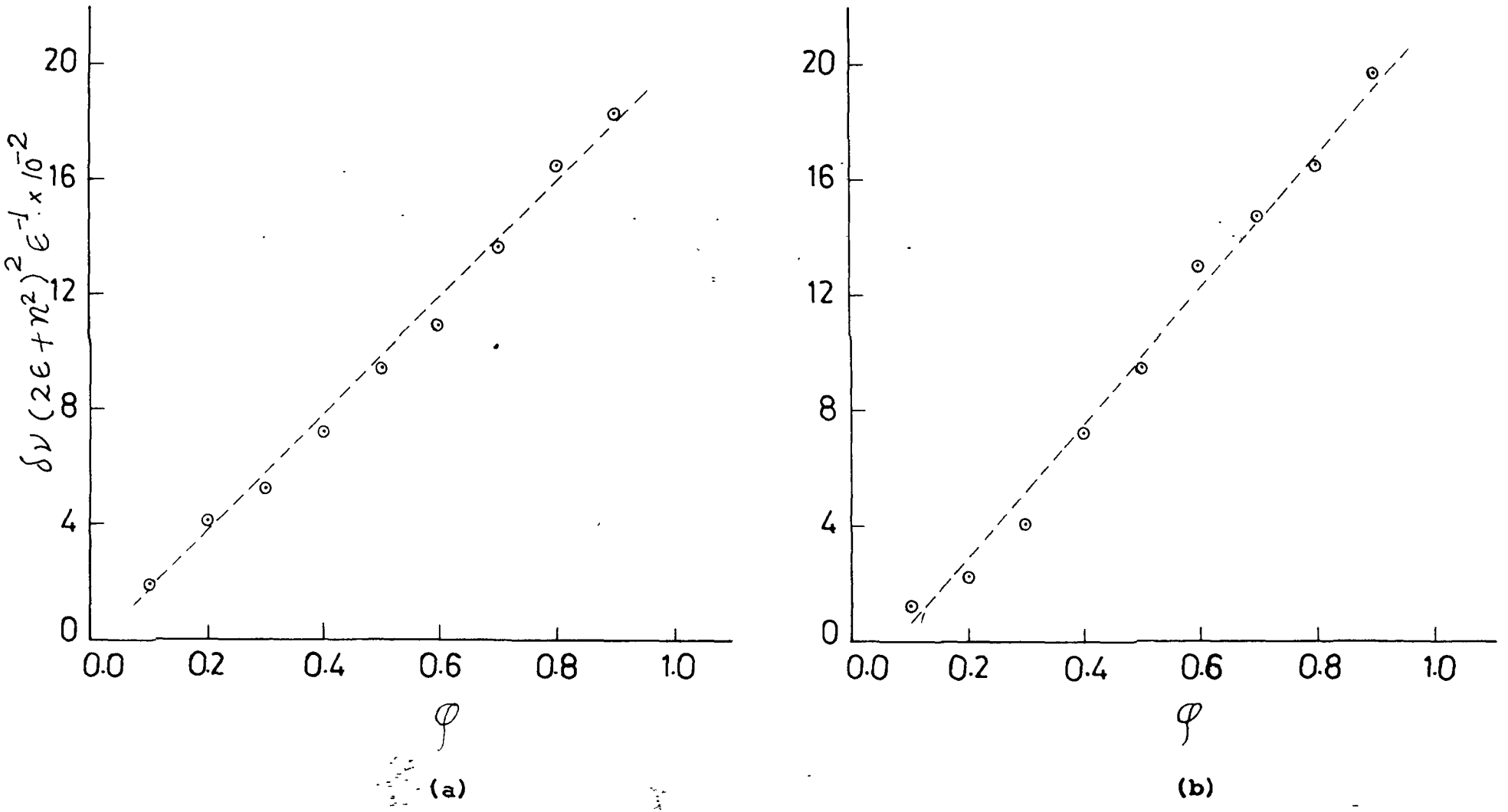

Fig. 5.7 The variation of the parameter $\delta\nu(2\epsilon+n^2)^2\epsilon^{-1}$ as a function of volume fraction φ of solute in solvent (a) CCl_4, (b) C_6H_6.

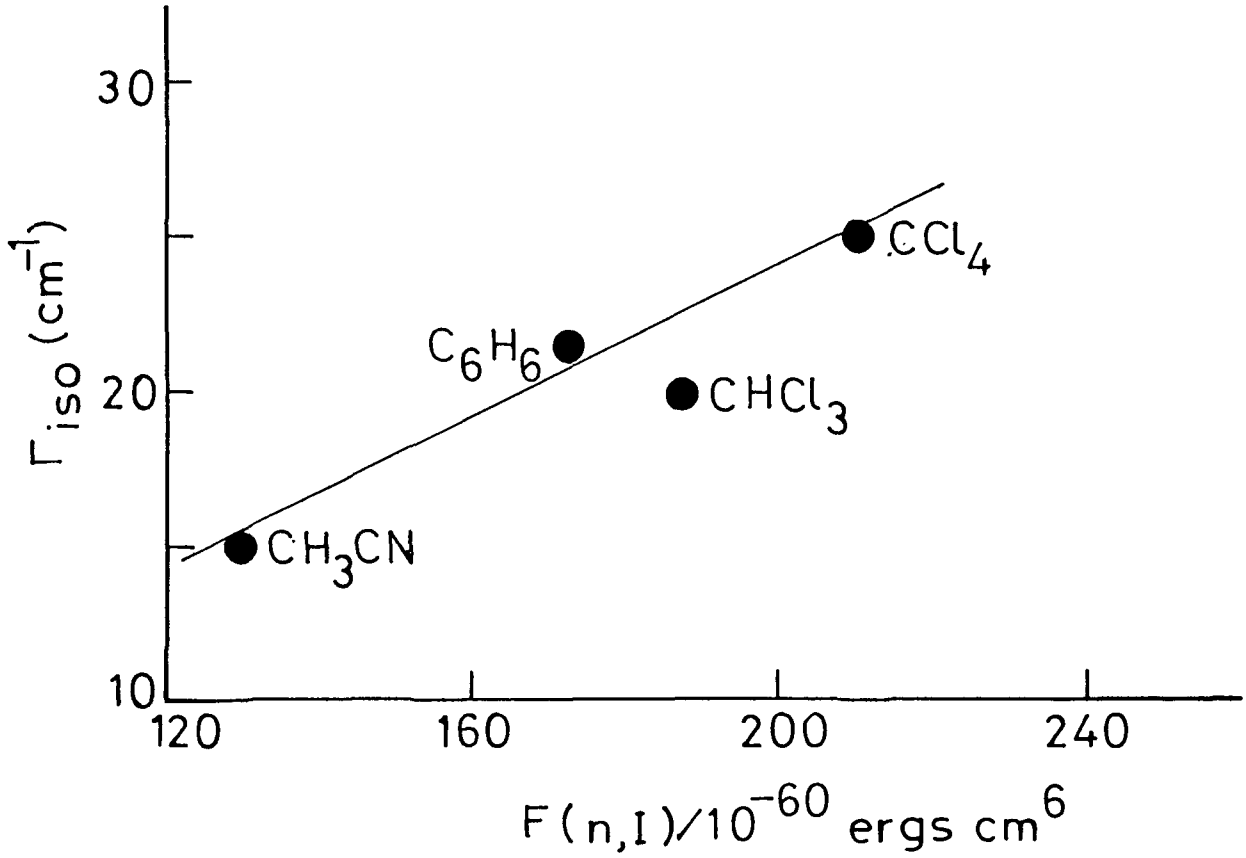

Fig. 5.8 The variation of the Γ_{iso} as a function of F(n,I) in various solvents.

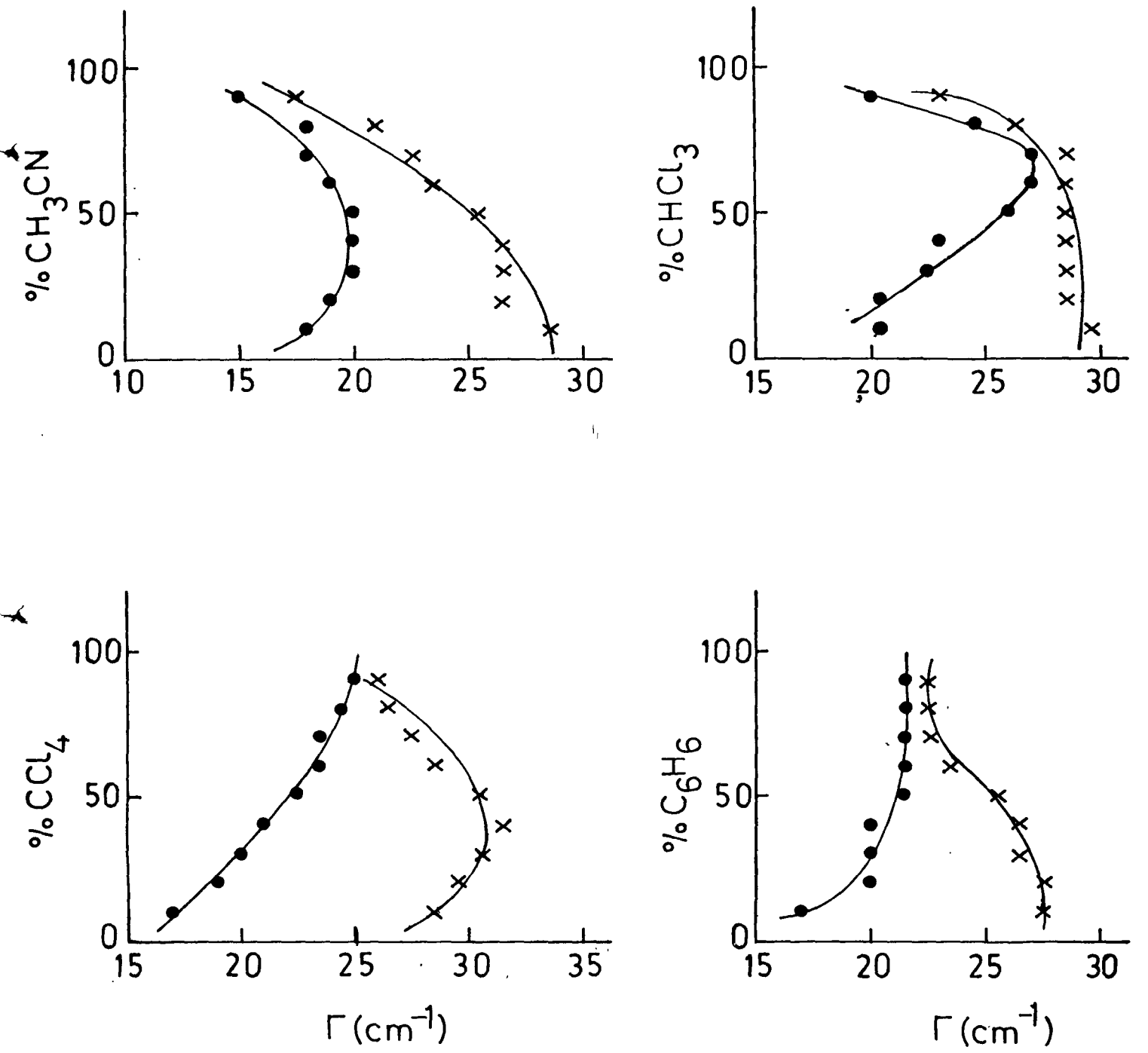

Fig. 5.9 The variation of FWHH as a function of solvent (s) concentration.

Γ_{iso} (•) , Γ_{aniso} (×) .

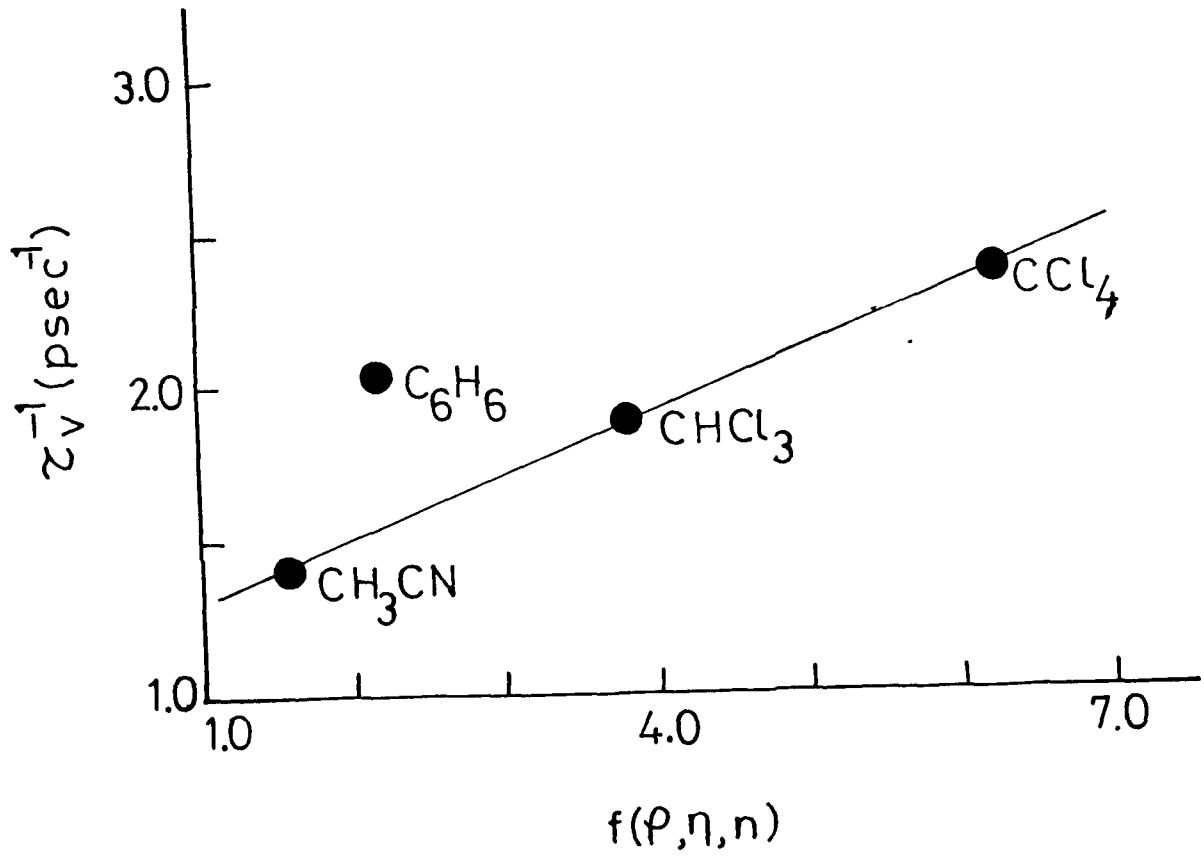

Fig. 5.10. The vibrational relaxation rate (τ_v^{-1}) dependence as a function of f (ρ, η, n). Concentration of DMF : Solvent, 10:90 v/v.

CHAPTER VI

VIBRATIONAL RELAXATION AND NONCOINCIDENCE EFFECT IN LIQUID CYCLOHEXANONE*

ABSTRACT

The vibrational relaxation and noncoincidence effect in liquid cyclohexanone molecule have been studied and explained in terms of molecular attraction parameters and van der Waals interactions. The line broadening of the isotropic component of the C=O stretching mode of cyclohexanone in different solvents is explained on the basis of dispersion forces. The parameter involving viscosity, density and refractive index has been correlated with the vibrational relaxation rate.

---

* Part of this work has been accepted for presentation: A Purkayastha and K. Kumar, International Conference on Laser Applications in Spectroscopy and Optics, Madras (1987)

CHAPTER VI

6.1 Introduction

The vibrational relaxation and reorientational motion in molecular liquids have been the subject of many theoretical and experimental studies in recent years[1-6]. These studies include the solvent dependence of the vibrational linewidth and frequency shifts in associated and non-associated liquids. However a systematic analysis of the effect of solvent on the structural and dynamic properties of the solute molecules is lacking. The analysis of the isotropic and anisotropic components of the Raman bands of a liquid can provide much information on the molecular structure and the vibrational and rotational motions of molecules.[4-10] Careful experimental studies indicate that in the Raman spectrum of some strongly polar molecules, the anisotropic component falls at a higher frequency than the isotropic component[4,11,12]. This noncoincidence between the isotropic and anisotropic components was interpreted as due to the coupling between vibrations of neighboring molecules with strongly polar modes (due to dipole-dipole interactions) in the liquid phase[4,13].

So far, the vibrational relaxation and noncoincidence effect have been studied extensively in some aldehydes, ketones and amides[4,6,11,12,14]. In this work the cyclohexanone ($C_6H_{10}O$) molecule was chosen for experimental study. The C=O stretching mode of cyclohexanone is a good example of a molecular

vibration which may show rather strong interactions. This molecule has not been investigated from the point of view of relaxation mechanism although some work related to conformational equilibrium has been done where it is shown that chair configuration is energetically more favourable[15]. The non-coincidence between the isotropic and anisotropic components of the C=O stretching mode of cyclohexanone was first reported by Fini and Mirone[11]. We have done an extensive study of the intermolecular interactions in this molecule. The solvent dependence of the vibrational relaxation time, frequency shifts and linewidth (FWHM) of cyclohexanone has been investigated. Raman spectral measurements were made for the pure liquid phase and in various solvents as a function of concentration. The infrared spectrum of the corresponding band was also recorded for the pure liquid. The experimental results were interpreted in terms of molecular attraction parameters, dipole-dipole interactions, dispersion forces etc.

6.2 Experimental

The sample of cyclohexanone and the solvents CCl_4, C_6H_6, $CHCl_3$ and CH_3CN were obtained commercially and were used without further purification. Raman spectra were recorded on a Spex Ramalog 1403 double monochromator with datamate equipped to use the 4880 A° line of a Spectra-Physics model 165 Ar^+ laser as the excitation source. The experiments were performed with a maximum power of about 500 mW. The slit

width employed was ~ 4 cm^{-1} for all recorded spectra. The polarized and depolarized parts of the band were obtained by changing the orientation of the analyzer placed in the scattered beam. The intensity of the isotropic component was calculated by using the standard formula

$I_{iso}(\omega) = I_{VV}(\omega) - \frac{4}{3} I_{VH}(\omega)$ and $I_{aniso}(\omega) = I_{VH}(\omega)$.

For the cases where the depolarization ratio is very small $I_{iso}(\omega) \approx I_{VV}(\omega)$. The finite slit width effect on the observed linewidth was corrected according to the usual formula (eqn.3.4). The accuracy of measurements is believed to be $\pm$ 1 cm^{-1} for Raman spectral measurements. The infrared spectra were recorded as a thin film of liquid between two KBr plates using Perkin-Elmer 983 infrared spectrophotometer.

6.3 Results and Discussion

The geometry of the cyclohexanone in the energetically favoured chair configuration has been described by Tai and Allinger[15]. The optimal bond lengths and valence angles are shown in Fig.6.1 where the atoms are numbered arbitrarily from 1 to 17 starting with oxygen[16].

The geometry assumed for cyclohexanone possesses a single element of symmetry, a plane through atoms 1,2,5,8,9. This yields two species of vibrations A' and A" which are respectively symmetric and antisymmetric to the symmetry plane. This system belongs to the point group C_s, and the 17 atoms are associated with 45 nondegenerate normal vibrations. Of

these, 25 belong to the A' species and 20 to the A" species. The three internal coordinates associated with the carbonyl group are the stretch, the in-plane bend and the out-of-plane bend (Fig 6.2). A priori, three corresponding group frequencies might be expected. The stretch plays a major part in organic structure analysis, but the two other vibrations have only minor value for structural diagnosis. It is to be emphasized that in this context "in-plane" and "out-of-plane" relate to the local site symmetry of the C-CO-C group and not to the symmetry plane of cyclohexanone.

The "C=O stretching band" is calculated for $C_6H_{10}O$ at 1715 cm^{-1} and observed at 1718 cm^{-1} in the infrared and at 1710 cm^{-1} in the Raman spectrum.[16] The potential energy coefficients indicate that five internal coordinates participate significantly in the 1715 cm^{-1} mode. The contribution from the C=O stretch coordinate is about 75% with the other contributions coming from the symmetric stretch of the -CC bonds 2, two symmetric angle bends 3,4 and the C=O in plane deformation 5. There are no significant contributions from bonds more remote than the $-CH_2$ groups.

The vibrations of neighboring molecules with strongly polar Raman bands are coupled by intermolecular interactions. The analysis of the lineshape of the isotropic and anisotropic components of Raman bands of a liquid gives information about the spherically symmetric part of inter, intramolecular forces

and anisotropic forces respectively. The information about vibrational relaxation and molecular reorientation processes may be obtained by the analysis of lineshapes of the isotropic and anisotropic components of Raman band. The Raman spectra of the cyclohexanone molecule show that the anisotropy shift is of the order of 7 cm^{-1} (Fig. 6.3) in neat liquid. The infrared absorption band corresponding to the Raman band under study is also very strong which indicates that the splitting factor is indeed related to the intensity of the infrared band.

The laser Raman spectrum of pure cyclohexanone (Fig.6.3) also shows that the I_{VV} component of the spectrum corresponding to the carbonyl stretching band has a shoulder whereas the I_{VH} (anisotropic) component is very symmetric with its peak shifted to higher frequencies. The differences between the peak frequencies ($\sim$ 7 cm^{-1}) and the asymmetry of the I_{VV} component may be explained by taking into consideration the resonant coupling due to transition dipole-transition dipole (TD-TD) interactions on the Raman band shape. This explanation that the two frequencies differ due to resonant coupling is supported by the experimental data related to the effect of solvent on the Raman band of cyclohexanone molecule. This difference in the frequencies decreases as the concentration of the solvent is increased irrespective of the nature of the solvent (Fig. 6.4). This is particularly explained on the basis of the data for the inert solvents where other interactions are supposed to be

minimum and the solvents are expected to turn off the resonant coupling between the cyclohexanone molecules for the carbonyl stretching mode of vibration.

The variations of the peak frequency and linewidth of the C=O stretching mode of cyclohexanone ($C_6H_{10}O$) are shown as a function of the concentration of CH_3CN, $CHCl_3$, CCl_4 and C_6H_6 solvents in Figs. 6.4 and 6.5. The behaviour of C=O band in different solvents may be summarized as follows:

CH_3CN - $C_6H_{10}O$ system

In CH_3CN the maximum frequency of the isotropic component increases linearly to higher wavenumbers compared to the pure liquid, whereas the anisotropic maximum decreases linearly. There is an almost linear decrease of both the isotropic and anisotropic half width as the concentration of solvent is increased. CH_3CN being a polar solvent is able to almost substitute for the cyclohexanone molecules.

$CHCl_3$ - $C_6H_{10}O$ system

On dilution with $CHCl_3$, the isotropic maximum tends to increase in the beginning (small concentration of the solvent). However, in $CHCl_3$ there is a possibility of the formation of hydrogen bond with the C=O group of cyclohexanone. As a result, with increasing dilution the isotropic part shifts to lower wavenumbers upto 40% concentration. This shift however, decreases on further dilution as the effect of resonant transfer of vibrational energy due to transition dipole-transition dipole

interaction on the band shape is removed. The anisotropic maximum frequency, on the other hand decreases linearly with dilution. Both the isotropic and anisotropic bands are found to be broadened at around 40% dilution.

CCl_4 - $C_6H_{10}O$ and C_6H_6 - $C_6H_{10}O$ systems

The behaviour of C=O stretching band in these two solvents is very similar. With increasing concentration of the solvents, the isotropic maximum frequency shifts to higher wavenumbers. The anisotropic maximum frequency, however, remains almost constant, (in C_6H_6) or increases a little (in CCl_4) in the region of high dilution. The anisotropy shift tends to vanish towards higher dilution in CCl_4, whereas in C_6H_6 the two frequencies coincide at about 90% solvent concentration. In CCl_4 solvent, there is not much change in the FWHH of both the components upto a certain concentration (70% solvent). However when the concentration of CCl_4 is increased further, the FWHH starts decreasing. In C_6H_6, Γ_{iso} remains almost constant upto 60% solvent concentration. Γ_{aniso}, on the other hand, decreases a little in the beginning of dilution and later it remains constant upto a concentration of 70%. Further as the amount of solvent is increased, both Γ_{iso} and Γ_{aniso} starts decreasing.

The validity of equation (4.17) was tested by plotting the quantity $\delta\nu\,(2\epsilon+n^2)^2\;\epsilon^{-1}$ as a function of the volume fraction (φ) of the solute. The screening factor S_t does not

vary much with the variation of the solvent and therefore may even be treated as constant. The variations are shown in Fig.6.6 and 6.7. Since the plots are almost linear it is clear that the equation holds good in case of cyclohexanone molecule also.

The van der Waals attractions are very important in case of liquids. For the case of large separations one may consider mainly three types of van der Waals interactions, as discussed in Chapter IV, depending upon whether the interacting molecules possess permanent dipoles or not. The total interaction energy in a medium of dielectric constant ϵ and refractive index n may be given by,

$$E = -\frac{1}{R_{ij}^6}\left[A + B + C\right], \qquad \ldots\ (6.1)$$

where $A = \frac{2\mu_i^2\mu_j^2}{3kT} \cdot \frac{1}{\epsilon^2}$,

$$B = \frac{\alpha_i \mu_j^2 + \alpha_j \mu_i^2}{\epsilon^2},$$

and $C = \frac{3}{2} \cdot \frac{1}{n^4} \frac{I_i I_j}{(I_i + I_j)} \cdot \alpha_i \alpha_j = F(n, I)$

The above three interaction terms are expected to play role in the full width at half height (FWHH) of isotropic component (Γ_{iso}) of the Raman band. Their relative contributions have to be calculated by taking into consideration the molecular parameters (ϵ, n, μ, α and I). It is expected that these three terms will give an idea about long-range interactions and its role in line broadening. The values of the interaction energy parameters for the systems $C_6H_{10}O$ - CH_3CN, $C_6H_{10}O$ -

$CHCl_3$, $C_6H_{10}O$ - CCl_4 and $C_6H_{10}O$ - C_6H_6 are given in Table VI.1. It can be seen from the table VI.1 that for all the interacting systems involving different solvents, the dispersion energy parameter has the maximum value even in case of solvent molecules with dipole moment. It is mainly because of the ε^2 dependence of dipole-dipole and dipole-induced dipole type of interactions for the solvents of high dielectric constant. Even in the case of highly polar solvents the dispersion energy is going to play a very important role. The variation of Γ_{iso} as a function of dispersion energy parameter in the four solvents was studied at 90% solvent concentration and is shown in Fig.6.8. It is a straight line which explains the experimental observation, by taking into consideration only the contribution from dispersion type long range forces.

The linewidth measurements may be of considerable value in order to understand the molecular dynamics. The inhomogeneous and homogeneous contributions to the linewidths may be separated by time dependent techniques[1,10]. The collisions with solvent molecules lead to homogeneous broadening. The randomization of vibrational phase due to elastic collisions leads to line broadening. This mechanism of line broadening is called pure dephasing. The discrimination between inhomogeneous (static) and homogeneous (dynamics) broadening is arbitrary in nature to some extent. The broadening mechanisms are inhomogeneous (slow modulated) or homogeneous (fast modulated) depending upon

whether $\langle \Delta\omega^2 \rangle^{1/2} \tau_c \gg 1$ or $\langle \Delta\omega^2 \rangle^{1/2} \tau_c \ll 1$. The lineshape is Lorentzian in case of homogeneous broadening ($\langle \Delta\omega^2 \rangle^{1/2} \tau_c \ll 1$). The $\langle \Delta\omega^2 \rangle^{1/2}$ and $1/\tau_c$ denote frequency shift and the rate of change between the various inhomogeneous components. The vibrational relaxation times were calculated assuming Lorentzian lineshapes for Raman band under study. The following relations[17] were used for calculation purpose:

$$\tau_v = (\pi c \Gamma_{iso})^{-1} \qquad \ldots\ldots (6.2)$$

where Γ_{iso} is the FWHH of the isotropic component.

The variation of the τ_v^{-1} as a function of $f(\rho,\eta,n)$, the parameter which is dependent upon the viscosity, density and refractive index as mentioned in Chapter V is shown in Fig.6.9. It is very clearly a linear variation and the fitting of the parameter in case of the four solvents is quite good. This therefore informed empirically that the linewidth or τ_v^{-1} is a function of all these parameters. This result is quite encouraging as it supports the idea presented in Chapter V in connection with the Dill vibrational relaxation studies. The role of the hydrodynamic force parameter η and the dispersion force parameter $\left(\frac{n^2-1}{2n^2+1}\right)^{-1}$ therefore seems to be significant in the line broadening mechanism of the cyclohexanone molecule.

References

[1] E.W. Knapp, J. Chem. Phys. 81, 643 (1984)

[2] D.W. Oxtoby, J. Phys. Chem. 87, 3028 (1983).

[3] F. Seifert, K.L. Oehme, G. Rudakoff, W. Hölzer, W. Carius and O. Schrötter, Chem. Phys. Lett. 105, 635 (1984).

[4] W. Schindler, T.W. Zerda and J. Jonas, J. Chem. Phys. 81, 4306 (1984).

[5] G. Döge, R. Arndt and J. Yarwood, Mol. Phys. 52, 399 (1984)

[6] L. Scheibe, J. Raman Spectrosc. 13, 103 (1982).

[7] V.F. Kalasinsky and T.S. Little, J. Raman Spectrosc. 14, 253 (1983).

[8] E.W. Knapp and S.F. Fischer, J. Chem. Phys. 74, 89 (1981).

[9] T. Bien and G. Doge, J. Raman Spectrosc. 12, 82 (1982).

[10] E.W. Knapp and S.F. Fischer, J. Chem. Phys. 76, 4730 (1982).

[11] G. Fini and P. Mirone, J. Chem. Soc. F. Trans. II 70, 1776 (1974).

[12] P. Mirone and G. Fini, J. Chem. Phys. 71, 2241 (1979).

[13] C.H. Wang and J. McHale, J. Chem. Phys. 72, 4039 (1980).

[14] J. Yarwood and R. Arndt, in "Molecular Association", Vol.2, Ed. by R. Foster (Academic Press, London, 1976) p.267.

[15] J.C. Tai and N.A. Allinger, J. Am. Chem. Soc. 88, 2179 (1966).

[16] H. Fuhrer, V.B. Kartha, P.J. Krueger, H.H. Mantsch and R.N. Jones, Chem. Rev. 72, 439 (1972).

[17] K. Fukushi and M. Kimura, J. Raman Spectrosc. 13, 9 (1982).

Table VI.1. The dipole-dipole, dipole-induced dipole and dispersion energy parameters for various solvent systems.

Molecular system	A /(ergs-cm^6) x 10^{-60}	B /(ergs-cm^6) x 10^{-60}	C /(ergs-cm^6) x 10^{-60}
$C_6H_{10}O$-CH_3CN	1.36	0.15	195.5
$C_6H_{10}O$-$CHCl_3$	6.14	3.71	282.48
$C_6H_{10}O$-CCl_4	0.0	16.71	318.63
$C_6H_{10}O$-C_6H_6	0.0	15.45	259.94

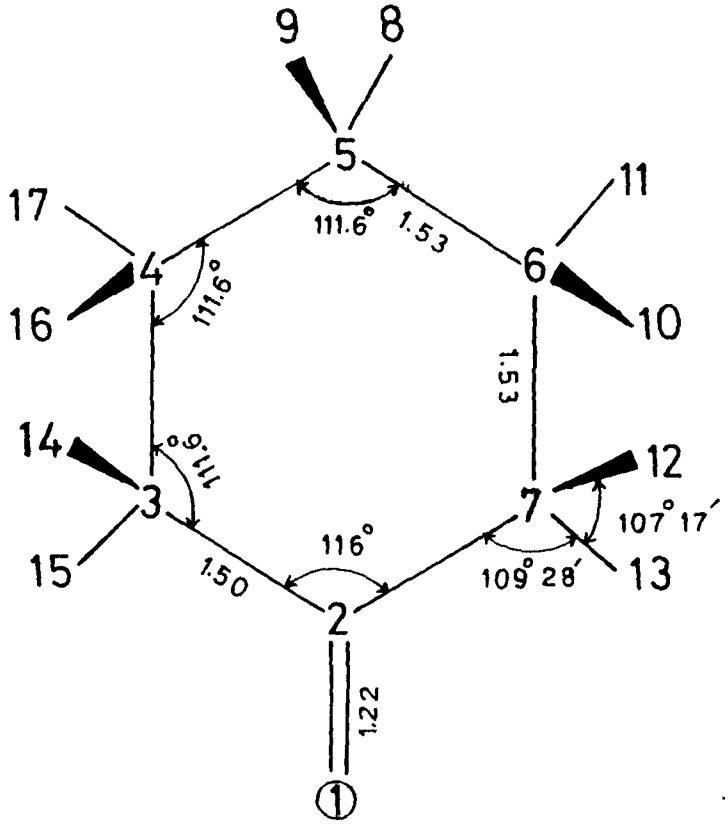

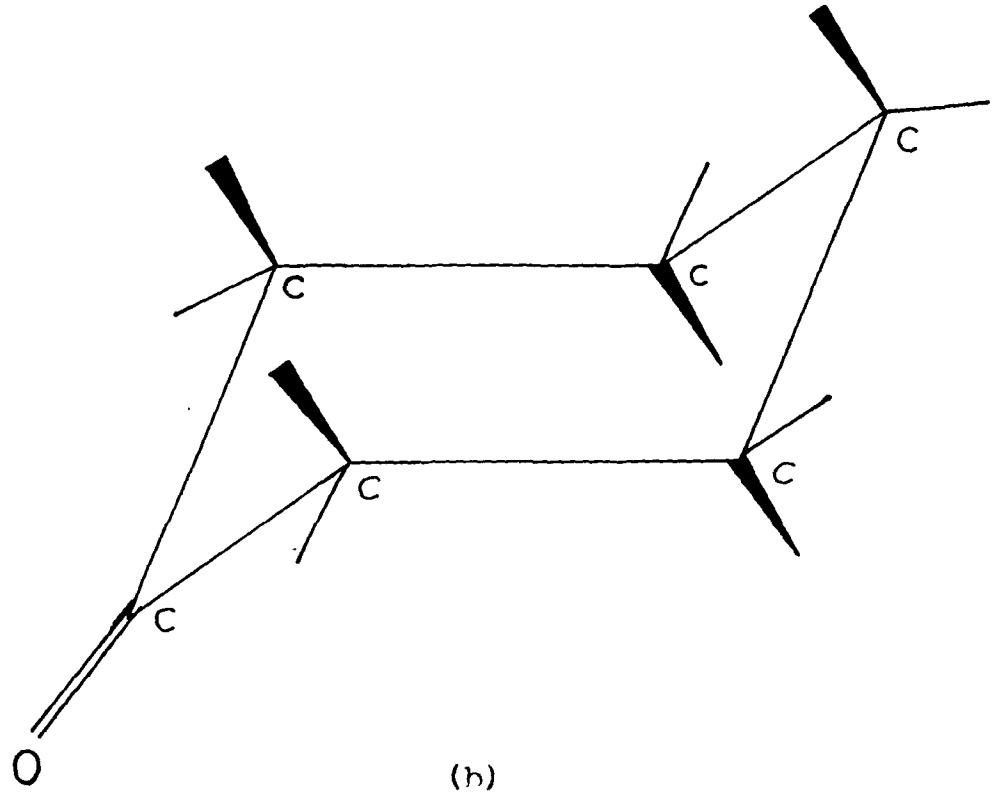

Fig. 6.1 (a) The structural parameters of cyclohexanone in chair conformation (b) The chair conformation of cyclohexanone

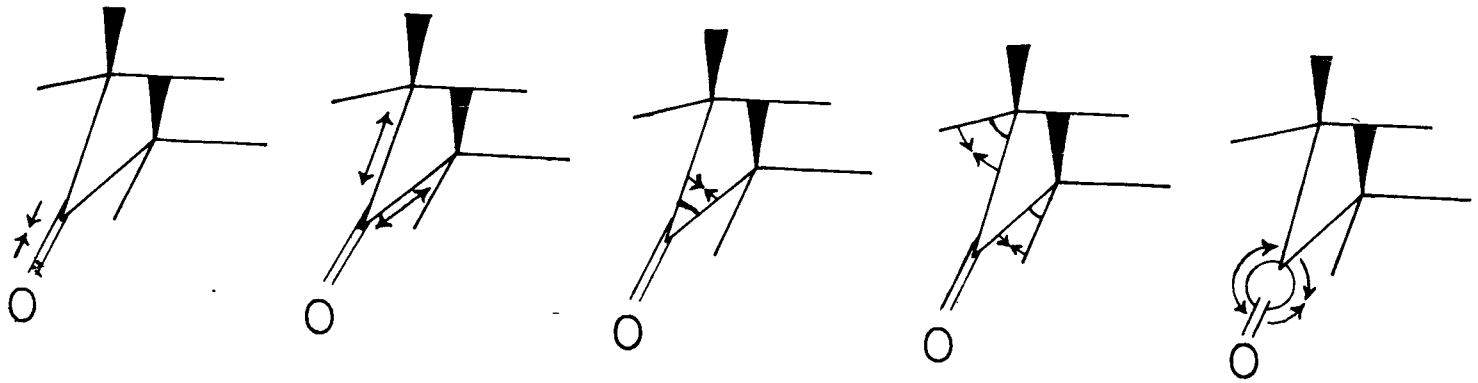

1 2 3 4 5

	1 (v)	2 (r)	3 (x)	4 (γ_α)	5 (ϵ)
ν_{calcd} = 1715 cm^{-1}	75	13	6	5	2

Fig. 6.2 **Vibrational motions participating in the carbonyl stretch band.**

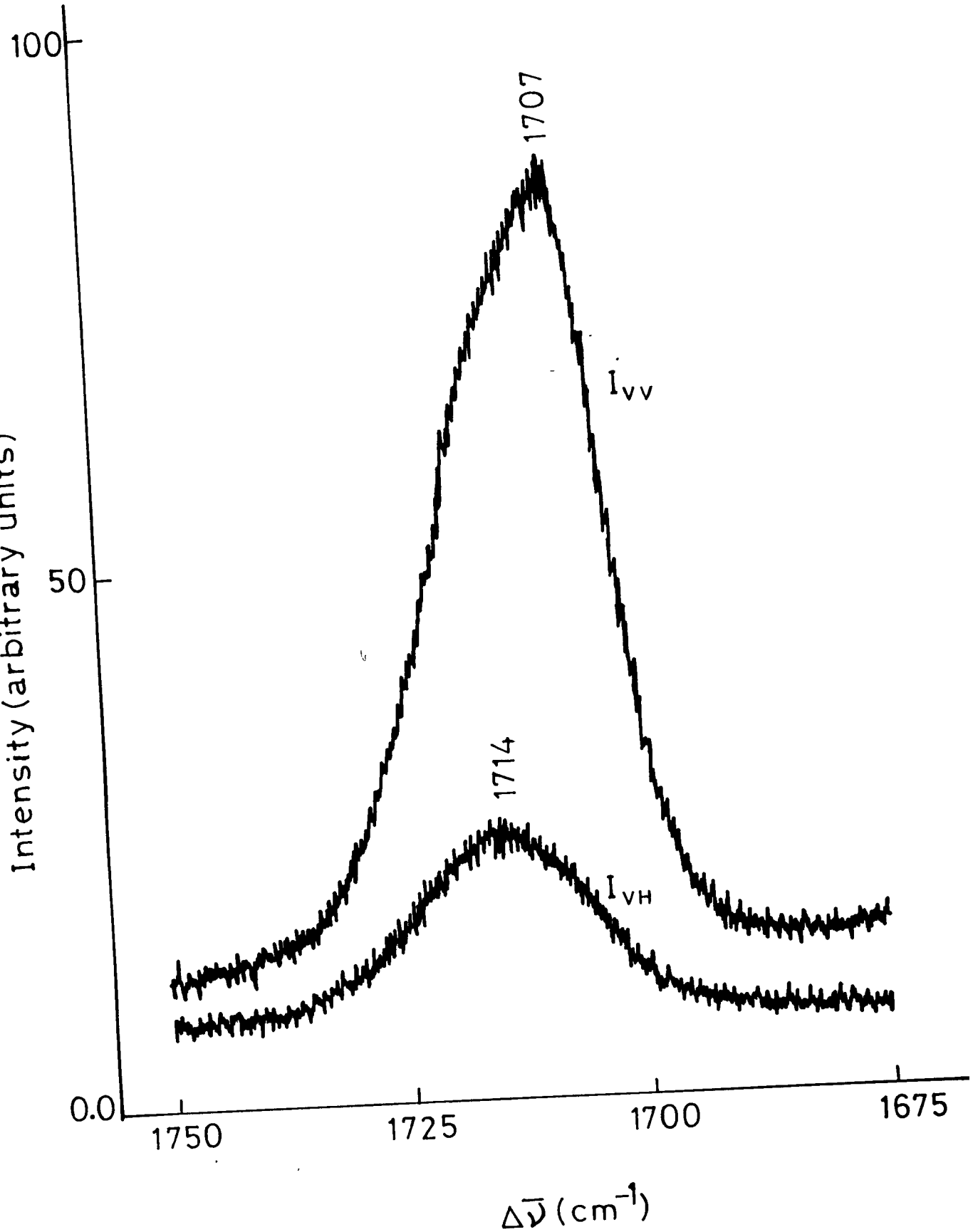

Fig. 6.3 The I_{VV} and I_{VH} components of the C=O st. vibrational mode
pure liquid cyclohexanone.

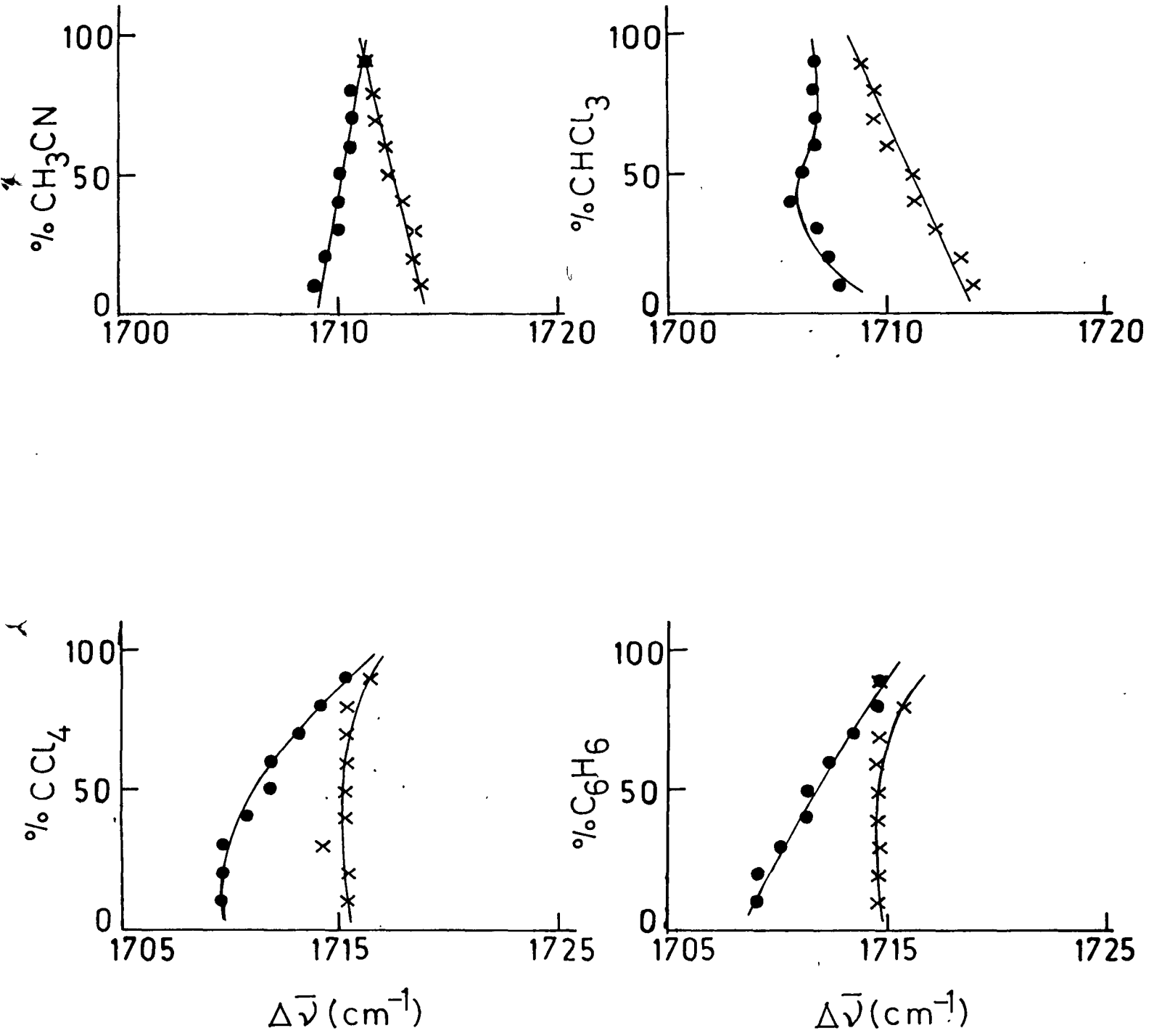

Fig. 6.4 The variation of isotropic (●) and anisotropic (x) maximum frequencies as a function of solvent (s) concentration.

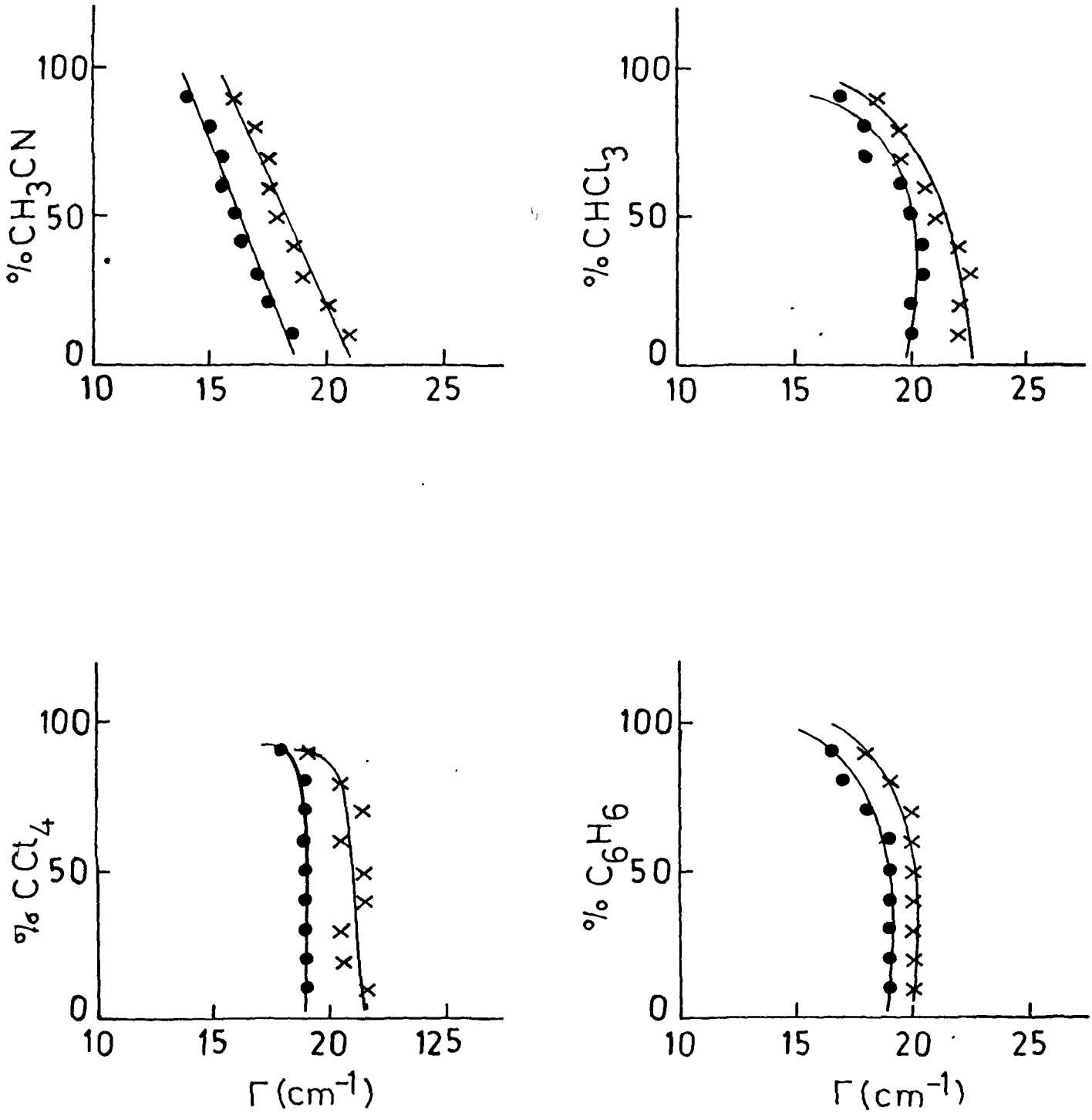

Fig. 6.5 The variation of isotropic (●) and anisotropic (x) FWHH as a function of solvent (s) concentration.

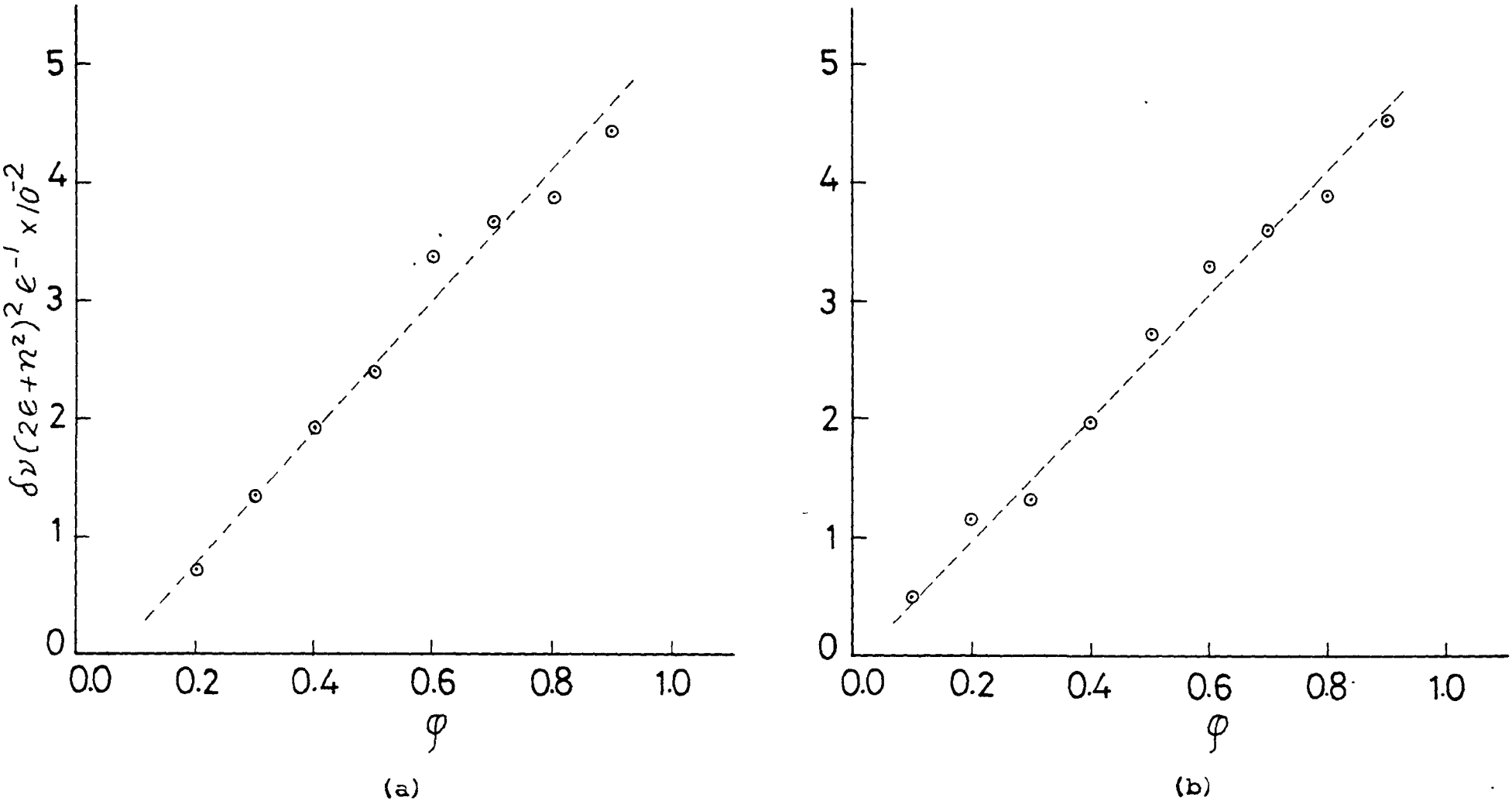

Fig. 6.6 The group showing the variation of $\delta\nu(2\epsilon + n^2)^2\ \epsilon^{-1}$ as a function of volume fraction φ of solute in solvent (a) CH_3CN, (b) $CHCl_3$.

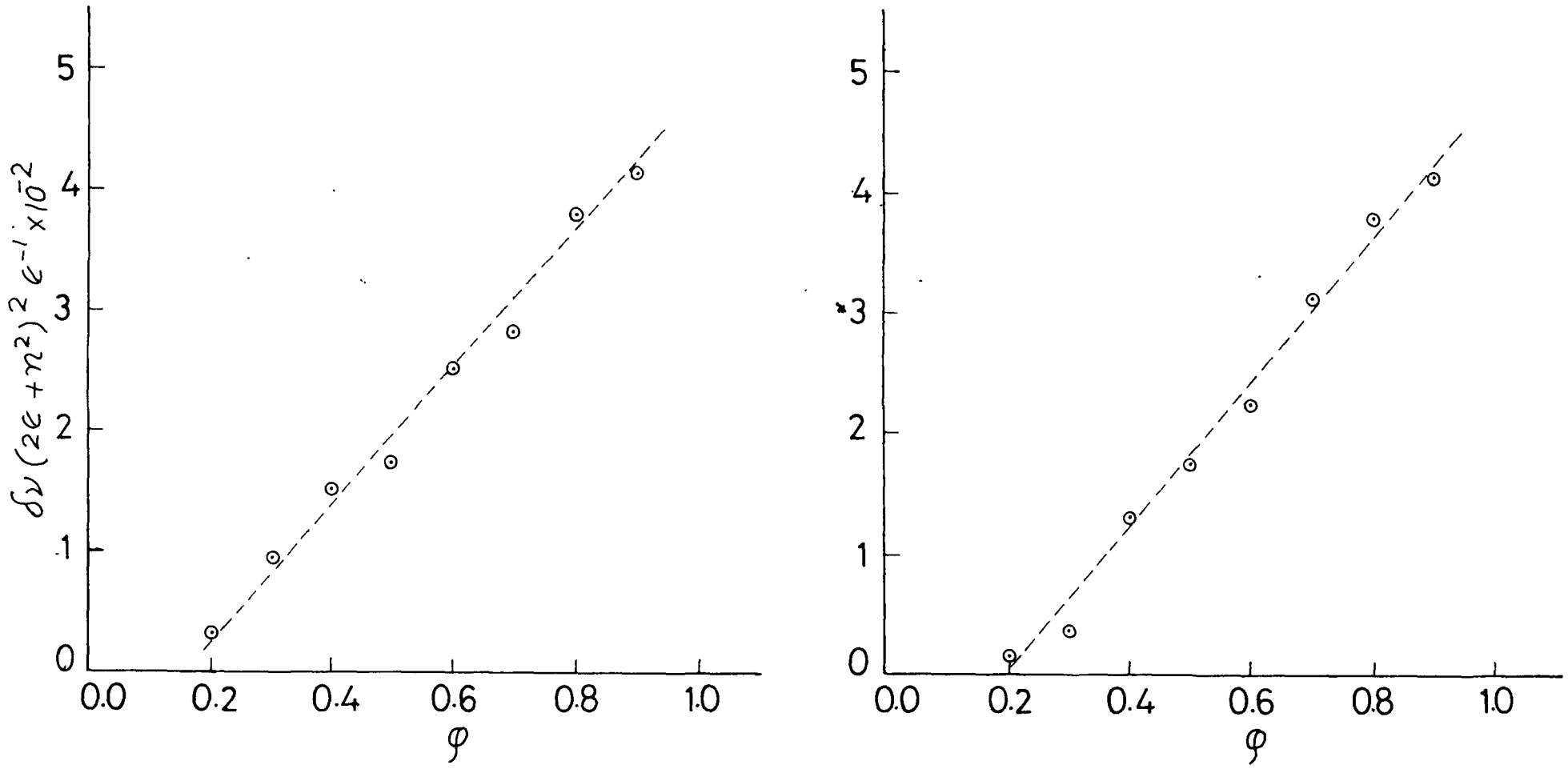

Fig. 6.7 The graph showing the variation of $\delta\nu(2\epsilon + n^2)^2\ \epsilon^{-1}$ as a function of volume fraction φ of solute in solvent (a) CCl_4, (b) C_6H_6.

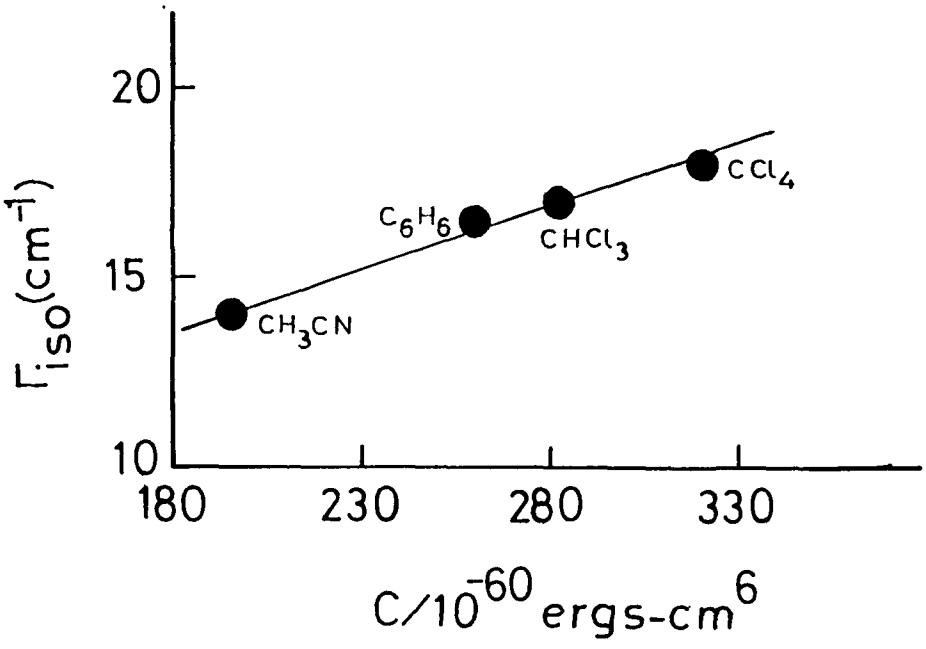

Fig. 6.8 The variation of Γ_{iso} as a function of dispersion energy parameter $C = F(n,I)$.

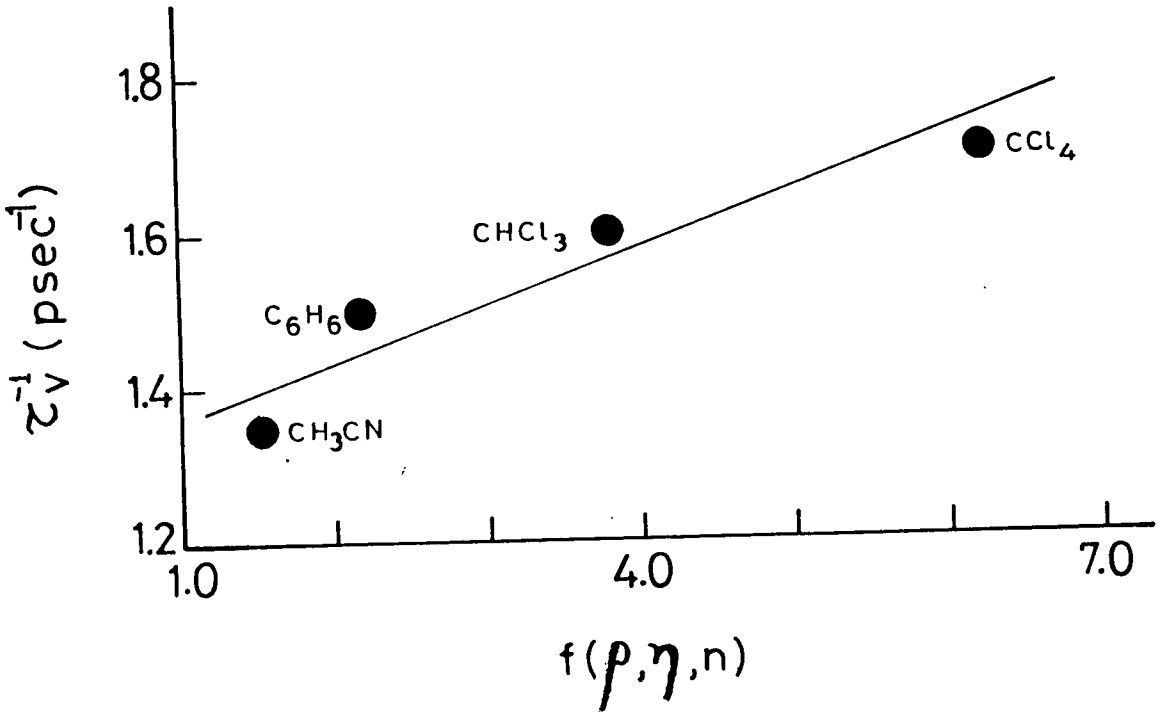

Fig. 6.9 The variation of τ_v^{-1} as a function of the parameter $f(\rho, \eta, n)$ for the cyclohexanone molecule.

CHAPTER VII

Conclusions

The laser-Raman scattering studies have been carried out on N,N-Dimethylacetamide (DMA), N,N-Dimethylformamide (DMF) and Cyclohexanone molecules. The amide I modes of DMA, DMF and C=O st. mode of Cyclonexanone were chosen for experimental study. These liquids have strong intermolecular interactions and the solvent dependence of the Raman band shapes were studied. The bands were recorded for various solutions as a function of concentration. These moleculeshave permanent dipole moments: DMA (μ=3.81 D), DMF (μ=3.82 D) and Cyclohexanone (μ=2.79 D). It may therefore be assumed that the liquid structure is mainly created by the orientation dependence dipole potential. Therefore only dipole interactions are considered for ordering of the molecules. The interaction potential between two permanent point dipoles has been considered taking care of the orientation dependent term. This potential of permanent dipoles is not involved directly in the vibrational spectrum, only its change during the vibration is effective. Therefore the interaction potential has to be considered as a function of the normal coordinate Q of the molecules. The interaction of the two transition dipole moments of the identical molecules (resonant vibration coupling) has been considered as the mechanism for the noncoincidence effect. The splitting of the frequency

of an isolated molecule by interaction with an identical neighbour (Anisotropy Shift) depends upon the geometrical relations between the two molecules. This anisotropy shift (splitting) is due to the inphase and out of phase vibration of the two identical molecules. The magnitude of the anisotropy shift depends on the magnitude of the splitting.

The Raman bands in liquids show a more or less broad distribution of frequencies. In case of isotropic part of the Raman band, the reorientational motion of the molecules can be neglected. The excited molecule in the liquid ensemble sees a somewhat different environment and therefore a different interaction situation, the vibrational frequency is therefore perturbed by various interaction potentials depending upon geometric relations. This leads to different frequency shifts and hence broadening of the band occurs.

Laser Raman measurements were made of the amide I modes of DMA and DMF in the pure liquid and in solutions of varying dipole moments (μ) dielectric constants (ϵ) and refractive indices (n). The solvent concentration were varied from about 10% (v/v) to 90% (v/v) in steps of 10% (v/v). The I_{VV} and I_{VH} components of the Raman bands were recorded in all the cases and the linewidth (FWHH) was obtained. The non-coincidence effect of the isotropic and anisotropic components was studied as a function of the solvent concentration in polar

as well as non-polar solvents. The Transition dipole-Transition dipole type of interaction was considered to be responsible for the anisotropy shift. It seems to be the dominant mechanism responsible for anisotropy shift in all the three molecules under study because the shift goes on reducing as the concentration of the solvent is increased. The solute molecules under these conditions become well separated and are therefore not able to interact much.

The effect of composition on the noncoincidence of the isotropic and anisotropic Raman frequencies was also considered in detail. In this connection the parameter involving the dielectric constant and the refractive index of the medium was taken into account. Two factors $S_p = \left(\frac{n^2+2}{2\epsilon+n^2}\right)^2 \epsilon^2$ and $S_t = \frac{(n^2+2)^2}{9n^2}$ corresponding to the permanent and transition dipoles were considered. The factor related to the permanent dipole is a variable one since it involves the dielectric constant of the solvent where as the factor S_t remains almost constant for all the solvents. The plot of the graph between $\delta\nu \frac{(2\epsilon+n^2)}{\epsilon}$ as a function of ϕ, the volume fraction of the solute is clearly a straight line showing the validity of the equation developed by earlier workers.

The variation of the isotropic linewidth (Γ_{iso}) as a function of the van der Waals interaction energy consisting of Dipole-Dipole (D-D), Dipole-Induced Dipole (D-ID) and Dispersion energy was considered by us in all the three molecules

DMA, DMF and Cyclohexanone. The calculations were performed to get the total interaction energy taking into account the dielectric properties of the medium. It has been observed by us that the linewidth (Γ_{iso}) is a linear function of the dispersion energy parameter $F(n,I) = \frac{3}{2n^4}\frac{I_i I_j}{I_i+I_j}\alpha_i\alpha_j$ where the symbols have their usual meaning defined earlier. It is quite an interesting result as it holds even for highly polar solvents. These results were obtained using four solvents (CH_3CN, $CHCl_3$, CCl_4 and C_6H_6). Having established this relationship we tried to correlate the vibrational relaxation rate (τ_v^{-1}) to the dispersion forces. The variation of vibrational relaxation rate (τ_v^{-1}) as a function of the density and the dynamic viscosity is known. In an attempt to put the parameter related to the dispersion force we considered various possible combinations and then found a linear relation between the vibrational relaxation rate (τ_v^{-1}) and a function $f(\rho,\eta,n) = \rho\eta\left(\frac{n^2-1}{2n^2+1}\right)^{-1}$. This function takes care of many molecular parameters and is therefore quite significant. The refractive index term has come from the expression for the Lorentz field. This relation is almost linear in case of DMF and Cyclohexanone molecule and correlation is very good for dilute solutions. From these studies, it is therefore possible to empirically correlate the vibrational relaxation rate with the hydrodynamic and dispersion forces. One very important and new result which one can derive from these investigation is that the key role

is played by the dispersion forces in the line broadening mechanism under the conditions of dilute solutions of the N,N-Dimethylacetamide, N,N-Dimethylformamide and Cyclohexanone molecules.

APPENDIX

APPENDIX

The dependence of the electronic transition moment on the normal coordinates of the system Q_k is small under Born-Oppenheimer approximation. The transition moment may be expressed as a rapidly converging Taylor series expanded around the equilibrium position (Herzberg-Teller expansion). Higher order terms in the Taylor expansion are normally sufficiently small to be neglected. The transition probability expression may then be simplified assuming that the electronic transition moments and the integral h^k_{es} do not under the approximation conditions for which the Born-Oppenheimer is valid, operate on the vibrational wavefunctions. One may therefore write,

$$\langle \alpha_{fg} \rangle_{an,\ gm} = A + B + C + D$$

where

$$A = \frac{1}{hc} \sum_{ev} \frac{\langle \mu_\rho \rangle^0_{ae} \langle \mu_\sigma \rangle^0_{eg} \langle n/v \rangle \langle v/m \rangle}{\tilde{\nu}_{ev,\,gm} - \tilde{\nu}_0 + i\,\Gamma_{ev}}$$

$$+ \frac{\langle \mu_\sigma \rangle^0_{ae} \langle \mu_\rho \rangle^0_{eg} \langle n/v \rangle \langle v/m \rangle}{\tilde{\nu}_{ev,\,an} + \tilde{\nu}_0 + i\,\Gamma_{ev}}$$

$$B = \frac{1}{h^2c^2} \sum_{ev} \sum_{s \neq e} \sum_{k} \left[\frac{\langle \mu_\rho \rangle^0_{as} \langle \mu_\sigma \rangle^0_{eg} h^k_{es} \langle n/Q_k/v \rangle \langle v/m \rangle}{(\tilde{\nu}_s - \tilde{\nu}_e)(\tilde{\nu}_{ev,\,gm} - \tilde{\nu}_0 + i\,\Gamma_{ev})} \right.$$

$$\left. \frac{\langle \mu_\sigma \rangle^0_{ae} \langle \mu_\rho \rangle^0_{sg} h^k_{es} \langle n/v \rangle \langle v/Q_k/m \rangle}{(\tilde{\nu}_s - \tilde{\nu}_e)(\tilde{\nu}_{ev,\,an} + \tilde{\nu}_0 + i\,\Gamma_{cv})} \right]$$

$$+ \frac{1}{h^2c^2} \sum_{ev} \sum_{s \neq e} \sum_{k} \left[\frac{\langle \mu_\rho \rangle^0_{ae} \langle \mu_\sigma \rangle^0_{sg} h^k_{es} \langle n/v \rangle \langle v/Q_k/m \rangle}{(\tilde{\nu}_s - \tilde{\nu}_e)(\tilde{\nu}_{ev,\,gm} - \tilde{\nu}_0 + i\,\Gamma_{ev})} \right.$$

$$\left. + \frac{\langle \mu_\sigma \rangle^0_{as} \langle \mu_\rho \rangle^0_{eg} h^k_{es} \langle n/Q_k/v \rangle \langle v/m \rangle}{(\tilde{\nu}_s - \tilde{\nu}_e)(\tilde{\nu}_{ev,\,an} + \tilde{\nu}_0 + i\,\Gamma_{ev})} \right]$$

$$C = \frac{1}{h^2c^2} \sum_{ev} \sum_{t \neq a,g} \sum_{k} \left[\frac{\Gamma\mu\rho_{te}^0 \Gamma\mu\sigma_{eg}^0 h_{at}^k \langle n/\Omega_k/v\rangle\langle v/m\rangle}{(\tilde{\nu}_t - \tilde{\nu}_a)(\tilde{\nu}_{ev,gm} - \tilde{\nu}_o + i\Gamma_{ev})} \right.$$

$$\left. + \frac{\Gamma\mu\sigma_{ae}^0 \Gamma\mu\rho_{tg}^0 h_{gt}^k \langle n/v\rangle\langle v/\Omega_k/m\rangle}{(\tilde{\nu}_t - \tilde{\nu}_g)(\tilde{\nu}_{ev,an} + \tilde{\nu}_o + i\Gamma_{ev})} \right]$$

$$+ \frac{1}{h^2c^2} \sum_{ev} \sum_{t \neq a,g} \sum_{k} \left[\frac{\Gamma\mu\rho_{ae}^0 \Gamma\mu\sigma_{et}^0 h_{gt}^k \langle n/v\rangle\langle v/\Omega_k/m\rangle}{(\tilde{\nu}_t - \tilde{\nu}_g)(\tilde{\nu}_{ev,gm} - \tilde{\nu}_o + i\Gamma_{ev})} \right.$$

$$\left. + \frac{\Gamma\mu\rho_{te}^0 \Gamma\mu\sigma_{eg}^0 h_{at}^k \langle n/\Omega_k/v\rangle\langle v/m\rangle}{(\tilde{\nu}_t - \tilde{\nu}_a)(\tilde{\nu}_{ev,an} + \tilde{\nu}_o + i\Gamma_{ev})} \right]$$

$$D = \frac{1}{h^3c^3} \sum_{ev} \sum_{s,s' \neq c} \sum_{k,k'} \left[\frac{\Gamma\mu\rho_{as}^0 \Gamma\mu\sigma_{sg}^0 h_{es}^k h_{es'}^{k'} \langle n/\Omega_k/v\rangle\langle v/\Omega_{k'}/m\rangle}{(\tilde{\nu}_s - \tilde{\nu}_c)(\tilde{\nu}_{s'} - \tilde{\nu}_e)(\tilde{\nu}_{ev,gm} - \tilde{\nu}_o + i\Gamma_{ev})} \right.$$

$$\left. + \frac{\Gamma\mu\sigma_{as'}^0 \Gamma\mu\rho_{sg}^0 h_{es'}^{k'} h_{es}^k \langle n/\Omega_k/v\rangle\langle v/\Omega_k/m\rangle}{(\tilde{\nu}_{s'} - \tilde{\nu}_e)(\tilde{\nu}_s - \tilde{\nu}_e)(\tilde{\nu}_{ev,an} + \tilde{\nu}_o + i\Gamma_{ev})} \right]$$